Indirect Dark Matter Detection CF2 Working Group Summary

Conveners: J. Buckley, D.F. Cowen, S. Profumo

A. Archer, M. Cahill-Rowley, R. Cotta, S. Digel, A. Drlica-Wagner, F. Ferrer, S. Funk, J. Hewett, J. Holder, B. Humensky, A. Ismail, M. Israel, T. Jeltema, A. Olinto, A. Peter, J. Pretz, T. Rizzo, J. Siegal-Gaskins, A. Smith, D. Staszak, J. Vandenbroucke, M. Wood

Executive Summary

1. Significant progress in theoretical studies has been made to assess the detectability of Dark Matter (DM) particle models by various experiments. These studies have been conducted both in the framework of UV-complete theories, for example supersymmetry (SUSY), and in the context of effective theories, such as with higher-dimensional contact operators. Both methods can be employed to relate accelerator constraints to the detectability of signatures from weakly interacting massive particles (WIMPs). SUSY scans including the latest constraints from the LHC, and cosmological constraints show that the *Cherenkov Telescope Array* (CTA) can greatly improve the current experimental sensitivity over the parameter space of many theoretical DM models.

2. CTA, with a critical enhancement provided by the U.S., would provide a powerful new tool for searching for dark matter, covering parameter space not accessible to other techniques (direct searches, accelerator). CTA would provide new information that will help identify the particle nature of the DM (mass, spectral signatures of the specific annihilation channel) and could provide a measurement of the halo profile. Given the importance of indirect detection (ID) to Dark matter science, DOE and NSF/Physics contribution to indirect detection experiment, on the level of its commitment to the G2 Direct Detection experiments, could result in a U.S. dark matter program with a realistic prospect for both detecting the dark matter in the lab and identifying it on the sky.

3. After the LHC has covered the *a priori* natural parameter space for SUSY, it is a priority in this field to further explore the viable theory parameter space of both supersymmetric models and other extensions to the Standard Model. Indirect detection experiments (gamma-ray and neutrino measurements in particular) can, in some cases, go beyond the limits of the *Energy Frontier* of terrestrial accelerators.

4. The field of indirect dark matter detection necessitates a coherent theoretical and observational effort to pinpoint via astrophysical modeling and measurements the relevant inputs to detection rates, such as the density, velocity distribution and substructure content of dark matter halos. Multi-wavelength and cosmic-ray searches are also in need of additional observational and theoretical efforts, especially in the realm of Galactic propagation and energy losses for charged species. We recommend, on both fronts,

a broad community based effort to improve measurements (e.g., identifying new Dwarf galaxies and improving the stellar velocity data on important objects; performing key multi-wavelength and cosmic-ray measurements to characterize the magnetic field structure in the Galaxy and determine secondary-to-primary ratios of light cosmic-ray nuclei) and conduct more realistic simulation studies (with higher resolution N-body simulations, and more detailed modeling of baryonic feedback). Progress in this field will allow us to both quantify uncertainties, and to converge on benchmark models for astrophysical inputs and for cosmic-ray diffusion models, which will allow for a direct comparison of performance and expected sensitivity for current and future experiments.

5. The Galactic center is a prime target for DM searches. Even without rejection of astrophysical backgrounds, observations of the GC provide strong constraints. For CTA, i.e. the next generation experiment, angular resolution is key to improving ability to reject astrophysical backgrounds in the GC. To achieve good angular resolution, and good sensitivity to southern sources doubling the size of the proposed southern CTA telescope is key. Merging telescopes in a single site, and improving angular resolution is much more than an incremental improvement.

6. IceCube with the DeepCore/PINGU/MICA enhancement (in-filling the instrument to achieve a significantly lower energy threshold) would provide the possibility of detecting a smoking-gun signal of DM (a high-energy neutrino signal from the Sun) as well as competitive limits on the *spin-dependent* SD nuclear recoil cross section compared with planned generation-2 (G2) direct detection experiments.

7. Continued operation of *Fermi*, HAWC, and VERITAS over the next $\sim$5 years will result in dramatic improvements in sensitivity to dark matter covering the energy range from GeV up to the unitarity limit of $\sim$100 TeV. These observations are projected to provide between a factor of 2 and order-of-magnitude improvements compared to existing limits over this range. Collectively, these experiments would provide the best sensitivity to the northern-hemisphere ("classical") dwarf galaxies, even after the first (southern) CTA array comes on line.

Contents

1 Overview of the CF2 Report

As part of the Snowmass process, the *Cosmic Frontier Indirect-Detection* subgroup (CF2) has drawn on input from the Cosmic Frontier and the broader Particle Physics community to produce this document. The scope of this report is to identify opportunities for dark matter science through indirect detection. Input was solicited at a number of meetings including the FNAL community planning meeting, the SLAC CF meeting and finally the Snowmass CSS2013 meeting. For this document, we have liberally drawn on work completed by the Dark Matter Complementarity (CF4) subgroup in the preparation of the Dark Matter Complementarity document [1], which puts indirect detection into the larger context of Dark Matter science.

The purpose of this report is to give an overview of the primary scientific drivers for indirect detection searches for dark matter, and to survey current and planned experiments that have, as a large part of their scientific program, the goal of searching for indirect (or astrophysical) signatures of dark matter. We primarily address existing experiments with a large U.S. role, or future experiments where a U.S. contribution is sought (see Table 0-1 for a summary of indirect detection experiments). We also address the limitations of this technique, and answer the tough questions posed by the HEP community through the Snowmass process.

The report is structured as follows: in the following §2 we give an introduction to dark matter science, and discuss the role of indirect detection in a comprehensive program for Dark Matter. §3 introduces the theoretical inputs needed for Indirect Dark Matter Detection. In §3.1 we describe the dependence on indirect detection signals to the beyond-standard-model particle physics framework, and in §3.2 to the halo model profile. From updated particle physics models (including the latest LHC constraints) and halo models (derived from N-body simulations and dynamical modeling of astrophysical data) we show that, even for conservative assumptions, the dark matter annihilation signal is within reach for next-generation experiments.

We then go through a description of the different indirect-detection methods, including cosmic-ray antimatter, gamma-rays and high-energy neutrinos in §4. For each discovery channel, we cover the basic theory for the indirect signal, and discuss current and future experiments quantifying the dark matter sensitivity for each case. In §4.1 we look at the current state of the art for cosmic-ray antimatter experiments including positron fraction measurements from PAMELA, *Fermi* and AMS and future positron measurements that might be made with Atmospheric Cherenkov detectors (§4.2). We discuss astrophysical backgrounds for these experiments, and describe the potential of future antideuteron experiments for obtaining less ambiguous results. We also describe results of ultra-high-energy (UHE) cosmic-ray measurements that already provide strong constraints on UHE gamma-rays and non-thermal WIMPs (or WIMPzillas) (§4.3). In §4.4 we cover gamma-ray experiments, demonstrating the potential for existing experiments (*Fermi*, VERITAS and H.E.S.S.) in the coming years. §4.5 we outline the status of future gamma-ray experiments. §4.6 briefly describes the case of indirect detection of decaying dark matter and the constraints on that scenario from gamma-ray observations. In §4.7 we then describe results from current neutrino experiments like Super-K and IceCube, showing that current limits on high energy neutrinos from dark matter collecting and annihilating in the sun give the best constraints on the spin-dependent cross-section (including direct detection experiments). Predictions for future enhancements of IceCube (in particular the PINGU upgrade) or Hyper-K point to the potential of these instruments to make further progress in dark matter constraints, as well as offering a unique avenue for discovery (§4.8). We consider other electromagnetic signatures of Dark Matter annihilation in galaxies, including radio synchrotron or inverse-Compton radiation from secondary electrons as well as unique hard X-ray signatures of non-WIMP dark matter, e.g., sterile neutrinos in §4.9. Table 0-1 schematically summarizes current and planned experiments relevant for indirect detection of dark matter.

A number of the primary experimental techniques for indirect detection as well as key enabling technologies are described in §5. We address the Snowmass "tough questions" pertinent to this subgroup in §6, and briefly comment on the issue of complementarity among dark matter detection in §7. Finally, we conclude in §8 by identifying important opportunities for constraining, detecting or identifying dark matter that are only possible with indirect detection methods.

Table 0-1: Current and planned indirect detection experiments.

Current:				
Experiment	Target	Location	Major Support	Comments
AMS	e^+/e^-, anti-nuclei	ISS	NASA	Magnet Spectrometer, Running
Fermi	Photons, e^+/e^-	Satellite	NASA, DOE	Pair Telescope and Calorimeter, Running
HESS	Photons, e^-	Namibia	German BMBF, Max Planck Society, French Ministry for Research, CNRS-IN2P3, UK PPARC, South Africa	Atmospheric Cherenkov Telescope (ACT), Running
IceCube/ DeepCore	Neutrinos	Antarctica	NSF, Australia, Belgium, Canada, Germany, Japan, New Zealand, Sweden)	Ice Cherenkov, Running
MAGIC	Photons, e^+/e^-	La Palma	German BMBF and MPG, INFN, WSwiss SNF, Spanish MICINN, CPAN, Bulgarian NSF, Academy of Finland, DFG, Polish MNiSzW	ACT, Running
PAMELA	e^+/e^-	Satellite		
VERITAS	Photons, e^+/e^-	Arizona, USA	DOE, NSF, SAO	ACT, Running
Planned:				
CALET	e^+/e^-	ISS	Japan JAXA, Italy ASI, NASA	Calorimeter
CTA	Photons	ground-based (TBD)	International (MinCyT, CNEA, CONICET, CNRS-INSU, CNRS-IN2P3, Irfu-CEA, ANR, MPI, BMBF, DESY, Helmholtz Association, MIUR, NOVA, NWO, Poland, MICINN, CDTI, CPAN, Swedish Research Council, Royal Swedish Academy of Sciences, SNSF, Durham UK, NSF, DOE	ACT
GAMMA-400	Photons	Satellite	Russian Space Agency, Russian Academy of Sciences, INFN	Pair Telescope
GAPS	Anti-deuterons	Balloon (LDB)	NASA, JAXA	TOF, X-ray and Pion detection
HAWC	Photons, e^+/e^-	Sierra Negra	NSF/DOE, CONACyT in Mexico	Water Cherenkov, Air Shower Surface Array
PINGU	Neutrinos	Antarctica	NSF, International Partners	Ice Cherenkov

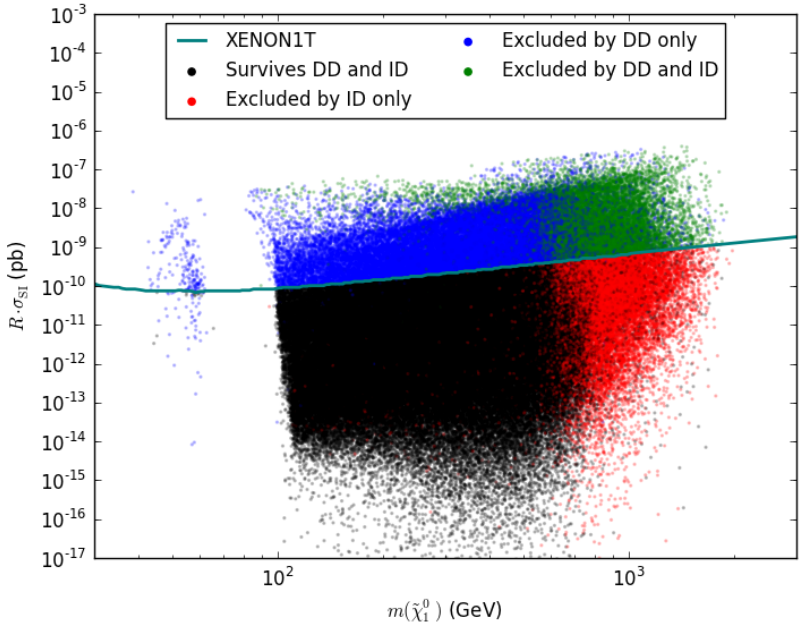

Figure 1: An example of the interplay between Direct and Indirect Detection (DD and ID, respectively) for a large collection of supersymmetric dark matter models.

2 Introduction to Dark Matter Indirect Detection

A large body of astrophysical evidence points to the fact that the dominant gravitational mass in the universe is in the form of non-baryonic dark matter. A 100 GeV thermal relic with weak scale interactions (WIMP) could provide the cold dark matter needed to explain the observed structure in the universe, and naturally provide the matter density derived by CMB measurements [2, 3]. DM has not been directly detected in the laboratory yet, but its gravitational effects have been observed on spatial scales ranging from the inner kpc of galaxies out to Mpc in clusters of galaxies, as well as on cosmological scales. Observations of separate distributions of the baryonic and gravitational mass in galaxy clusters indicate that the DM is likely composed of particles with a low interaction cross section with ordinary matter.

Numerous well-motivated particle physics models predict new particles in the 100 GeV to TeV scale. Often, these new particles are involved in solving the so-called hierarchy problem, associated with explaining the large hierarchy between the Planck and the electroweak scale, and with softening the associated fine-tuning problem. Supersymmetry (SUSY), a theory that provides an elegant solution to the quadratic divergence of the Higgs mass, also provides a natural candidate for the DM, the *neutralino* or lightest mass eigenstate resulting from a mixture of the neutral bino, wino and Higgsino [4]. Remarkably, a weakly interacting particle with a mass of m_χ ~100 GeV, if stable, would have a relic density close to the observed total matter density inferred from the CMB measurements. This follows from the fact that weakly interacting particles fall out of equilibrium earlier in the expansion history of the universe, avoiding Boltzmann suppression $\sim \exp(-m_\chi c^2/kT)$, making weakly interacting massive particles (WIMPs) a natural candidate for the DM. This feat (sometimes dubbed the "WIMP miracle") also sets the scale for the annihilation rate of dark

matter today, under certain assumptions. The fact that such a particle interacted with ordinary matter in the early universe means that such interactions should still take place in the present epoch.

In regions of high DM density the annihilation (or decay) of WIMPs into Standard Model particles including gamma rays, neutrinos, electrons and positrons, protons and antiprotons, and even antideuterons. Annihilation through various channels could produce distinctive signatures such as high energy neutrinos from the sun, or gamma-rays from the center of galaxies including our own Milky Way. Almost any annihilation channel will eventually produce gamma rays either through pion production (for hadronic channels), or via final state bremsstrahlung and inverse Compton from leptonic channels. Moreover, the spectrum from annihilation would be universal (barring the effect of energy losses and diffusion on the secondary electrons and positrons), with the same distinctive spectral shape detected in every DM halo. Unlike direct detection, the detected signal could potentially provide strong constraints on the particle mass, and help to identify the particle through the different kinematic signatures predicted for different annihilation channels.

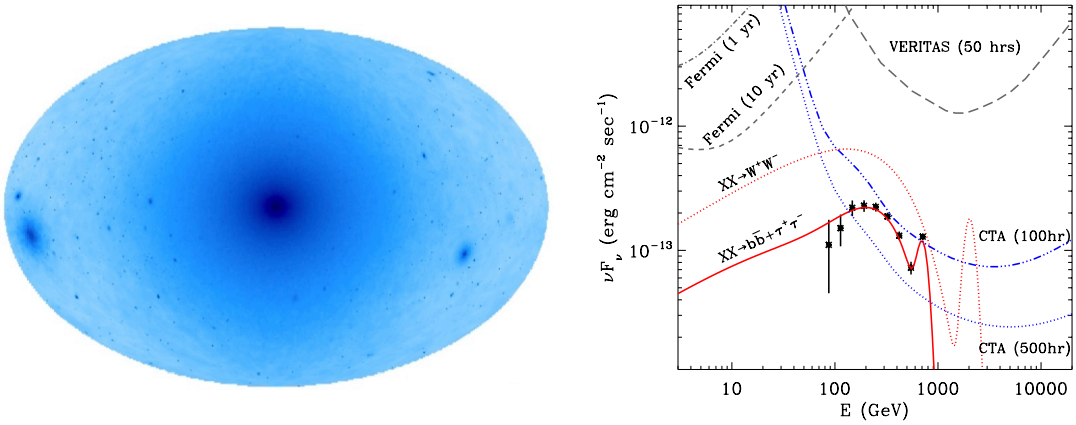

Figure 2: *Left:* Angular distribution of the gamma-ray signal from DM annihilation (Galactic coordinates) calculated from the line-of-sight integral (J-value) of a Milky-Way-sized halo as generated by the VL Lactea N-body simulation. *Right:* Simulated gamma-ray spectra as they would be measured using an augmented-CTA instrument. The two models correspond to two (arbitrary) annihilation channels assuming SUSY model points with an annihilation cross section is close to the natural value (with a Sommerfeld boost for the high-mass case) and assuming an NFW halo profile for the GC. Sensitivity curves are calculated for a southern hemisphere instrument with VERITAS or H.E.S.S.-like sensitivity, together with the sensitivity curve of the augmented CTA instrument.

Several tantalizing observations of cosmic and gamma-ray fluxes have been linked to the possible signals from annihilation or decay of DM particles. The bright 511-keV line emission from the bulge of the Galaxy detected by the SPI spectrometer on the INTEGRAL satellite [5], the excesses of microwaves and gamma-rays in the inner Galaxy revealed by the WMAP and *Fermi* satellites [6], the evidence for a 130 GeV spectral line in the *Fermi* data [7, 8], or the rise in the positron fraction above 10 GeV observed by PAMELA and AMS-02 [9, 10], have been attributed to the physics associated with DM [11, 12, 13, 14, 15]. Currently a dark matter interpretation for these signals is far from clear, given limited statistics (for the *Fermi* line) or large systematics or astrophysical backgrounds (for the positron, and 511-keV emission).

For almost all of these signals, the flux exceeds the predictions of the most generic, conservative models, requiring a *boost* in either the present-day cross-section for particle interactions, or in the astrophysical factor, e.g., a steepening of the halo profile or a modification of usual assumptions about dark matter halo

substructure. Some of these scenarios require boost factors that, while not the most conservative, are also not ruled out by observations. Indeed, these tentative associations of signals with DM have motivated numerous important theoretical studies that quantify the possible boosts. For example, since the fluxes from DM annihilations depend on the square of the density, some astrophysical processes (for example the steepening of the halo profile from the adiabatic growth of the central massive black hole) could change the inner profile near the Galactic center, so strong boosts near the galactic center are possible. Another boost could result if the present day annihilation cross-section is substantially larger than the cross section at decoupling, in particular, if there is a strong dependence of cross section on the relative velocity v between dark matter particles. Since the DM particles were relativistic at decoupling, but are moving at non-relativistic speeds in the halo of the present-day Galaxy, a *p-wave* velocity dependent flux, $\sigma v \sim b v^2$, can result in the right relic density for a light MeV dark matter particle that annihilates into non-relativistic $e^{\pm}$ pairs with $\sigma v \sim 10^{-5}$ pb giving a possible, if not completely natural, explanation for the observed 511 keV emission from the bulge [16, 17].

Similarly, for the positron excess, one requires significant boosts compared with the most generic expectations. In fact, barring the presence of a nearby DM clump [18, 19], the thermal cross-section falls short by about two orders of magnitude to explain the AMS-02 data. Here, the correct relic abundance and a larger annihilation cross-section can be reconciled if the annihilation follows $\sigma v \propto 1/v$. This so-called *Sommerfeld enhancement* results from the exchange of new light particles, and is at the basis for the DM explanation of the rising positron fraction at GeV energies [20, 21, 22, 23]. These scenarios face stringent constraints from anti-proton, gamma-ray and synchrotron data, and there is some tension with the higher DM density in the galactic center predicted by the steep NFW and Einasto profiles favored by N-body simulations [24, 25, 26, 27, 28].

Most recently, the possible observation of a gamma-ray line in the *Fermi* data from the GC region has sparked considerable interest [29]. Since the excess is offset from the center, there is no prior hypothesis for the line energy and the line-to-continuum ratio exceeds *a-priori* expectations, it is difficult to assign an a-posteriori probability that accurately accounts for trials factors. Moreover, the *Fermi* team has argued that the line profile is too narrow to match the instrument energy resolution reducing the inferred significance. Additional data is needed to elevate this hint of a signal to a detection; a significant increase in the *Fermi* GC exposure together with *Fermi* and observations with the new H.E.S.S.-II low-threshold ground-based observatory. Other hints of excesses at $\sim$10 GeV in the Galactic halo [30], or even in the stacked *Fermi* dwarf analysis [31] continue to motivate more careful studies of systematics, and theoretical exceptions. Many of these results are of marginal statistical significance $<$3 sigma, much like hints of signals seen in accelerator experiments that eventually fade with increased statistics.

3 Theoretical Input to Indirect Detection Signals

Ultimately, the goal of indirect detection experiments is to provide a measurement that helps to determine both the nature of dark matter and the distribution of dark matter on the sky. But to estimate the signals in different ID detectors, we must make reasonable assumptions about just such unknown parameters. For these estimates, we must consider specific *benchmark models* for the particle physics, and must use empirical fits to the best (gravitational) measurements of the distribution of dark matter in halos. While it is important to maintain a somewhat agnostic attitude about the exact nature of beyond-the-standard model physics that might result in a viable dark-matter candidate, it is important to make generic predictions about the signals, and to consider some specific well-motivated scenarios to provide benchmarks by which different ID techniques can be compared, and through which ID constraints can be compared to accelerator and direct-detection data. Here we discuss the particle physics models that might provide a framework for dark matter, and summarize our understanding about the phase-space distribution of dark matter particles in halos.

In full generality, the indirect detection signal flux resulting from the annihilation of a WIMP with a mass m_χ to gamma-rays (or neutrinos) an be cast as the product of a particle physics term $\mathcal{P}$ and an astrophysical ter J

$$\frac{d\phi}{dE\, d\Omega} = \mathcal{P} J. \tag{1}$$

Since the self-annihilation rate is proportional to the square of the density, the astrophysical term can be derived by integrating the square of the halo density profile $\rho(r)$ along a line-of-sight making an angle of ψ with respect to the source direction:

$$J(\psi) = \int_{\rm l.o.s} \rho^2(r) dl(\psi). \tag{2}$$

This line-of-sight integral requires a simple geometrical relationship between the line-of-sight distance l, the radial distance from the center of the halo r for a particular viewing angle ψ.

The particle physics term can be written

$$\mathcal{P} = \sum_i \frac{\langle \sigma v \rangle_i}{M_\chi^2} \frac{dN_{\gamma,i}}{dE} \tag{3}$$

The sum over the index i represents the different possible secondary production mechanisms, and annihilation channels.

To calculate the total signal, it is necessary to convolve the J-factor with the angular distribution with the point-spread-function of the instrument, convolve the spectrum with the energy resolution function and then to integrate over solid angle and energy to derive the total flux. Since the halo may appear to be quite extended, the cutoff in the solid angle integral is typically determined so that the ratio of the annihilation signal strength to the integrated diffuse background is maximized.

While the annihilation rate depends on the density profile, understanding the full *phase-space density* (including the velocity distribution) is important for deriving a self-consistent halo model, consistent with dynamical measurements (e.g., stellar velocities and rotation curves). Moreover, in some cases the cross-section may depend on velocity, demanding more care in specifying the full distribution function for the dark matter.

We define the phase-space density of dark matter as:

$$dN = f(\mathbf{x}, \mathbf{v}, t) d^3\mathbf{x} d^3\mathbf{v}, \tag{4}$$

such that the number of particles within a phase-space element $d^3\mathbf{x}d^3\mathbf{v}$ centered on coordinates $(\mathbf{x}, \mathbf{v})$ is dN. The phase-space density of dark matter affects indirect detection in the following ways:

(1) If the phase-space density is separable, $f(\mathbf{x}, \mathbf{v}) = n(\mathbf{x}) f_v(\mathbf{v})$, and dark matter is self-annihilating, then the annihilation rate of dark matter in a halo is simply

$$\Gamma \propto \langle \sigma_A v_{rel} \rangle \int d^3\mathbf{x} n^2(\mathbf{x}), \tag{5}$$

where $\langle \sigma_A v_{rel} \rangle$ is the velocity-averaged annihilation cross section, and where the average is taken over the relative velocities of particles with respect to each other. In cases in which the phase-space density is not separable and the cross section is velocity-dependent, it is not possible to simplify the expression for the collision term in the Boltzmann equation and this must be evaluated by preforming the integral over the full phase-space distribution function. However, we typically assume a velocity-independent (s-wave) annihilation cross section, so we can estimate the annihilation rate in the above form. However, one note

of caution is that in simulated halos (see below), the phase-space density is in general *not* separable, so to calculate, e.g., p-wave-type cross sections, one formally must calculate the collision term in the Boltzmann equation instead of using the above simplified formula.

In contrast to the case for dark matter annihilation, for dark matter decay, the signal is proportional to the line of sight integral of the density (not the density squared), giving slightly less sensitivity to the detailed halo model.

For annihilation to charged particles, the situation is a bit different since diffusion and energy loss also affect the observed signal (see [32, 33, 34] for details of the calculation). One convolves the source function for annihilation with the Green's function for cosmic-ray propagation including diffusion, and energy loss from inverse-Compton and synchrotron radiation for electrons (or losses from ionization and nuclear interactions for protons and deuterons). For electrons, energy losses are dominated by synchrotron and inverse Compton losses, both of which have the same dependence dependence on energy (for Compton scattering in the Thomson regime) and can be combined to give $dE/dt = -b\,E^2$. Combining this with diffusion with diffusion constant κ, the transport equation can be solved to give the Green's function which gives the intensity of positrons seen at x=0, time t and energy E given an impulse at position x and energy E':

$$G(x,t,E,E') = (4\pi\kappa t)^{-3/2}(1-b\,E\,t)^2 \exp\left(-\frac{x^2}{4\kappa t} - t/\tau\right)\delta\left(E_0 - \frac{D}{-1-b\,E\,t}\right) \tag{6}$$

One then folds this with the source function that gives the annihilation rate

$$Q(E,x) = 4\pi\frac{dN_{e^+}}{dE\,d^3x\,dt} = \sum_i \frac{\langle\sigma v\rangle_i}{M_\chi^2}\frac{dN_{e^+,i}}{dE} \times \rho(r)^2 \tag{7}$$

and integrates over time (assuming steady state emission) and over the spatial distribution of dark matter to give the observed, nearly isotropic, electron spectrum:

$$\frac{dN_{e^+}}{dE_{e^+}} = \int dt \int d^3x \int dE' G(x,t,E,E')Q(E',x) \tag{8}$$

This can be accomplished either analytically, or by using numerical codes like GALPROP that make an effort to include more detailed information[35]

For cosmic ray electrons, regardless of the source spectrum, there will be a sharp cutoff in the observed spectrum at energy $\frac{E_c \approx 4\kappa}{b\,d^2}$ where d is the distance to the source. Plugging in typical numbers for the interstellar magnetic field, the range of 1 TeV electrons is limited to about $d \sim 1$ *kpc*. Thus, at high energies, the observed electron or positron spectrum is dominated by the local dark matter (or cosmic-ray background) distribution.

3.1 Particle Physics

While a plethora of particle physics models have been envisioned to provide viable DM candidates, a special category of DM particles stands out as especially well motivated: that of weakly interacting massive particles, *i.e.* WIMPs. WIMPs have both phenomenological and theoretical appeal, in that on the one hand a weak-scale mass and pair-annihilation cross section naturally produces a thermal relic density in accord with the observed dark matter density, and on the other hand WIMP candidates are ubiquitous in extensions to the Standard Model of particle physics where new particles exist at the electroweak scale.

One such extension that has attracted the interest of the theory community, for many reasons unrelated to the problem of featuring a DM candidate, is supersymmetry. However, the recent LHC results have put stringent limits on some of the particles predicted by weak-scale supersymmetry. For example, direct searches for strongly interacting squarks and gluinos imply that the mass of those particles , if they exist, must be in the TeV range, with some (although not dramatic) implications for the phenomenology of supersymmetric DM candidates. The electroweak sector of the supersymmetric particle content is much less constrained, at least directly, by LHC results. As part of this sector, the lightest neutralino – the supersymmetric WIMP *par excellence* – and its phenomenology are not severely constrained by LHC results (with the possible exception, for example, of resonant annihilation channels through the SM Higgs, or of direct detection cross sections mediated dominantly by SM Higgs exchange).

Another framework that produces a natural WIMP dark matter candidate is that of universal extra dimensions, or UED [36, 37]. In UED, all Standard Model fields propagate in a 5th compactified extra dimension, giving rise, in the four-dimensional theory, to a tower of Kaluza-Klein states. Momentum conservation in the extra dimension leads to a discrete symmetry, in the four-dimensional picture, known as Kaluza-Klein parity, which corresponds to the parity assignments $(-1)^N$, with N the Kaluza-Klein level. As a result, the lightest Kaluza-Klein level-1 particle is stable. For the Higgs mass recently pinpointed at the LHC, and for minimal boundary conditions, this lightest Kaluza-Klein particle is the first excitation of the hypercharge gauge boson, $B^{(1)}$.

In the following sections we limit our detailed estimates to a single benchmark model corresponding to neutralino dark matter. However, we expect to obtain similar results for any thermal WIMP. In general, any thermal relic must have interacted with ordinary matter in the universe, and must interact with such matter in the present epoch, ultimately producing gamma-rays, and in many cases producing cosmic-ray electron-positron pairs, protons and antiprotons and neutrinos. When one subjects the predictions to cosmological constraints, the level of the allowed cross section for different models must hover around the generic total annihilation cross section of $\langle \sigma\, v \rangle \sim 10^{26} \mathrm{cm}^3 \mathrm{s}^{-1}$. Thus the estimated sensitivity of experiments to WIMP dark matter is generic. Typically, the natural range of dark matter masses is expected to extend from a few GeV to a few TeV. However, this argument based on *naturalness* in supersymmetry, the upper limit on generic WIMP masses is significantly higher. Ultimately, the upper bound on the mass of a thermal relic is set by unitarity at 120 TeV [38] or even higher, if one takes into account co-annihilations (changing the relic abundance) or a strong velocity dependence in the cross section [39].

3.1.1 Expected Annihilation Cross-Sections for SUSY WIMPs

One of the main motivations for R-parity conserving supersymmetry (SUSY) is the prediction that the lightest SUSY particle (LSP) is stable and may be identified as a candidate dark matter (DM) particle if it is both electrically neutral and colorless. Quite commonly the LSP corresponds to the lightest neutralino, χ_1^0, a linear combination of the neutral higgsinos, wino and bino, and this be will assumed in the discussion that follows. While DM searches are superficially focused on the nature of the LSP, the properties of all the other super-particles as well as those of the extended SUSY Higgs sector also come into play. Thus it is impossible to completely separate searches for DM, *i.e.*, the LSP, from searches for and the examination of the rest of the SUSY spectrum. However, even in the simplest SUSY scenario, the MSSM, the number of free parameters (~ 100) is too large to study in all generality. The traditional approach is to assume the existence of some high-scale theory with only a few parameters (such as mSUGRA[40]) from which all the properties of the sparticles at the TeV scale can be determined and studied in detail. While such an approach is quite valuable [41], these scenarios are somewhat phenomenologically limiting and are under increasing tension with a wide range of experimental data including, in some cases, the ~ 126 GeV mass of the recently discovered Higgs boson[42, 43]. One way to circumvent such limitations is to examine instead

the far more general 19-parameter pMSSM[44]. We adopt this approach for one of our benchmarks in the sensitivity estimates presented below.

3.1.2 Generic WIMPs and contact operator constraints

A model-independent approach to WIMP phenomenology consists in making the assumption that the particles mediating dark matter's interactions with the Standard Model are very heavy, leading to a description in terms of contact interactions in the context of an effective field theory (EFT). Depending on the relevant process, and on the spin and nature (e.g. Dirac or Majorana) of the DM candidate, it is possible to write down a complete set of relevant operators of a given dimension. Much like Fermi's theory of the weak interaction the *strength* of each operator is expressed in terms of a quantity Λ with the dimensions of mass. Constraints can then be obtained from a variety of experimental results as a function of Λ. A key advantage of this approach is that it captures the phenomenology of a wide variety of dark matter models (although naturally not all) and that it is especially simple to compare various different detection methods.

3.1.3 Indirect Detection of Non-WIMP DM models

WIMPs do not nearly exhaust the huge variety of known particle physics candidates for dark matter. Many *non-WIMP* DM models can be tested by the same experiments relevant for indirect WIMP detection (sometimes this is the only practical means of detection). In other cases, direct detection may provide the only avenue for discovery. Non-WIMP dark matter is covered at much greater length in the CF3 report. Here we give a partial list of non-WIMP DM scenarios, and describe the implications for indirect detection.

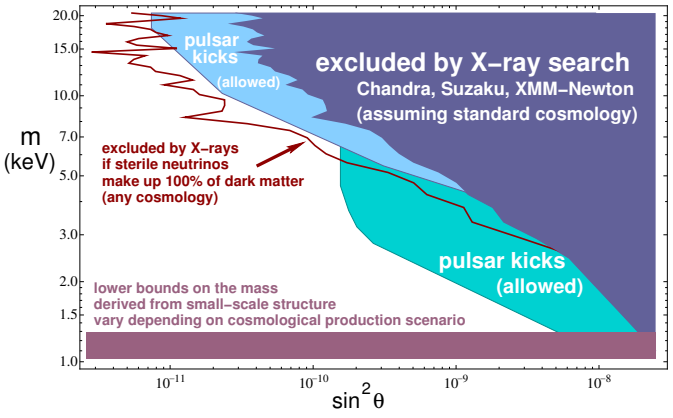

Figure 3: Summary of astrophysical constraints on in the $m_{\rm st} - \theta$ plane for sterile neutrino dark matter assuming a standard cosmology below the temperature when neutrino oscillations occur, adapted by Kusenko from Ref.[45].

Sterile neutrinos provide another candidate for non-WIMP dark matter. [45]. Sterile neutrinos are motivated by a variety of arguments besides the necessity of a DM candidate (for example, the generation of a baryon asymmetry, and the non-zero value of SM neutrino masses). Sterile neutrinos generically decay into ordinary

SM neutrinos plus a photon, in a two-body decay that produces nearly monochromatic photons in the final state, with an energy corresponding to half the sterile neutrino mass. Preferred sterile neutrino mass ranges makes the relevant observational window the X-ray to hard X-ray range. Ideal targets are nearby clusters of galaxies or nearby galaxies such as Andromeda or local dwarf spheroidal galaxies. Other non-WIMP candidates such as gravitinos can be unstable, either because of R-parity breaking operators, or because they are not the LSP but they are long-lived enough to act as dark matter. Gravitino decay can lead, similarly to the case of sterile neutrinos, to two-body decays featuring a photon in the final state. The emitted radiation would be monochromatic, producing a line in the spectrum. The location of the line in the electromagnetic spectrum is theoretically rather weakly constrained, and it could occur anywhere in the X-ray to gamma-ray regime.

Another novel possibility is that some or all of the cosmological dark matter may be a leftover of a primordial asymmetry between DM and anti-DM. The resulting dark matter candidate is typically referred to as *asymmetric dark matter*. A key benefit of the asymmetric dark matter scenario is the possibility to relate the DM asymmetry to the observed baryon asymmetry, via a careful choice of quantum number attribution to the dark matter candidate. Although by definition annihilation does not occur in asymmetric DM models, a residual population of anti-DM particle could well trigger important indirect detection signatures. In particular, in certain scenarios asymmetric dark matter could produce interesting and unique features for example in antimatter spectra [46].

Super-heavy DM candidates could also in principle produce interesting indirect dark matter signals, especially at ultra-high energy cosmic ray experiments. There are a number of proposed scenarios that involve physics beyond the Standard Model (SM) where the existence of massive particles, generically called "X" particles, of mass $M_X \gg 10^{20}$eV, originate from processes in the early Universe. These scenarios are called *top-down* (TD) scenarios in the context that they may produce the extreme energy cosmic rays (cosmic rays with energies around 10^{20}eV) through the decay of these massive X particles instead of the conventional *bottom-up* scenarios where acceleration happens in extreme astrophysical environments.

Two general possibilities for the origin of the X particles have been discussed in the literature: They could be short-lived particles released in the present Universe from cosmic topological defects such as cosmic strings, magnetic monopoles, etc., formed in a symmetry-breaking phase transition in the early Universe. Alternatively, they could be a metastable (and currently decaying) particle species with lifetime larger than or of the order of the age of the Universe. This second scenario arises in models where the dark matter is a heavy particle such as "WIMPzillas" etc. (See [47] for a list of TD models.)

Since the mass scale M_X of the hypothesized X particle is well above the energy scale currently available in accelerators, its primary decay modes are unknown and likely to involve elementary particles and interactions that belong to physics beyond the SM. However, irrespective of the primary decay products of the X particle, the observed UHECR particles must eventually result largely from *fragmentation* of the SM quarks and gluons, which are secondaries to the primary decay products of the X particles, into hadrons.

The most abundant final observable particle species in the TD scenario are expected to be photons and neutrinos from the decay of the neutral and charged pions, respectively, created in the parton fragmentation process, together with a few percent baryons (nucleons). Therefore, searches of ultrahigh energy (UHE) photons and neutrinos strongly constrain TD models.

3.1.4 Benchmark particle physics models for gamma-rays, neutrinos, positrons, antiprotons and antideuterons

The CF2 group recommends that particle physics benchmarks be adopted to help facilitate the comparison of performance of different search channels (including but not limited to gamma-rays, neutrinos, positrons, antiprotons and antideuterons). Such comparison necessitates not only of particle physics benchmarks, but also of additional choices for the relevant dark matter density distribution and for the propagation and energy loss properties of cosmic particles in the Galaxy, as discussed below.

As a step toward this particle physics benchmarking activity, some of us have recently begun a detailed study of the indirect detection signals for neutralino dark matter derived from the phenomenological SUSY parameter space (pMSSM). These pMSSM models are constrained by observations at the 7 and 8 (and eventually 14) TeV LHC, supplemented by input from previous DM experiments as well as from precision electroweak and flavor measurements[48, 49, 50]. The pMSSM is the most general version of the R-parity conserving MSSM when it is subjected to several experimentally-motivated constraints: (*i*) CP conservation, (*ii*) Minimal Flavor Violation at the electroweak scale, (*iii*) degenerate first and second generation sfermion masses, (*iv*) negligible Yukawa couplings and A-terms for the first two generations. In particular, no assumptions are made about physics at high scales, e.g., the nature of SUSY breaking, in order to capture electroweak scale phenomenology for which a UV-complete theory may not yet exist. Imposing the constraints (*i*)-(*iv*) decreases the number of free parameters in the MSSM at the TeV-scale from 105 to 19 for the case of a neutralino LSP or 20 when the gravitino mass is included as an additional parameter when it plays the role of the LSP[1].

Independent of the LSP type, it is not assumed that the thermal relic density as calculated for the LSP necessarily saturates the WMAP/Planck value[51] to allow for the possibility of multi-component DM. For example, the axions introduced to solve the strong CP problem may may make up a substantial amount of DM. The 19 pMSSM parameters and the ranges of values employed in these scans are listed in Table 0-2. To study the pMSSM, many millions of model points were generated in this space (using SOFTSUSY[52] and checking for consistency using SuSpect[53]), each point corresponding to a specific set of values for these parameters. These individual models were then subjected to a large set of collider, flavor, precision measurement, dark matter and theoretical constraints [48]. Roughly 225k models with neutralino LSPs that survive this initial selection were used for these studies. (A model set of similar size has been obtained for the case of gravitino LSPs.) Decay patterns of the SUSY partners and the extended Higgs sector are calculated using a modified version of SUSY-HIT[54].

In addition to these two large pMSSM model sets, a smaller, specialized neutralino LSP set of $\sim$ 10k *natural* models have been generated, all of which result in the correct Higgs mass $m_h = 126 \pm 3$ GeV, have an LSP that *does* saturate the WMAP relic density and which produce values of fine-tuning (FT) better than 1% using the Barbieri-Giudice measure [55, 56]. This low-FT model set will also be used in the future as part of the present study.

As a result of the scan ranges going up to masses of 4 TeV, an upper limit chosen to enable phenomenological studies at the 14 TeV LHC, the LSPs in these model sets are typically very close to being a pure electroweak eigenstate since the off-diagonal elements of the chargino and neutralino mass matrices are at most $\sim M_W$. Figure 4 shows some of the properties of nearly pure neutralino LSPs (with a single electroweak eigenstate comprising over 90% of the mass eigenstate). In the left panel we see the distribution of the LSP mass for nearly pure bino, wino, and Higgsino LSPs while in the right-hand panel we see the corresponding distribution for the predicted LSP thermal relic density. Note that the masses of all of our neutralino LSPs lie below $\sim$ 2 TeV since the scan ranges only extend to 4 TeV and the entire SUSY spectrum must be heavier

[1] Here we will limit our discussion to the case of neutralino LSPs

$m_{\tilde{L}(e)_{1,2,3}}$	100GeV − 4TeV
$m_{\tilde{Q}(q)_{1,2}}$	400GeV − 4TeV
$m_{\tilde{Q}(q)_3}$	200GeV − 4TeV
$\lvert M_1\rvert$	50GeV − 4TeV
$\lvert M_2\rvert$	100GeV − 4TeV
$\lvert\mu\rvert$	100GeV − 4TeV
M_3	400GeV − 4TeV
$\lvert A_{t,b,\tau}\rvert$	0GeV − 4TeV
M_A	100GeV − 4TeV
$\tan\beta$	1 - 60
$m_{3/2}$	1 eV−1TeV ($\tilde{G}$ LSP)

Table 0-2: Scan ranges for the 19 (20) parameters of the pMSSM with a neutralino (gravitino) LSP. The gravitino mass is scanned with a log prior. All other parameters are scanned with flat priors, though we expect this choice to have little qualitative impact on our results [57].

than the LSP and less than $\sim$ 4 TeV (by definition). The fraction of models that are nearly pure bino is found to be rather low in this model set since pure binos generally result in predictions of too high of a relic density unless they co-annihilate with another sparticle, happen to be close to some (Z, h, A) funnel region or have a suitable Higgsino admixture. Note that only in the rightmost bin of the right panel is the relic density approximately saturating the WMAP thermal relic value. These LSP properties will be of particular importance in the discussion that follows.

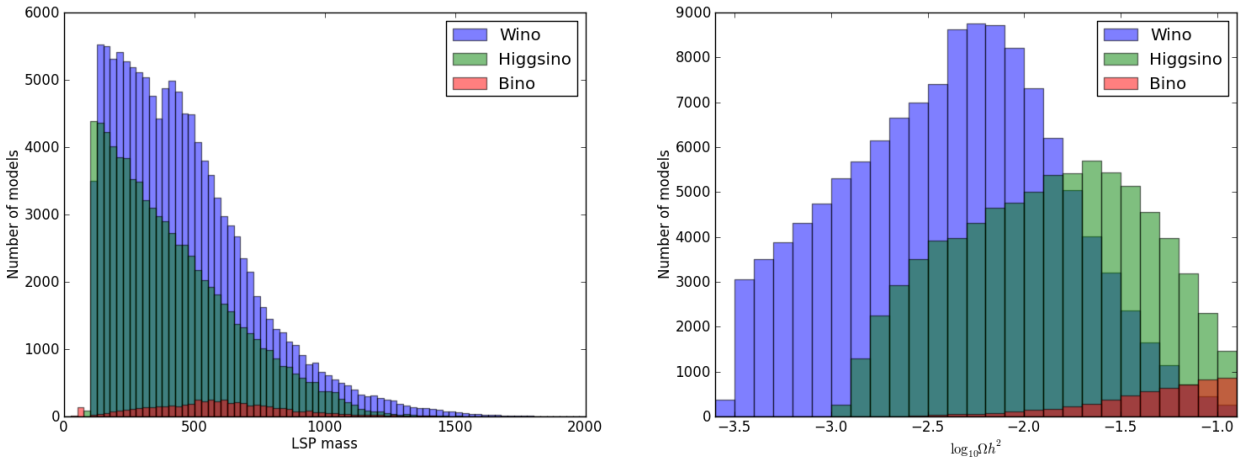

Figure 4: Number of models associated with a given LSP mass (left) and predicted relic density (right) for neutralino LSPs which are almost pure Wino, Higgsino or Bino-like.

Figure 4 shows the histogram of the distribution of LSP mass (left) and predicted relic density (right) for neutralino LSPs which are almost pure Wino, Higgsino or Bino-like. Essentially every possible mechanism to obtain (or be below) the WMAP relic density is seen here: (i) The set of models at low masses on the left-hand side forming 'columns' correspond to bino and bino-Higgsino admixtures surviving due to their

proximity to the Z, h-funnels. (*ii*) The bino-Higgsino LSPs saturating the relic density in the upper left are of the so-called 'well-tempered' variety. (*iii*) the pure[2] bino models in the middle top of the Figure are bino co-annihilators (mostly with sleptons) or are models near the A-funnel region. (*iv*) The green (blue) bands are pure Higgsino (wino) models that saturate the relic density bound near $\sim 1(1.7)$ TeV but dominantly appear at far lower relic densities. Wino-Higgsino hybrids are seen to lie between these two cases as expected. (*v*) A smattering of other annihilator models are seen to be loosely distributed in the lower right-hand corner of the plot. These pMSSM model sets will be used in subsequent sections, for calculating anticipated cross sections.

3.2 Astrophysics

To calculate the indirect detection rates one must combine benchmark models for the particle physics with an assumed form for the halo profile. Detailed N-body simulations of structure formation in a ΛCDM cosmology provide us with information about the density profile. But this work is by no means complete; new measurements of stellar velocities coupled with more complete simulations of structure formation including not only CDM but also baryonic physics continue to change our understanding of halo profiles. Here we discuss some of the common parameterizations of the halo profile, that, when calibrated using astrophysical measurements (e.g., stellar velocities), provide us with the requisite astrophysical information for the annihilation rate calculation.

Theoretical Input from N-body Simulations:

Simulated Halo Density Profiles:

Most cosmological simulations focus on dark matter that was non-relativistic at the time of decoupling, collisionless, and stable (the defining characteristics of WIMPs). Astronomically, this sort of dark matter is called *cold dark matter*, or CDM. CDM-only simulations now include $> 10^{10}$ simulation particles, where each simulation *particle* is actually a tracer for hundreds to thousands of solar masses and a vast number ($\gtrsim 10^5 4$) of dark matter particles [58, 59, 60]. The two most important results of these simulations for typical indirect searches are: (1) the gross properties of the density profile, and (2) the amount and mass function of substructure. As simulations improve, information about the velocity distribution is becoming available, and may have an impact on the calculation of some indirect signals.

In the absence of baryons, CDM simulations indicate that dark-matter halos are cuspy ($\rho \sim r^{-1}$ approximately) [61, 62, 63], with their central concentration dependent on the mass of the halo and the halo formation time [64, 65]. Small halos tend to form earlier than big halos, and are much more densely concentrated than big halos. While halos certainly do not show the pronounced disks of baryonic matter in galaxies and are typically assumed to be spherically symmetric, simulations show that halos are, in fact, somewhat *triaxial* or ellipsoidal with triaxiality increasing in the center and more pronounced for smaller halos [66]. Summarizing, these simulation results imply that annihilation signals should be centrally concentrated and that there may even be a non-spherically-symmetric shape to the emission, with the emission shape and normalization perhaps somewhat dependent on the orientation of the halo with respect to the line of sight.

The major caveat to the inferences of these CDM-only simulations is that the centers of halos, where we expect the highest dark-matter annihilation rates, are also the places where baryons (here defined as atomic, ionic, and electronic matter) settle and dominate the gravitational potential well (except in the largest and

[2]Here again, 'pure' means having an eigenstate fraction $\geq 90\%$. Points shown as bino-wino, bino-Higgsino, or wino-Higgsino mixtures have less than 2% Higgsino, wino, or bino fraction, respectively. Mixed points have no more than 90% and no less than 2% of each component.

smallest dark-matter halos). There are many arguments as to how baryons should affect dark-matter halos, but there is as yet no consensus on what actually happens. On one hand, when baryons cool, they can drag (by gravity) the dark matter with them, leading to a steepening of the dark-matter density profile [67, 68, 69]. On the other hand, violent ejections of gas generated by supernovae or active galactic nuclei reduce the central potential, and thus the density profile of dark matter [70, 71]. Ref. [72] makes a heat-engine-type argument that repeated cycles of slow baryon infall and violent ejection lead to an irreversible trend toward shallower dark-matter density profiles and central densities. However, it is not clear if baryon cooling is slow enough, or gas ejection violent enough, for this argument to work. Unfortunately in Galaxy simulations, the effect on the density profile depends extremely sensitively on the prescription for the sub-grid physics of star formation/death and the impact of any active galactic nucleus (AGN) [73].

Halo Substructure:

In addition to informing our knowledge of the gross structure of halos, N-body simulations also reveal significant substructure that can have a large impact on indirect detection signals. However, substructure has a different impact on the different types of indirect detection. For the purpose of the discussion, it is useful to consider the effect of substructure on (1) photons produced as the primary or secondary products of dark matter annihilation in the center of our own Galaxy, or more remote objects (2) cosmic-ray antimatter signals from relatively nearby in our own Galaxy, and (3) solar neutrino signals produced as the very local halo is collected in our own Sun. For gamma-ray observations, the signal is proportional to density squared and any clumps along the line of sight can lead to potential boosts in the signals. Eventually, for sources with redshifts of $Z \gtrsim 0.1$, the signals of gamma-rays with energies of $\gtrsim 100$ GeV will be affected by absorption and pair-production as the high energy gamma-rays interact with diffuse extragalactic background light (EBL). For cosmic ray positron experiments, however, only relatively local substructure is important since the range of high energy positrons is limited to several kpc.

For indirect detection, the amount and impact of substructure is quantified as the *boost factor* B, which is the ratio of the flux from a halo with all its subhalos to the flux the halo would have if it only had a smooth, virialized component. It is useful to differential substructure into two different categories: substructure that is self-bound, typically called subhalos; and substructure that is the un-virialized debris of tidally stripped subhalos. For the typical indirect searches, what matters most is the properties of subhalos—the variations in density induced by tidal debris is not significant [74]. Simulations find that the subhalo mass function is approximately $dN/dm \sim m^{-1.9}$ down to the resolution limit of the simulations (on the order of 10^3 solar masses for present N-body simulations). It is important to note that the mass function is unconstrained for masses smaller than this resolution limit, even though substructure is expected to continue for up to ~ 10 orders of magnitude from this point down to the typical WIMP free-streaming and kinetic decoupling scale [75, 76]. Since the substructure of galaxy clusters includes a number of objects more massive than this resolution limit (including Galaxies, Dwarf Galaxies, and even Galactic substructure), we can, with a high degree of confidence, attribute a substantial boost factor to these objects. For smaller subhalos, like those hosting dwarf galaxies, the amount of substructure is probably much lower and there is scant observational data indicating subhalos. Current thinking is that B is likely of order unity for Milky Way dwarf galaxies, but $B \sim 100 - 1000$ for galaxy clusters, depending on the precise form of the subhalo mass function below simulaion resolution limits [77, 78, 79, 80].

Even for CDM-only-models, simulations show that substructure can be destroyed by dynamical friction, especially in the inner parts of galaxies where the the boost factor is not significant. But, once again, the inferences from dark-matter-only simulations may be substantially modified by the presence of interacting, baryonic matter. Specifically, the presence of centrally concentrated baryons greatly affects tidal stripping of subhalos. Subhalos passing through disk galaxies may also undergo substantial tidal disruptions. It is predicted that the amount of substructure near the centers of halos should be significantly reduced with respect to simulations that only contain CDM [81, 82, 83, 84].

One significant way that Baryonic matter could change our expectations for indirect detection signals is that dark-matter subhalos could preferentially be destroyed in the plane of the Milky Way disk [85, 86], boosting the local density as well as the relative speed between WIMPs and the Sun, and perhaps dramatically enhancing the solar WIMP signal. However, more recent, high resolution simulations do not find evidence of a significant *dark disk*.

We note that in the case where dark matter has a strong elastic self-interaction, the interactions between particles drive the halo toward isothermality. This means that there is a core at the center, the velocity distribution is well modeled by a Maxwell-Boltzmann distribution near the center, and substructure tends to get erased [87, 88]. This implies slightly smaller boost factors due to substructure (although the subhalo mass function itself is not significantly altered, especially near halo outskirts), but this effect has not been quantified as yet. For solar WIMP searches, this implies that the simplest assumptions made about the local phase-space density (Maxwellian distribution) are especially reasonable for strong dark-matter self-interactions.

The Dark Matter Velocity Distribution:

In the simplest WIMP models the annihilation flux is mostly *s-wave*, and independent of the relative velocity between annihilating particles, i.e., $\sigma v \sim a$. As mentioned above, then the flux from DM annihilations varies through the halo tracking the square of the density, which is expected to be larger at the center of the halo or in the dwarf Spheroidal satellites of the Milky Way [89]. When the annihilation is velocity dependent, however, the flux is also affected by the distribution of DM particle velocities, which depends on the location in the halo. For instance, for the same density profile, a p-wave annihilating DM gives a shallower distribution of the halo flux [90] and results in a different power spectrum for the diffuse cosmological signal [91]. In the case of Sommerfeld enhancement, the flux is greatly increased towards the center of the halo due to smaller DM velocities [92].

The resolution of numerical simulations has increased dramatically in recent years, but the number of particles is still too small to sample the possible velocities at each point in the synthetic halo. However, there has been some progress in characterizing the velocity distribution in the solar neighborhood.

To estimate the velocity distribution at the particular location of the solar system, an average over 100 randomly distributed sample spheres centered at 8.5 kpc was performed in [93] to capture about 10^4 particles among the billion particles in *Via Lactea II*, an N-body simulation of a Milky-Way-size galaxy. The results provide insight into the non-gaussian shape of the velocity distribution and on the influence of substructure.

An analysis of a large number of halos from the Rhapsody and Bolshoi simulations was used in [94] to find an empirical model to the velocity distribution. Nevertheless, a subsequent study by the same authors concluded that the results of different experiments cannot be directly compared, even when restricting to a single parametrized model of the VDF [95].

A promising strategy is to use VDF-independent methods, which only compare the region of $v_{\rm min}$ probed by each experiment [96, 97]. We note that for solar WIMP searches, the expected signal is far less sensitive to sub-parsec variation in the density and velocity distribution (currently unquantified by simulations) than direct searches are.

3.2.1 Observational Constraints and Uncertainties in Halo Models

Observations of Milky Way dwarf galaxies: The Milky Way is known to host at least two dozen satellite galaxies. About half of those were discovered in the Sloan Digital Sky Survey using color-magnitude-diagram filtering techniques (e.g., [98, 99, 100]). The SDSS galaxies (with the exception of CanVen I [101])

are extremely faint, and thus were only detected because they were so nearby. This implies that there could be a large number of other dwarf galaxies in the Milky Way halo that we do not yet have the sensitivity to find [102, 103]. Big, deep wide-field surveys like the Dark Energy Survey and, critically, LSST, should find more. In particular, it is likely that we should find substantially more galaxies in the southern hemisphere, since this area was not explored with SDSS. Even with conservative assumptions about the boost factor, the resulting stacked Milky Way dwarf analysis (with these additional objects) will provides annihilation cross section constraints that are competitive with Galactic Center constraints, but with no foreground systematics [104, 105].

The predicted gamma-ray signals from Dwarf galaxies are less sensitive to the detailed distribution of dark matter since, unlike the Galactic Center, for typical halo profiles most of the emission will be concentrated in an angular region that is not much larger than the width of the gamma-ray point spread function. Still, the dominant uncertainty for the dwarf limits is the dark-matter distribution. Using dynamical modeling, e.g. a Jeans analysis, one may use the line-of-sight velocities of individual stars in the dwarf galaxies to estimate the mass profile [106, 77]. There are two complicating factors, even if one assumes spherical symmetry both for the gravitational potential of the system and the distribution of tracer stars. First, the enclosed mass of the system is degenerate with the velocity anisotropy of the stars. It is difficult to break that anisotropy without proper motions, and those are often prohibitive to get for individual stars in the dwarfs. The one place at which the degeneracy breaks is at the half-light radius. Thus, we have a good idea of the average density of dark matter within one (or in the case of multiple stellar populations, a few [107]) specific fixed radii [108]. But the detailed density profiles are not that well constrained [109]. For example, there is some indication that several of the "classical" dwarfs have constant-density cores [107, 110]. The second complicating factor is that many of these galaxies simply do not have enough stars for detailed modeling. For some of these objects the resulting density-profile estimates will always be limited by the small number of measurements, even with the advent of thirty-meter telescopes and the LSST. In addition to assumptions about isotropy used in modeling, or limitations in the available data on some objects, other systematics may also enter into the determination of the details of the halo distribution. One such systematic error, in fact a dominant one for many objects, is the effect of tidal forces on stellar kinematics, from past interactions of Milky-Way satellites with the Milky way disk. A number of objects now show long tidal tails indicating close encounters with concentrations of matter in the Milky Way. The spread in velocities in these tidal tails (sometimes hidden along the line of sight direction) bias the mass estimates derived using the Jeans equation, which may only be rigorously applied to equilibrium systems. We also note that other dynamical equilibrium methods, distribution function and Schwarzschild modeling, have also been applied to the Milky Way dwarfs for mass profile inference [111, 110, 112]. While these more detailed analyses of the distribution functions are not as susceptible to the simplifying assumptions made in a simple Jeans analysis, it is impossible for any method to fully compensate for the limited number of velocity measurements or the unknown effects of tidal disruption.

Additional stellar kinematic data will help estimate the magnitude of tidal effects, to determine whether the galaxies are tidally disturbed to the point that equilibrium modeling breaks down. Another key element of current work has been the development of equilibrium modeling techniques aimed at properly handling multiple stellar populations, which has an impact on determining the appropriate range of models for both the dark-matter and stellar distributions. There is an ongoing debate over a single key point, with a significant bearing on expected dark matter signals: whether the density profile is cusped (with an NFW-like profile down to small radii) or cored (with a constant density central region that may reduce the line of sight integral of $\rho^2(r)$ compared to a cusped halo of similar mass. For most cases, either type of profile can provide an adequate fit to the data, but for several Milky Way dwarf galaxies, there is fairly good evidence for cored density profiles. But such cored profiles are not produced by CDM-only N-body simulations, and the origin of such profiles is still poorly understood. The two likely candidates for driving cores are either baryonic feedback or new dark-matter physics. The latter is intriguing in the context of this report.

Observations of the Milky Way: The brightest DM source for conventional WIMP dark matter is expected to be the Galactic Center, but astrophysical backgrounds and uncertainties in the inner halo profile result in relatively large uncertainties in the dark matter sensitivity when compared with other sources, like the dwarf galaxies discussed above. [76, 113]. A large number of astrophysical foregrounds in the direction of the Galactic Center must either be removed from the region of interest or included (as an additional contribution to the background) in sensitivity calculations. Most of these foregrounds (e.g., emission from supernova remnants, or molecular clouds illuminated by cosmic-rays) have high energy $E > 100GeV$ spectra steeper than $E^{-2.2}$, significantly different from the expected spectrum of dark matter annihilation which, to first order, appears as a hard power-law $\sim E^{-1.5}$ with an exponential cutoff near the neutralino mass. But there are a few astrophysical sources with similar spectra, especially at somewhat lower energies (in the 1-10 GeV regime measured by *Fermi*). At these lower energies, a particularly troublesome background comes from pulsars which have energy spectra and Galactic distributions not dissimilar to dark matter [114, 115]. Fortunately, all of these foregrounds, whether they are from diffuse cosmic-rays or point sources, are significantly reduced at the higher energies observed with ground-based telescopes. Moreover, ground-based telescopes have very good angular resolution allowing many of these sources to be identified and removed from the regions-of-interest for dark matter searches. We discuss in what follows present upper limits on the GC that exclude the astrophysical point source at the center, and other resolved structures near the center. Even with this relatively minimal subtraction of astrophysical foregrounds, present dark matter limits fall within an order of magnitude of the natural cross-section. Thus, while these backgrounds somewhat reduce the sensitivity of GC observations, the relative strength of the GC signal is high enough to largely compensate for these backgrounds (at least in determining upper limits).

Implicit in the assumption that the GC is a much stronger source than other more distant halos is that the density profile of dark matter follows a power-law ("cuspy") profile down to the inner few kpc. While this expectation follows from CDM-only N-body simulations, there is little observational evidence either directly supporting or contradicting this. Two factors make it difficult to obtain good observational constraints on the DM profile in the GC region. First, since the mass and the gravitational potential within the solar circle are dominated by baryons the impact of the inner DM halo profile on dynamical measurements (e.g., velocities of molecular clouds or stars) is minimal. Second, since we are viewing the GC from within the Milky-Way disk, projection effects and foregrounds make it particularly difficult to determine the inner rotation curve for our own Galaxy compared, for example, to other nearby spiral galaxies. Even local estimates of the dark-matter density at the position of the solar system have substantial systematic errors. Therefore, our understanding of the inner halo-profile of the Milky Way (and hence our inferences about the brightness of the GC) must be based almost entirely on N-body simulations. These simulations show a relatively universal power-law cusp of dark matter in the centers of dark matter halos on various scales. While these results are probably robust down to $\sim$1 kpc scales, to quantify the dark matter profile in the inner Galaxy one must extrapolate these results well below the resolution limit of current simulations. The presence of baryonic matter may lead to large enhancements or reduction in signals. Perhaps the only observational reassurance we have in assuming that the cusp extends down to the inner parsecs of the GC is that stellar distributions in spiral galaxies also show such power-law cusps, and, to a crude first-order approximation, these stars are effectively non-interacting particles that should behave in a similar way to dark matter particles. However, other galaxies (including giant elliptical and Dwarf galaxies) do not show such stellar cusps. (For a nice review see [116].)

Observations of Galaxy Clusters: Galaxy clusters are observed to have density profiles consistent with those predicted in CDM-only simulations, except within the inner $\sim$ 50 kpc. These inferences are based on X-ray surface-brightness modeling, stellar kinematics of the brightest cluster galaxy, and weak and strong lensing [117, 118, 119, 120]. Their concentrations are approximately what one would predict from CDM simulations. There are estimates of the subhalo population (the subhalos hosting observed galaxies) [121, 122].

The potential multi-wavelength signals from dark matter have been discussed in the context of galaxy clusters including at gamma-ray (e.g., [123, 124, 125]), radio [126, 127], and X-ray [128, 129] wavelengths. In particular, clusters are good targets for searches for secondary inverse-Compton (IC) or synchrotron radiation signals due to the fact that the high energy electrons and positrons produced in dark matter annihilation or decay events are typically expected to lose energy through these processes much faster than the time needed for them to diffuse out of the cluster [127], making diffusive losses insignificant (compared to smaller systems like dwarfs). Gamma-ray observations of cluster also give comparably strong constraints on the dark matter decay lifetime given the associated J factors (see e.g. Ref.[130, 124]).

3.3 Halo Benchmark Models

The assumed form for the halo density profiles typically follow from fits to numerical N-body simulations. The parameterization of these fits varies, based, at times, on a parameterization used for stellar distributions (e.g., the Hernquist models), at other times based on profiles with desirable analytical features such as a finite total mass or well-defined phase-space distribution. The exact parameterization tends to have an unintended impact on the estimated flux, since this functional form often is used to extrapolate density profiles to the inner ∼100 parsecs of halos, where stellar velocity or rotation curve measurements become unreliable, and below the resolution limit of current N-body simulations. In order to address these limitations, we advocate adopting benchmarks that bracket the range of possibilities, and allow us to marginalize our estimates over what, for estimates of ID sensitivity, is a nuisance parameter. The best choices for such benchmarks are probably a cusped halo profile (like the NFW profile) and a cored profile. For measurements of p-wave, or Sommerfeld-enhanced cross sections, the velocity distribution should be determined from the density distribution in a self-consistent manner. For most of our sensitivity curves, the NFW profile is the de-facto benchmark distribution. Here we describe some other possible choices for the halo profile.

The particular shape of the density profile can be inferred from observations of stars tracing the gravitational potential of the halo or from numerical N-body simulations. Although simulations favor a universal cusped profile, some sub-galactic sized objects are better described by assuming the presence of a central core. We, hence, consider both cusped and cored distributions.

NFW profile

The Navarro, Frenk, and White (NFW) profile provides a good fit to DM-only N-body simulations over a wide range of halo masses [131].

The NFW profile is given by the equation:

$$\rho_{\rm nfw}(r) = \frac{\rho_0}{(r/r_s)(1+r/r_s)^2} \tag{9}$$

where r_s is the scale radius of the halo, M is the total halo mass and the remaining free parameter, the scale density ρ_0 can also be written in terms of a concentration parameter c defined as the ratio of the scale virial radius $R_{\rm virial}$ to the scale radius r_s. The relationship between ρ_0 and c can be shown to be:

$$M = 4\pi\rho_0 r_s^3 \left[\ln(1+c) - \frac{c}{1+c}\right] \tag{10}$$

To model a dwarf Spheroidal (dSph) satellite of the Milky Way with an NFW profile, we note that observations are consistent with the known satellites having a mass of about $10^7 M_\odot$ within their central 300 pc [132], while a scale radius $a = 0.62$ kpc fits the observed radial velocity dispersion of the stars [89]. The

total mass of the dSph dark matter halos is difficult to determine, since their extent beyond the observed stellar distributions is largely unknown [133]. Hence, $c = 4.8$ in eq. (10), which is substantially lower than the typical values $c \sim 20$ for halos of this size found in simulations [134].

3.4 Einasto profile

In addition to describing the luminosity profiles of early-type galaxies and bulges and the surface density of hot gas in clusters, the Einasto profile is as good a fit as the NFW profile, if not better, to simulated galaxy-sized dark matter halos.

The Einasto density profile is based on the observation that the logarithmic slope of the density profile, $d\ln\rho/d\ln r$ appears to vary continuously with radius can be written as

$$\frac{d\ln\rho}{d\ln r} = -2\left(\frac{r}{r_{-2}}\right)^{1/n} \tag{11}$$

where r_{-2} is the radius at which the logarithmic slope is -2 and n is a parameter describing the degree of curvature of the distribution.

$$\rho_{\rm einasto}(r) = \rho_s e^{-2n\left[(r/r_s)^{1/n}-1\right]} \tag{12}$$

As an example of the parameters for this model, consider the case of the Segue 1 dwarf. Here the parameters $\rho_s = 1.1\times10^8\,M_\odot{\rm kpc}^{-3}$, $r_s = 0.15kpc$ and $n = 3.3$ provide a good fit to the data [135]

3.5 Burkert profile

The fact that the best NFW fit to the observations of dSphs can be far less concentrated than expected from simulations suggests that the NFW profile provides a poor fit to the dynamics of some dSphs. In particular, detections of distinct stellar sub-populations provide mass estimates at different radii for Fornax and Sculptor that are consistent with cored potentials, but largely incompatible with cusped profiles [136, 137].

The Burkert profile is a cored profile that appears to provide a good fit to the DM distribution in dSph galaxies [138]. This model was developed by Burkert to capture the observation that some halo profiles appear to have flat inner density profiles, that role over into an outer r^{-3}. The Burkert profile is given by the expression

$$\rho_{\rm burkert}(r) = \frac{\rho_0 r_s^3}{(r+r_s)(r_2+r_s^2)} \tag{13}$$

where ρ_0 is the central density, and r_s is a scale radius.

A scale radius of $r_s = 650$pc and $\rho_0 = 1.8\times10^8 M_\odot$ in 13 were found in [139] to fit the kinematics of Draco.

4 Current and Future Indirect Detection Experiments

In this section we overview current experiments with a significant U.S. involvement, for which indirect detection is a large part of the overall scientific program. We do not try to survey all instruments, and omit a number of important experiments which are primarily led by non-US international collaborations.

4.1 Charged Cosmic-Ray/Antimatter Experiments

Dark matter could annihilate through a number of channels (quark-antiquark, W and Z or heavy leptons) with a similar branching ratio. These annihilation channels can ultimately produce cosmic-ray particles including protons and antiprotons and even deuterons and antideuterons. Annihilation to lighter leptons (in particular electrons) is also possible, but will generally be helicity suppressed unless some other mechanism contributes such as internal bremsstrahlung, or some new light mediator that could give rise to a Sommerfeld enhancement.

The transport of cosmic ray particles can be described by a combination of spatial diffusion, energy gains and losses, losses and gains in the number of a given particle species due to interactions with the ISM, and escape from the source region or galaxy. Since cosmic-rays are charged particles, to a good approximation, the random magnetic fields in the Galaxy randomize their directions hiding their directions. However, a small anisotropy may remain due to contributions from local sources. Unlike gamma-ray and neutrino observations of dark matter signals that would point back to the centers of galactic halos or to the sun, the identification of a dark matter signal from cosmic rays requires the detection of a spectral feature that stands out against the background. The best signal to background ratio is likely to be obtained for cosmic ray antimatter, which is produced in roughly equal proportions in DM annihilation, but subdominant in the production at cosmic ray sources such as supernova remnants.

4.2 Cosmic-Ray Positron Measurements

The recent measurement of the cosmic-ray positron fraction by the AMS-02 magnetic spectrometer on the International Space Station [10] confirms (with excellent precision) earlier measurements that showed a positron fraction, $e^+/(e^+ + e^-)$, increasing with energy from 0.05 at 10 GeV to 0.15 between 200 and 350 GeV. It is well known that some cosmic-ray positrons must be created in interstellar space as secondary products of interaction of cosmic-ray nuclei (mostly protons and helium nuclei) with nuclei of the interstellar medium (mostly hydrogen and helium). However, widely used models of propagation of cosmic rays in the Galaxy[35] predict that such secondary positrons would give a positron fraction falling in this energy range from about 0.04 to less than 0.03. Thus, other explanations for the rising positron fraction must be considered. Here we consider several possible explanations for the positron excess:

- *Dark matter:* Perhaps the most interesting explanation for the rising positron fraction would be that these positrons originate in the decay or annihilation of dark matter [140, 141]. Since such positrons cannot have energy greater than the rest mass of the dark-matter particles, if the AMS-02 positrons are interpreted as due to dark matter, those dark-matter particles must have mass greater than 350 GeV. Furthermore, as pointed out in §2 there must be a large boost in the dark matter signal caused by an enhancement in the present day cross-section (e.g., due to a Sommerfeld enhancement), a mechanism to suppress the large (but unobserved) channel for annihilation to antiprotons and an enhancement in the astrophysical factor due, e.g., to a nearby dark matter clump. Any such boost in the cross-section for annihilation to electrons would produce an even larger source of electrons and positrons in the galactic center. These electrons and positrons would produce a large radio synchrotron and gamma-ray inverse Compton signal that should be readily detected. Upper limits on these signals seem to already strongly contradict a dark matter interpretation for the excess.

  AMS-02 is capable of identifying cosmic-ray positrons with energy up to ∼1 TeV; currently the AMS-02 positron fraction is limited to energies below 350 GeV by the low flux of particles at higher energy. With

several more years of data, that instrument should be able to extend its determination of the positron fraction to energies close to 1 TeV. Despite the difficulties with a dark matter interpretation discussed above, if the positron fraction should display an abrupt decrease at some energy, E, between 350 GeV and 1 TeV, one would certainly take a closer look at the possibility of a dark matter source for the positrons since none of the astrophysical explanations for the observed positrons (summarized below) would produce such an abrupt decrease. Since such leptonic annihilation channels must also result in gamma-rays (either as final-state radiation, internal bremsstrahlung, or inverse-Compton emission) ground-based gamma-ray observations (with there good sensitivity about a few hundred GeV) should readily detect the expected gamma-ray signal – if not with the current generation experiments, certainly with future gamma-ray instruments.

In any event, lacking an abrupt drop in the positron fraction, it would be very difficult to attribute the observed positrons to dark matter with any confidence, since there are several plausible astrophysical mechanisms for producing them, including primary positrons produced near pulsars, secondary positrons produced in the normal cosmic-ray sources and accelerated there, and secondary positrons produced in the interstellar medium with that production modeled in a manner different from the widely used cosmic-ray propagation model.

- *Primary positrons from pulsars:* Electrons can be accelerated in a pulsar magnetosphere and induce an electromagnetic cascade through the emission, by curvature radiation in the pulsar, strong magnetic field, of photons above threshold for pair production. Acceleration of the positrons thus produced can yield a hard spectrum that could account for the rising positron fraction. Many papers have discussed this possible origin of the positron excess (e.g. [142, 143, 144]).

- *Secondary positrons produced in the sources:* In addition to the secondary positrons produced by cosmic rays interacting in interstellar space, there are likely to be secondary positrons produced by interactions with material in the source regions. These secondary positrons would then participate in the same acceleration process that produces cosmic-ray protons and electrons. The positrons thus accelerated are likely to have a harder spectrum than the Galactic secondaries calculated by Moskalenko & Strong and could thus account for rising positron fraction [145]. As Blasi stated, "*This effect cannot be avoided though its strength depends on the values of the environmental parameters during the late stages of evolution of supernova remnants.*"

- *Modifications of the widely used model of Galactic cosmic-ray propagation:* Four approaches, each different from the others, have been proposed that account for the observed rise in positron fraction above 10 GeV as being due entirely to secondary positrons produced as the cosmic-ray nuclei propagate through the interstellar medium.

  One approach ignores the details of propagation models and simply assumes that positrons are produced at the same places as secondary nuclei like boron (which is the fragmentation product of carbon, oxygen, and other heavier nuclei interacting with interstellar gas). From the ratio of production of positrons to production of boron, one infers an upper limit to the positron fraction. (It is an upper limit because it ignores energy loss processes suffered by positrons but not by nuclei.) The upper limit thus calculated matches the peak of the positron fraction observed by AMS-02. [146, 147]

  Another approach notes that the Moskalenko & Strong model of Galactic cosmic-ray propagation is cylindrically symmetrical, but in fact cosmic-ray sources are likely to be concentrated in the spiral arms of the Galaxy. Taking into account energy loss of primary cosmic-ray electrons from those sources, while noting that secondary positrons are produced from primary nuclei that are distributed more uniformly throughout the Galaxy, a model has been developed that produces a rising positron fraction above 10 GeV [148]. (It must be noted, however, that another calculation of Galactic cosmic-ray propagation, in which the spiral structure is incorporated, fails to match the observed positron fraction without invoking some primary positron source.)

A more radical modification of the commonly used Galactic propagation model invokes the "Nested Leaky Box" model [149]. In this model boron and other nuclear secondaries are primarily produced in "cocoons" around the sources, from which escape is energy dependent, going as $\sim E^{-0.6}$, while the positrons, which are produced by interactions of protons and other nuclei of much higher energy, are mainly produced outside the cocoons, in the general Galaxy from which escape is energy independent. In this model, one can easily reproduce the observed positron fraction over the entire energy range for which we have observations, from 1 to 350 GeV [150, 151]

- Another possible explanation of the apparent tension between the observed positron excess and propagation models might lie in the simplifying assumptions that are currently made about magnetic field structure, diffusion and energy losses made in cosmic-ray propagation models. For example, Kistler, Yuksel and Friedland [152] looked at the implications of the hierarchical structure of the Milky Way magnetic field on cosmic-ray propagation. They argue that for positrons, the diffusion approximation to charged-particle propagation is simply inappropriate.

  Although a more detailed discussion lies beyond the scope of this document, we wish to emphasize the crucial role played by diffusion and energy losses uncertainties in cosmic-ray propagation models. We point the interested reader to, e.g., Ref. [153]. The importance of future cosmic-ray experiments in pinpointing critical observables such as secondary-to-primary ratios and unstable-to-stable isotope ratios cannot be overemphasized.

4.2.1 VERITAS Positron and Electron Measurements

Cosmic ray electrons and positrons provide a unique astrophysical window into our local Galaxy. In contrast with hadronic cosmic rays, electrons and positrons lose energy quickly through IC scattering and synchrotron processes while propagating in the Galaxy. These processes effectively place a maximum propagation distance of ∼1 kpc for electrons with ∼TeV energy[154]. Prior to H.E.S.S.[155] all cosmic ray electron measurements came from balloon-based and satellite-based experiments. The effective area of IACTs is 5 orders of magnitude larger and thus offers a method to extend the spectrum to higher energies. The electron+positron spectrum is now measured by the *Fermi*-LAT[156] from 7 GeV to 1 TeV and by H.E.S.S.[155, 157] and MAGIC[158] from 100 GeV to 5 TeV (a VERITAS result is forthcoming). These overlapping results agree within statistical+systematical uncertainties and give evidence of an additional harder component within the spectrum that is not accounted for in our standard picture of the local environment. This additional piece becomes significant at ∼30 GeV and steepens above ∼700 GeV.

IACTs have the ability to extend the positron fraction spectrum to higher energies. To measure the positron flux, IACTs can utilize a combination of the Earth's geomagnetic field with the cosmic ray moon shadow to create a spectrometer. This technique was developed by the Artemis[159, 160] experiment using data from the Whipple 10m telescope to search for the anti-proton shadow. While all IACTs currently collect data in some moonlight conditions, the positron ratio measurement is particularly difficult because it requires observations within a few degrees of bright moon phases (up to ∼50%, where the phase represents the fraction of the moon lit by the sun). In these conditions the background rates are very large and the potential to damage the sensitive PMTs is very real. To alleviate this, VERITAS has developed filters that cover each of the four cameras and let in the peak of the Cherenkov spectrum, 250-400 nm, while rejecting the bulk of the reflected solar spectrum. MAGIC [161] is also attempting this difficult measurement and estimates that it will require 50 hours spread over several years to accomplish, assuming that the missing flux is on the order of a few percent.

4.2.2 Future Cosmic-Ray Antimatter Measurements

The cosmic-ray antiproton spectrum has been measured from balloons and satellites between 60 MeV to 180 GeV [162]. Secondary antiprotons are created as cosmic rays propagate through the Galaxy, and the flux of these antiprotons is very sensitive to the propagation processes of cosmic rays. Above $\sim$ 10 GeV, the $\bar{p}/p$ ratio from secondary production is expected to decline. Various new-physics scenarios can increase the $\bar{p}/p$ ratio above 100 GeV, with predictions up to 10^{-3} for contributions from dark matter [163] and up to several % for contributions from extragalactic sources, such as antigalaxies [164]. Antiprotons can also be produced by primordial black hole evaporation [165]. Existing measurements up to $\sim$ 180 GeV are consistent with secondary production. Atmospheric Cherenkov telescopes have the effective area to make an important contribution in the 200 GeV to few TeV range, where to date only limits exist.

Electrons and positrons can likewise be produced by secondary processes during propagation or interaction in SNRs or pulsars, or via pair production in nearby pulsars. However, they can also be among the final-state products from annihilation of dark matter particles. The combined $e^+ + e^-$ spectrum from 7 GeV to 1 TeV has been measured by the *Fermi* satellite [166], and up to 6 TeV by HESS [155] and MAGIC [161].

Over the next decade, *Fermi* and CREST will measure the total $e^+ + e^-$ spectrum to several TeV [167], and CALET will measure it to $\sim$20 TeV [168]. AMS will extend its positron fraction measurement beyond 350 GeV, measure the total $e^+ + e^-$ spectrum to 1 TeV or beyond, and provide a precise measurement of antiprotons. The AMS team estimates that with an 18-year exposure, the sensitivity to the anti-helium/helium ratio will reach 10^{-4} in the 400 GV to 1 TV range. The sensitivity improves rapidly with decreasing rigidity, reaching 10^{-9} for energies below 50 GV. AMS will measure the charge-separated e^+ and e^- spectra up to several hundred GeV.

CTA will complement these satellite- and balloon-based instruments by providing a high-precision combined $e^+ + e^-$ spectrum from $\sim$100 GeV to $\sim$100 TeV, well beyond the range feasible for satellite- or balloon-based experiments due to their limited effective area. CTA can also provide strong constraints on large-scale anisotropies (an important signature in distinguishing source models) in the $e^+ + e^-$ spectrum by comparing flux measurements made in opposite directions on the sky [169]. CTA will also measure the charge-separated electron, positron, and antiproton spectra using the Moon's shadow and the geomagnetic field, a technique pioneered by ARTEMIS [170] and more recently pursued by MAGIC [171, 161] and VERITAS.

The US extension to CTA will is anticipated to be an array of 25-36 mid-size telescopes (MSTs) with 8° diameter field of view and cameras instrumented with SiPMs. The US extension of MSTs provides three important advantages for these measurements. First, an increase in the point-source sensitivity by a factor of 2-3 in the energy range ($\sim$1 TeV) where CTA can contribute best to the positron spectrum measurement [172]. Second, SiPMs (unlike PMTs) are not endangered by bright moonlight, so observations can be made under a wider range of conditions and a greater overall sensitivity can be achieved. Third, the improved optical point spread function and smaller pixel size of the innovative dual-mirror design planned for the US extension enables improved hadronic/electromagnetic shower discrimination. This is important because hadron showers are much more numerous than electron and positron showers and even a small fraction of residual background can present a significant challenge to these measurements.

Instruments on balloons, satellites, and on the ground will provide important new measurements of charged cosmic particles over the next decade, extending the surprising discoveries that have generated a great deal of excitement among particle physicists in the past few years. These new measurements are essential to distinguishing among the many competing models. Charged particles are an important component of indirect dark matter searches, complementing gamma-ray and neutrino measurements. CTA will contribute unique measurements of cosmic electrons, positrons, and antiprotons at the highest energies.

4.2.3 GAPS Anti-Deuteron Search

About a decade ago it was pointed out that antideuterons produced in WIMP-WIMP annihilations ("primary" antideuterons) offered a potentially attractive signature for cold dark matter (CDM) ([173] hereafter DFS). The reason is that the flux of primary antideuterons is fairly flat in the 0.1 to 1.0 GeV/n energy band, while the "secondary/tertiary" antideuterons, those produced in cosmic ray interactions in the interstellar medium (secondaries) and subsequent reprocessing (tertiaries), have fluxes that sharply decrease with decreasing energy. The lower antideuteron background results because of the higher cosmic-ray energy required to create an antideuteron compared to an antiproton, combined with a cosmic-ray spectrum steeply falling with energy. In addition, the collision kinematics disfavors the formation of low-energy antideuterons.

Despite the low astrophysical background and a signature which is rather generic in many "beyond-the-Standard-Model" models, there has been no dedicated, optimized search for antideuterons. An upper limit on antideuterons was obtained by the BESS experiment [174], but it is three orders of magnitude higher than the interesting range for dark matter searches. The AMS experiment on the ISS has sensitivity for antideuterons [175], but other complementary experiments, optimized for making a clean measurement of antideuterons are being considered. Just such an optimized search for antideuterons has been proposed, the General Antiparticle Spectrometer experiment (GAPS) [176], and it recently had a successful prototype flight [177].

It is important to understand the complementarity of different types of antideuteron measurements, as well as the complementarity of these measurements with direct and indirect detection experiments. There are a number of interesting hints of low-mass neutralinos in a number of direct detection experiments (DAMA/LIBRA, CoGent and CDMS). Since the detected events are very near threshold, at present it is difficult to make a convincing case for dark matter, rather than contamination of some new background. Because antideuteron searches are very sensitive to SUSY models that provide low mass neutralino candidates, their overlap with direct detection experiments is potentially of great utility. Together with *Fermi* observations of dwarf spherical galaxies which are also beginning to place strong limits on low-mass neutralinos (few tens of GeV), antideuteron measurements can provide an important corroborating role in the discovery (and identification) of a low-mass dark matter particle. Antideuteron searches are also generally sensitive to much higher neutralino masses than direct detection searches with massive target nuclei, thus also extending the reach to higher masses. AMS and GAPS have mostly complementary kinetic energy ranges, but also some overlap in the interesting low energy region, which allows the study of both a large energy range, confirming the potential signals, and the best chance for controlling the systematic effects. Another very important virtue comes from the different detection techniques of both experiments. AMS follows the principle of typical particle physics detectors. Particles are identified by analyzing the event signatures of different subsequent sub-detectors, also using a strong magnetic field. The GAPS detector will consist of several planes of Si(Li) solid state detectors and a surrounding time-of-flight system. The antideuterons will be slowed down in the Si(Li) material, replace a shell electron and form an excited exotic atom. The atom will be de-excited by characteristic X-ray transitions and will end its life by annihilation with the nucleus producing a characteristic number of protons and pions. The approach of using two independent experimental techniques is important in providing confidence in any potential primary antideuteron detection.

There are substantial uncertainties in predictions of the primary antideuteron flux. The dominant uncertainty in the primary flux is due to propagation uncertainties. During the next years the AMS high precision observations will tightly constrain the cosmic ray propagation parameters. However, some degeneracy in the parameters will most likely remain. There is also an uncertainty due to the halo model employed, but the antideuteron production is averaged over the halo and over fairly long scale lengths, so whether or not a cored or un-cored halo profile is used is somewhat reduced in importance. Recently, increasing attention has been paid to details of the hadronization process. In the coalescence model, the antineutron and antiproton

combine when their momentum difference is less than a critical value, the coalescence momentum, p_0. But since p_0 is smaller than the QCD phase transition temperature, there is a strong sensitivity to the hadronization model. Recent studies emphasize the need for event-by-event determination of the production rates and are probing the sensitivities when different hadronization models are employed [178, 179, 180]. While theoretical progress is made, the best way to pin down the production uncertainty is unquestionably to make a good accelerator measurement of p_0, given the considerable discrepancy in the various measurements. One possible source of uncertainty, which only drives up the expected primary flux, is due to the boost factor. It was previously fashionable to consider boost factors up to 100 times or more, but recent simulations seem to have definitively settled this issue, with boost factors in the range of 1-10 being the largest allowed [181] . However the sensitivity curves presented here assume no boosting effect (i.e., boost factor 1), and a factor of 2 or 3 in boost would provide very substantial reach into discovery space for a number of models presented here. Similar observations pertain to the secondary/tertiary background, except that in this case it is the production uncertainties that dominate [182]. Most of the secondary/tertiary antideuterons are produced in the Galactic disk, so the propagation is more local and thus less important. At any rate, for the antideuteron searches the nominal or optimistic propagation and production parameters are very promising for dark matter searches. The most pessimistic numbers would make prospects for detection problematic.

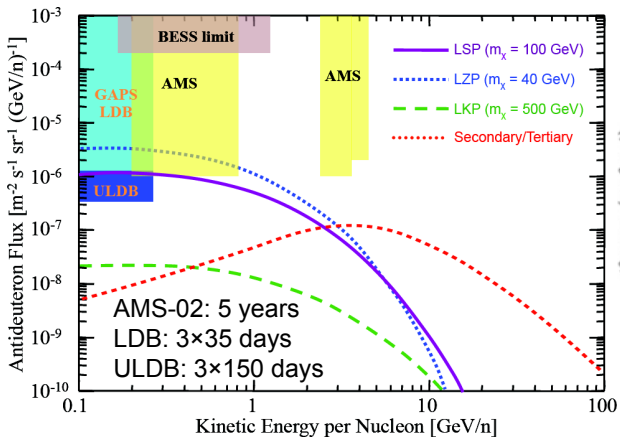

Figure 5: LSP, LKP and LZP models along with the antideuteron background and the sensitivity of GAPS, BESS and AMS (5 years) [183].

Figure 6 shows a scan of SUSY models overlaid on the sensitivity for a dedicated antideuteron search experiment under various scenarios. The experimental curves correspond to a generic GAPS-like experiment for balloon flights of various duration from a few to 10 months. This plot illustrates some of the opportunities as well as challenges of antideuteron searches. An ensemble of supersymmetric (SUSY) model parameters is shown, all yielding the same neutralino-annihilation cross-section and mass. To the right of the vertical green line are results from a low-energy minimal SUSY model, and to the left are shown results from a low mass non-universal gaugino model. The latter admits light neutralinos, which have recently been argued to provide a candidate for the controversial DAMA/LIBRA, CoGENT and CDMS II signals [184, 185, 186]. The red dots indicate parameter space in the WMAP preferred density range, while the blue dots correspond to models in which the thermally-generated neutralinos are subdominant. The gray models are ruled out by antiproton searches. It has been argued that it is important to search the entire parameter space, not just the WMAP preferred range, since there are many mechanisms to under-produce WIMPS in the early universe and still have them detectable today [187]. The solid and dashed lines indicate the sensitivity of

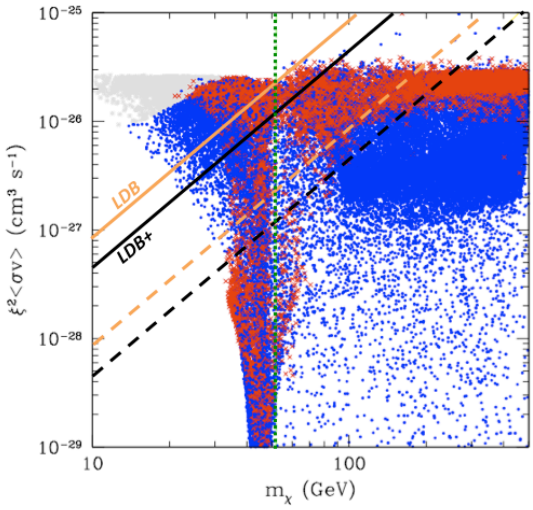

Figure 6: Sensitivity of a dedicated antideuteron experiment (diagonal lines) for long-duration balloon (LDB) and ultralong duration balloon (ULDB) flights; the green vertical line separates low mass non-universal gaugino SUSY models (left) from MSSM models. Solid (dashed) lines for the sensitivity correspond to median (high) antideuteron propagation models [183].

the antideuteron search for the case of nominal (solid) and maximal (dashed) propagation models. There are several points illustrated by this figure. Firstly, antideuteron searches are quite sensitive to models with low energy neutralinos, and they maintain sensitivity up high neutralino masses. Secondly, the plot illustrates both the opportunity and the curse of an antideuteron search, antideuteron propagation and production uncertainties. This is discussed more below, but we note here that the reach into parameter space for primary antideuterons is sensitive to details of the propagation (and less so the production) of the antideuterons in the interstellar medium, which are still poorly constrained. Thus, for the best case uncertainties, antideuterons provide a deep reach into parameter space. Conversely, compounding the most pessimistic values of the uncertainties can lead to a reach, in a short balloon observation, that is not much better than has been obtained for antiproton searches.

4.3 UHECR Measurements

Currently the strongest constrains on TD models and therefore heavy dark matter models with decaying particles come from limits on the flux of UHE photons from the Pierre Auger Observatory in Malargue, Argentina [188]

Although the contribution of X particles to the observed UHECR flux is now constrained to be subdominant, the existence of long-lived X particles continues to be viable below the current observation limits.

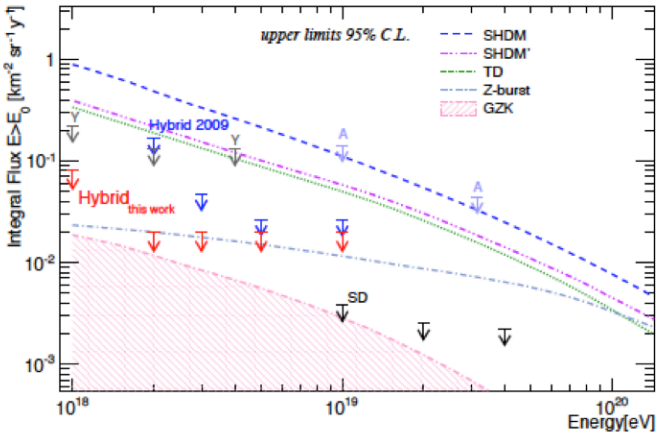

Figure 7: Figure from Ref. [189] showing Auger Surface Detector (SD) limits and Hybrid (SD and fluorescence events) limits. Also shown are predictions from models of super-heavy dark matter (SHDM), TD , Z-bursts, and the expected flux due to the GZK (Greisen-Zatsepin-Kuzmin) effect.

4.4 Gamma-ray Experiments

In regions of high DM density the annihilation (or decay) of WIMPs into Standard Model particles could produce a distinctive signature in gamma rays potentially detectable with ground- and space-based gamma-ray observatories. In fact, almost any annihilation channel will eventually produce gamma-rays either through pion production (for hadronic channels), or final state bremsstrahlung and inverse Compton from leptonic channels. Moreover, the spectrum from annihilation would be essentially universal, with the same distinctive shape detected in every DM halo. Unlike the signals that can be measured by direct DM detection experiments, the gamma-ray signature would provide strong constraints on the particle mass and help to identify the particle through the different kinematic signatures predicted for different annihilation channels.

The gamma-ray flux from DM annihilations scales with the integral of the square of the DM density along the line of sight to the source (the J-factor as defined in Eq. 2). Thus, the detectability of the DM signal from a given target depends critically on its DM density distribution, as well as on the possible presence of substructure along the line of sight. The ideal targets for DM annihilation searches are those that have both a large value of J and relatively low astrophysical gamma-ray foregrounds. These criteria have motivated a number of Galactic and extragalactic targets including the Galactic Center (GC), dwarf spheroidal satellite galaxies of the Milky Way (dSphs), and galaxy clusters. While the sensitivity to the DM halo profile provides the largest systematic uncertainty, it also provides an avenue for inferring the DM halo profile from the shape of the gamma-ray emission and connecting the detected particle to the missing gravitational mass in galaxies.

The GC is expected to be the brightest source of DM annihilations in the gamma-ray sky by several orders of magnitude. Although the presence of many astrophysical sources of gamma-ray emission toward the inner Galaxy make disentangling the DM signal difficult in the crowded GC region (see § 3.2.1), the DM-induced gamma-ray emission is expected to be so bright there that one can obtain strong upper limits at the level of the natural cross section $\langle \sigma\, v \rangle \sim 10^{26} \mathrm{cm}^3 \mathrm{s}^{-1}$. In addition, with the improved angular resolution of CTA, the astrophysical foregrounds can be more easily identified and separated from the diffuse annihilation signal.

Also, the large concentration of baryons in the innermost region of the Galaxy might act to further increase the expected DM annihilation flux by making the inner slope of the DM density profile steeper, a mechanism known as "adiabatic contraction" [190, 191, 192]. While the exact role of baryons is not yet well understood, new state-of-the art numerical studies of structure formation that include baryonic physics along with the non-interacting DM are beginning to provide valuable insights.

Since the astrophysical foregrounds in the GC make it difficult to unambiguously interpret any detected signal, it is important to identify other sources that combine the characteristics of high J values, but very low backgrounds. In the event of a detection from the GC, deeper observations of such sources could provide an important confirmation of any putative dark-matter signal. As discussed in § 3.2.1 the inner halo profile of the GC has large uncertainties that lead to significant (order-of-magnitude) uncertainties in the expected signal A promising class of objects for study are the dwarf spheroidal satellite galaxies of the Milky Way (dSphs).

dSphs are thus attractive for DM searches in gamma rays for a number of reasons including their close proximity, high DM content, and the absence of intrinsic sources of gamma-ray emission. These objects are also predominantly found at high galactic latitudes where the astrophysical foregrounds are much weaker. Because they are highly DM-dominated, the DM mass on small spatial scales ($\sim$100 pc) can be directly inferred from measurements of their stellar velocity dispersions. The uncertainty of the line of sight distribution of DM for these systems is therefore much less than for other candidates. Additionally, smaller DM subhalos may not have attracted enough baryonic matter to ignite star-formation and would therefore be invisible to most astronomical observations from radio to X-rays. All-sky monitoring instruments sensitive at gamma-ray energies, like *Fermi*-LAT, may detect the DM annihilation flux from such subhalos [193], while follow-up observations with CTA would characterize the distinctive spectral cut-off that would eventually determine the DM particle mass.

4.4.1 *Fermi*

The Large Area Telescope (LAT), the primary instrument on the *Fermi Gamma-ray Space Telescope*, launched in 2008, possesses unprecedented sensitivity in the GeV energy range. In the first weeks of operation, the LAT collected more gamma rays with energy > 100 MeV than all previous missions combined. The LAT is a pair-conversion gamma-ray detector. It has a modular arrangement of silicon strip trackers interleaved with tungsten converter foils (1.5 radiation lengths on-axis) above calorimeters with a hodoscopic arrangement of CsI crystals (8.5 radiation lengths on-axis). A 4×4 array of these tracker/calorimeter modules is surrounded by tiled plastic scintillators for charged-particle rejection. The LAT is approximately 1.8 m square, with a squat aspect ratio. Positron-electron pairs from gamma rays that convert in the tungsten are followed through the silicon strip tracker and into the calorimeter, where the light yield in the CsI crystals is recorded. This information is used in ground processing to precisely reconstruct the direction and energy of the incident gamma ray. The flux of celestial gamma rays is several orders of magnitude smaller than that of cosmic rays at the orbit of *Fermi* and the design of the LAT and the ground processing enables very efficient rejection of this background. The LAT is sensitive to gamma rays from 20 MeV to greater than 300 GeV with $\sim$10% resolution over much of that range. The effective collecting area peaks at about 8000 cm^2 at 10 GeV and the field of view is 2.4 sr. The per-photon angular resolution ranges from several degrees at 100 MeV to $\sim$ 0.1 deg at the highest energies (Atwood et al. 2009). The scanning and rocking pattern of the attitude control system of *Fermi* allows the LAT to observe the entire sky every 3 hours. The characteristics of the LAT make it an excellent instrument for the discovery of faint new gamma-ray sources.

Searches for gamma-ray signals from annihilation or decay of massive dark matter particles were a principal scientific driver for the *Fermi* mission. Searches in the LAT data have been undertaken in a variety of

ways, to try to maximize sensitivity and to overcome limitations from astrophysical foregrounds. The cross section limits obtained for annihilation necessarily depend on the assumed decay channels, e.g., through $b\bar{b}$, $\tau^+\tau^-$, W^+W^-, with gamma rays also produced via interactions of secondaries. The limits also depend on the assumed spatial distribution of particle dark matter. Theoretically well-motivated predictions for the distributions have a range of "cuspiness" for the cores; in addition substructure on the smallest scales can be very important to the overall annihilation rate because the rate depends on the square of the density. Such 'boost factors' are typically quite uncertain and limits for annihilation cross sections are generally conservatively quoted for unit substructure boosts. For the searches, templates of the expected gamma-ray emission for the assumed mass and annihilation channel and density distribution are compared to the LAT data. As discussed further below, annihilation can also be directly into two gamma rays. This would produce a spectrally-distinct signal (a narrow line) but the branching ratios are expected to be very small.

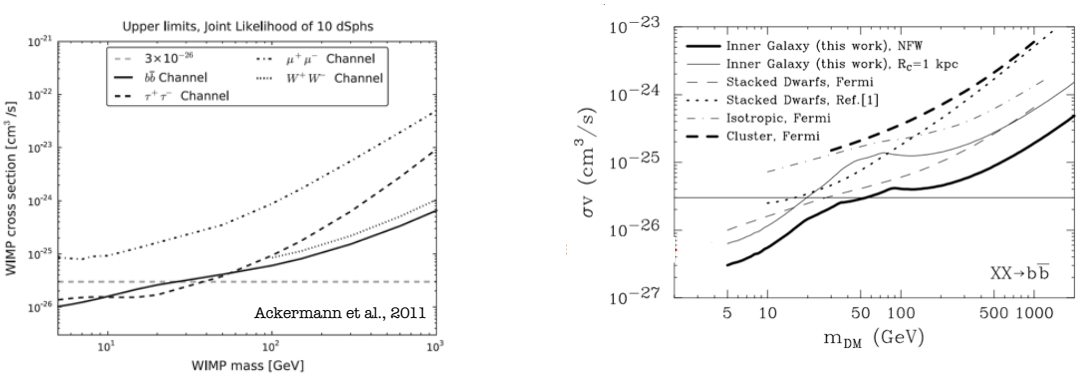

Figure 8: *Left:* Constraints on the total annihilation cross section derived by combining *Fermi* data on a number of dSphs [31] Dwarf stacking. *Right:* Compilation of *Fermi* DM constraints (courtesy D. Hooper).

The density of dark matter is greatest in the Galactic center (GC) region and the annihilation fluxes are expected to be greatest from the GC. However, the astrophysical foregrounds are extremely bright and challenging to model toward the GC. Conservative limits on the annihilation cross section have been obtained using the entire observed gamma-ray intensity as an upper limit for the dark matter signal. Less conservative limits have relied on (uncertain) modeling of the foreground astrophysical signals and/or masked the lowest-latitude regions where the foreground is brightest.

Searches for gamma-ray lines in the GC region suffer much less from foreground confusion. An analysis of publicly-available LAT data has reported evidence for a line-like feature near 130 GeV from the GC region. (The actual region analyzed was optimized for sensitivity to the assumed distribution of dark matter.) The implied cross section was much greater than expected theoretically. This finding has stimulated a number of follow-up studies, characterizing the potential systematics and looking for similar line-like signals from other directions, including galaxy clusters and the Sun.

The distribution of dark matter is expected to be clumpy on a wide range of scales and in particular the halo of the Milky Way should contain a number of massive sub-halos, which would themselves be sources of annihilation gamma rays. Some searches have looked for unidentified LAT sources that have the right spectral and spatial distributions. The most constraining limits have come from stacking analyses of observations of dwarf spheroidal (dSph) galaxies in the halo of the Milky Way. These are the largest sub-halos and are expected to be dominated by dark matter. Additionally, they host essentially no on-going star formation and

so have little non-thermal emission from astrophysical processes. The limits for annihilation cross sections from a joint analysis of the best-characterized dSphs are now below the thermal cross section limit for some energy ranges and annihilation channels.

A novel search for a dark matter signal in the isotropic gamma-ray background has been developed using the angular power spectrum to distinguish various extragalactic and Galactic foregrounds. The ultimate sensitivity of the method should be sufficient to detect a dark matter contribution to the isotropic diffuse spectrum at the several percent level.

4.4.2 VERITAS

Figure 9: The VERITAS IACT array.

The VERITAS IACT array[194], located in Southern Arizona, is an additional key contributor to the indirect search for particle dark matter. VERITAS is comprised of four, 12 meter diameter Davies-Cotton optical reflectors which focus light from gamma-ray air showers onto four 499 pixel photomultiplier tube(PMT) cameras. The array, with a total field of view of 3.5°, is sensitive in the range of 100 GeV to 50 TeV, easily covering a large range of parameter space favored by the SUSY models discussed previously. Since the commissioning of the array in 2007, VERITAS has accrued approximately 350 hours of observations on a range of putative dark matter targets including dSph galaxies, galaxy clusters and the GC. The analysis of these observations is ongoing, however, the results already published from subsets of the observations have resulted in some of the strongest DM constraints available from indirect searches. While VERITAS focuses on a range of potential dark matter targets such as the Galactic Center, and galaxy clusters; one of VERITAS' key contributions to indirect matter searches thus far has been in the study of dwarf spheroidal galaxies (dSphs).

The first VERITAS dSph results [195] were composed of observations of the dSph galaxies Draco, Ursa Minor, Bootes I, and Willman I. This result was based on a relatively small observational exposure (10-15 hours per source) and was significantly improved by the result of [135] in which over 50 hours of observation on the dSph Segue I was presented (Figure 2). While these limits do not constrain the most conservative realizations of minimal SUSY, the VERITAS dSphs limits (in particular the Segue I limits) provide much stronger constraints on alternative models of SUSY (for example, invoking a Sommerfeld enhancement at very high mass from W and Z exchange, or at a lower mass from a new scalar mediator [21]). Models with a kinetically enhanced cross section are already constrained by current VERITAS observations, and may be all but excluded over the next few years of VERITAS observations.

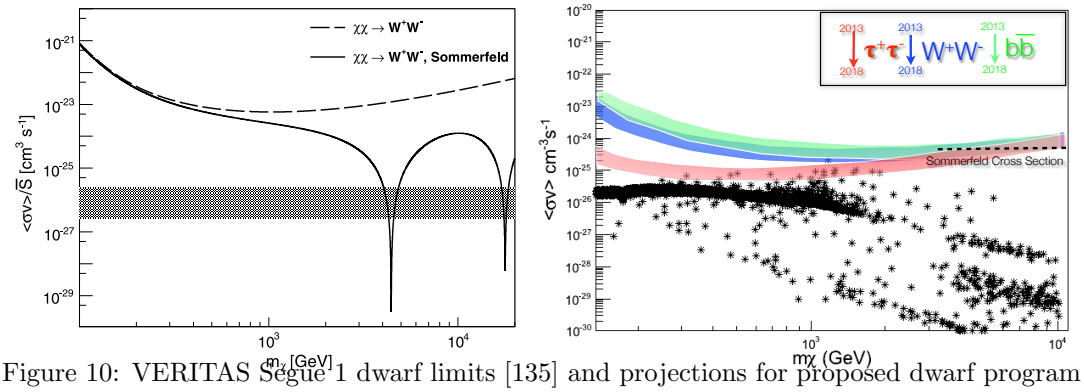

Figure 10: VERITAS Segue 1 dwarf limits [135] and projections for proposed dwarf program

Of particular importance, VERITAS dSph observations have now provided strong constraints on models of dark matter annihilation invoked to reproduce the PAMELA positron excess[9]. In these models, DM annihilates exclusively into $\mu^+\mu^-$ (leptophillic models). In order for these models to explain the PAMELA excess, a boost factor B is required (both astrophysical and particle physics boosts are convolved into B. The VERITAS Segue I observations places strong constraints on B, limiting the allowed parameter space that can be utilized to explain the PAMELA excess within a DM framework. These results are especially relevant in light of the recent results from the AMS experiment [10]. As with the constraints on $\langle\sigma v\rangle$, these limits will improve with additional observations.

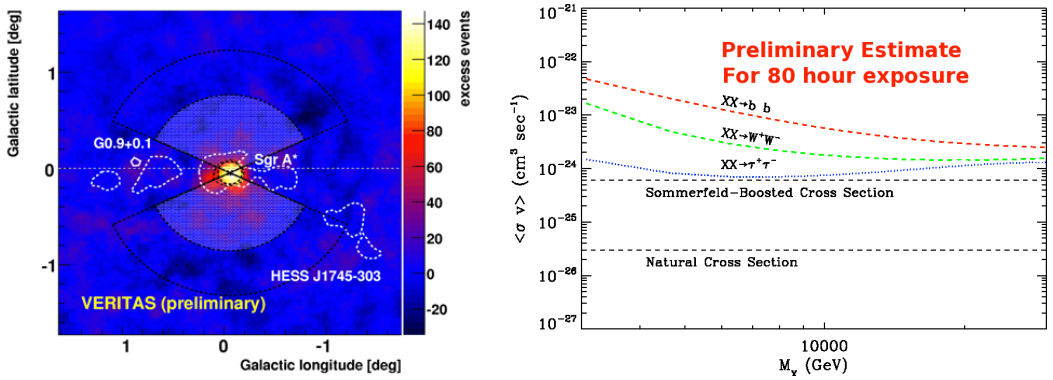

Figure 11: *Left:*VERITAS GC exposure showing the bright source at Sgr A*, and DM signal and background regions [196]. *Right:* VERITAS projected sensitivity for an 80 hr exposure (JB)

As observations for the VERITAS DM program are ongoing and will continue through the operational lifetime of the array, these constraints will only be improved with time. Recently, VERITAS has dramatically increased the time allocation for Dark Matter observations with a goal of acquiring ∼250 hours of data on Dwarf galaxies every year. This change represents an order-of-magnitude increase in observing time compared to that of previous published DM results. Together with the recent upgrade of VERITAS [197] (replacing the PMTs to realize a 50% increase in light collection efficiency), this will substantially improve DM sensitivity.

As shown in Figure 10, the anticipated dwarf galaxy limits with 5 years with VERITAS are surprisingly good, pulling within an order of magnitude of the natural cross-section, a result not significantly different from some predictions for CTA (e.g., the analysis of Ref. [198] for the baseline CTA instrument without the U.S. extension). There are a number of reasons why VERITAS (a current generation experiment) might be competitive with the baseline CTA instrument. First, VERITAS has made observations of dSph's one

of the highest priority science programs and should accumulate very deep dwarf exposures long before CTA is fully on-line and when other higher-priority scientific programs could dominate the CTA schedule (U.S. participation in CTA might change these priorities). Thus the large exposure time assumed in these limits reflects the higher priority of dark-matter science in the U.S. community compared with the European-led CTA consortium. Another significant factor comes from the fact that, of the currently known dSphs, the best candidates are in the northern hemisphere. In particular, the Segue 1 Dwarf that appears to have a higher J-factor than any of the presently known dwarfs (a factor of 2 larger than any of the new Sloan sources, and a factor of $\gtrsim$10 larger than the best "classical" dwarfs (see Table. 0-3). These limits also include a new advanced analysis technique which makes use of an optimal weighting of each event based on the reconstructed energy and angular position [104]. Thus, with 5 years of continued (post-upgrade) observations, the extensive dark matter search program with VERITAS offers one of the strongest avenues available for the possible detection of WIMP dark matter and, in the absence of detection, can severely constrain many conservative SUSY models (see Figures 10,11).

Since the GC transits at large zenith angles at the VERITAS site, the energy threshold is raised compared with southern hemisphere experiments like H.E.S.S., or the future Southern-CTA array. However, the effective area increases at large zenith angle (LZA) and the VERITAS team has developed a new LZ analysis technique that exploits the large effective area, providing VERITAS observations of the GC region a similar sensitivity to H.E.S.S. but in $\sim$1/6th of the observing time for energies above a few TeV [196]. At lower energies (below a TeV) the H.E.S.S. limits on the GC now come within an order of magnitude of the natural cross section, better than any of the current dSph limits [199]. As shown in Fig. 11 with 5 years of observation, VERITAS will extend the cross-section energies to higher WIMP masses, in some cases reaching the natural cross-section when non-perturbative boosts in the cross section are taken into account.

In addition to VERITAS, the other major ground-based instruments MAGIC and H.E.S.S have performed observations of dSphs to obtain DM upper limits. While we do not discuss all of these results in detail, these measurements are summarized in Table 0-3 below.

Table 0-3: J-factors for Dwarf Galaxies

Source	J-factor [GeV^2 cm^{-5}]	Profile	Reference
Draco	7.1×10^{17}	NFW	[200]
Willman I	8.4×10^{18}	NFW	[201]
Segue I	1.7×10^{19}	Einsasto	[202]
Ursa Minor	2.2×10^{18}	NFW	[200]
Boötes I	-	-	-
Sagittarius	-	-	-
Sculptor	8.9×10^{17}	NFW	[200]
Carina	2.8×10^{17}	NFW	[200]

Table 0-4: Flux Upper Limits from IACTs

Source	VERITAS $\Phi^{u.l.}$ $cm^{-2}s^{-1}$	MAGIC $\Phi^{u.l.}$ $cm^{-2}s^{-1}$	H.E.S.S. $\Phi^{u.l.}$ $cm^{-2}s^{-1}$
Draco	0.49×10^{-12} [a][201]	1.1×10^{-11} [b][203]	-
Willman I	1.17×10^{-12} [c][201]	9.87×10^{-12} [d][204]	-
Segue I	7.6×10^{-13} [e][205]	2×10^{-12} [f][206]	-
Ursa Minor	0.40×10^{-12} [g][201]	-	-
Boötes I	2.19×10^{-12} [h][201]	-	-
Sagittarius	-	-	3.6×10^{-12} [i][207]
Sculptor	-	-	5.1×10^{-13} [j][208]
Carina	-	-	1.6×10^{-13} [k][208]

[a] $E_{min} = 340$ GeV [b] $E_{min} = 140$ GeV [c] $E_{min} = 320$ GeV
[d] $E_{min} = 100$ GeV [e] $E_{min} = 300$ GeV [f] $E_{min} = 200$ GeV
[g] $E_{min} = 380$ GeV [h] $E_{min} = 300$ GeV [i] $E_{min} = 250$ GeV
[j] $E_{min} = 220$ GeV [k] $E_{min} = 320$ GeV

Table 0-5: dSph upper limits on $\langle \sigma v \rangle$ for VERITAS, MAGIC and H.E.S.S. collaborations.

Source	VERITAS $\langle \sigma v \rangle^{u.l.}$ $cm^3\ s^{-1}$	MAGIC $\langle \sigma v \rangle^{u.l.}$ $cm^3\ s^{-1}$	H.E.S.S. $\langle \sigma v \rangle^{u.l.}$ $cm^3\ s^{-1}$
Draco	2×10^{-23} [a][201]	10^{-23} [b][203]	-
Willman I	10^{-23} [c][201]	-	-
Segue I	2×10^{-24} [d], 10^{-23} [e][205]	2×10^{-24} [f][202]	-
Ursa Minor	10^{-23} [g][201]	-	-
Boötes I	10^{-22} [h][201]	-	-
Sagittarius	-	-	10^{-25} [i], 3×10^{-26} [j][207]
Sculptor	-	-	4×10^{-23} [k][208]
Carina	-	-	2×10^{-22} [l][208]

[a] For a composite neutralino spectrum and $m_\chi \sim 1$ TeV
[b] For Model D' given by [209] and with $m_\chi \sim 200$ GeV
[c] For a composite neutralino spectrum and $m_\chi \sim 900$ GeV
[d] For $\tau^+\tau^-$ and $m_\chi \sim 300$ GeV
[e] For $b\bar{b}$ and $m_\chi \sim 1$ TeV
[f] For $\tau^+\tau^-$ and $m_\chi \sim 500$ GeV
[g] For a composite neutralino spectrum and $m_\chi \sim 1$ TeV
[h] For a composite neutralino spectrum and $m_\chi \sim 800$ GeV
[i] For pMSSM + Cored profile and with $m_\chi \sim 200$ GeV
[j] For Kaluza-Klein + Cored profile with $m_\chi \sim 300$ GeV
[k] For self annihilation into WW and ZZ pairs and with $m_\chi \sim 2$ TeV
[l] For self annihilation into WW and ZZ pairs and with $m_\chi \sim 3$ TeV
[m] Note: All values for $\langle \sigma v \rangle^{u.l.}$ are approximate minimum values taken from plots of $\langle \sigma v \rangle^{u.l.}$ for a range of values of m_χ.

4.5 Future Gamma-Ray Experiments

4.5.1 Anticipated *Fermi* 10-Year Data

While the *Fermi* LAT data reach the natural cross section below 30 GeV, they do not presently constrain any of the pMSSM benchmark models. Here we estimate the improvements expected over a 10 year mission lifetime. In the low-energy, background dominated regime, the LAT point source sensitivity increases as roughly the square-root of the integration time. However, in the high-energy, limited background regime (where many pMSSM models contribute), the LAT sensitivity increases more linearly with integration time. Thus, 10 years of data could provide a factor of $\sqrt{5}$ to 5 increase in sensitivity. Additionally, optical surveys such as Pan-STARRS [210], the Dark Energy Survey [211], and LSST [212] could provide a factor of 3 increase in the number of Milky Way dSphs corresponding to an increased constraining power of $\sqrt{3}$ to 3 [103]. Ongoing improvements in LAT event reconstruction, a better understanding of background contamination, and an increased energy range are all expected to provide additional increases in the LAT sensitivity. Thus, we find it plausible that the LAT constraints could improve by a factor of 10 compared to current constraints.

In Figure 12 we display the boost required to constrain the various pMSSM models at 95% CL based on the *Fermi*-LAT dwarf analysis employing only the first 2 years of data colored-coded by either the annihilation cross section or the LSP thermal relic density. Here we see that the LAT analysis does not currently constrain any of our pMSSM models. However, as discussed above with more dwarfs and longer integration times we would expect an $\sim$ 10-fold improvement in the sensitivity and thus all models with boost factors less than 10 would become accessible. We will assume this $\sim$ 10-fold improvement in sensitivity assumption for the analysis that follows.

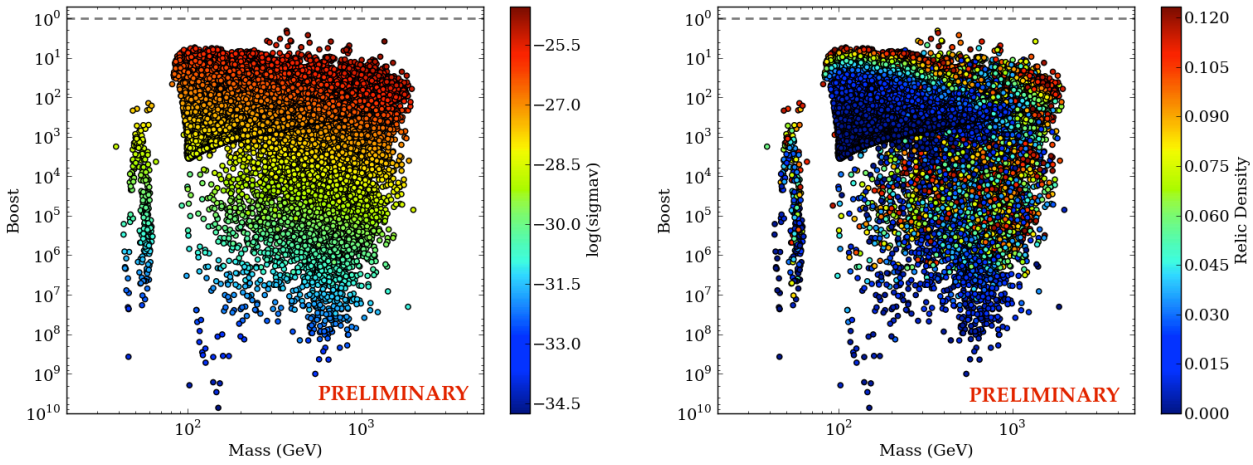

Figure 12: (Left) *Fermi*-LAT boost factor vs. LSP mass for the pMSSM model set. The true cross section, $\langle\sigma v\rangle$, for each model is plotted on the color scale. (Right) Here the corresponding relic density for each model is plotted on the color scale.

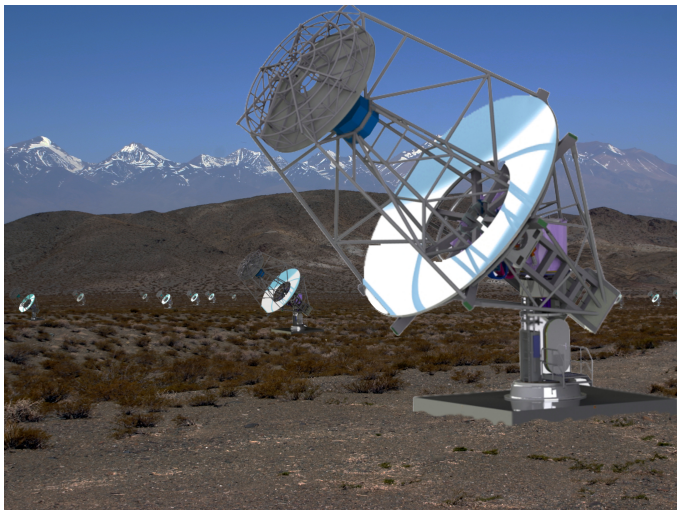

Figure 13: Artist's concept of an array of SCT telescopes as being developed by the U.S. CTA group to extend the baseline CTA array providing a factor of 2 to 3 in sensitivity, improved angular resolution and larger field of view compared with the baseline CTA concept.

4.5.2 The Augmented Cherenkov Telescope Array (CTA)

The planned (baseline) Cherenkov Telescope Array (CTA) [213] will have great sensitivity over the energy range from a few tens of GeV to 100 TeV. To achieve the best sensitivity over this wide energy range CTA will include three telescope types: Large Size Telescope (LST, 23 m diameter), Medium Size Telescope (MST, 10-12 m) and Small Size Telescope (SST, 4-6 m). Over this energy range the point-source sensitivity of CTA will be at least one order of magnitude better than current generation imaging atmospheric Cherenkov telescopes such as H.E.S.S., MAGIC, and VERITAS. CTA will also have an angular resolution at least 2 to 3 times better than current ground-based instruments, improving with energy from 0.1° at 100 GeV to better than 0.03° at energies above 1 TeV.

The potential of CTA for DM searches and testing other exotic physics has been studied in detail by [198] using the projected performance of several alternative array configurations [214] with 18–37 MSTs and different combinations of SSTs and LSTs. For this study we use the projected sensitivity of a candidate CTA configuration with 61 MSTs on a regular grid with 120 m spacing [215]. This telescope layout is similar to the anticipated layout of the baseline MST array with 18–25 telescopes with an additional US contribution of 36 MSTs. This configuration has a gamma-ray angular resolution that can be parameterized as a function of energy as $\theta \simeq 0.07^\circ (E/100\ \mathrm{GeV})^{-0.5}$ and a total effective area above 100 GeV of $\sim 10^6$ m^2. We define the GC signal region as an annulus centered on the GC that extends from 0.3°–1.0° and calculate the sensitivity of CTA for an integrated exposure of 500 hours that is uniform over the whole region. An energy-dependent model for the background in the signal region is taken from a simulation of residual hadronic contamination. The uncertainty in the background model is calculated for a control region with no signal contamination and a solid angle equal to five times the signal region (14.3 deg^2).

Figure 14 shows the projected sensitivity of our candidate CTA configuration. We evaluate the sensitivity to a WIMP particle annihilating through three possible final states: $b\bar{b}$, W^+W, and $\tau^+\tau$. For the Sculptor dSph, one of the best dSph candidates in the south, CTA could reach $\sim 10^{-24}\mathrm{cm}^3 s^{-1}$ at 1 TeV which is comparable to current limits from H.E.S.S. observations of the GC halo. For an observation of the GC

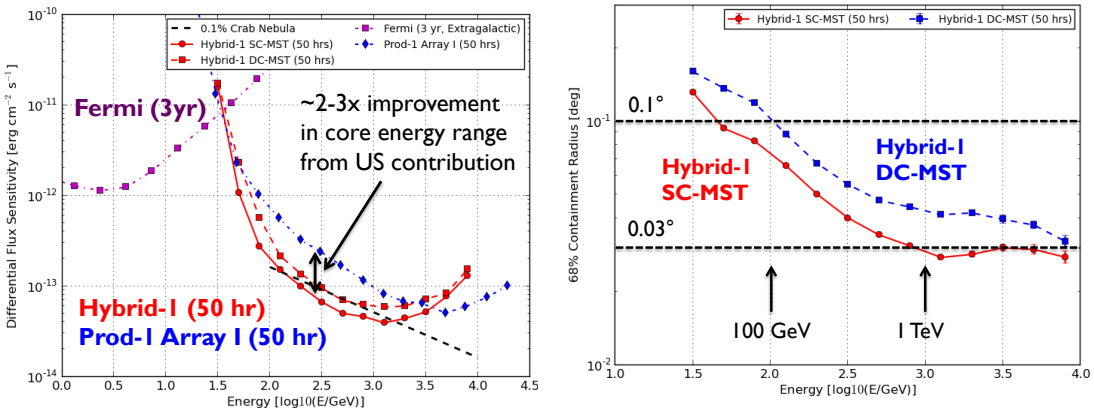

Figure 14: Projected sensitivity of a candidate CTA configuration, see the text for details.

utilizing the same 0.3° to 1.0° annular search region as the H.E.S.S. analysis CTA could rule out models with cross sections significantly below the thermal relic cross section down to $\sim 3 \times 10^{-27}\mathrm{cm}^3\mathrm{s}^{-1}$. Overlaid in the figure are WIMP models generated in the pMSSM framework that satisfy all current experimental constraints from collider and direct detection searches. Approximately half of the models in this set could be excluded at the 95% C.L. in a 500 hour observation of the Galactic center.

We compute the sensitivity of CTA using a two-dimensional likelihood analysis that models the distribution of detected gamma-rays in energy and angular offset from the GC. Following the same procedure as the *Fermi*-LAT analysis, we compute the model boost factor as the ratio of the model cross section with the 95% C.L. upper limit on the annihilation cross section of a DM model with the same spectral shape. For models with LSP masses below 1 TeV, the sensitivity of CTA is dominated by events at low-energy ($E \lesssim 300$ GeV).

The optimal DM search region for CTA will be limited by the CTA FoV of 8° to the area within 2° to 3° of the GC. On these angular scales the DM signal is predominantly determined by the DM distribution in the inner Galaxy ($R_{GC} < 1$ kpc). We model the Galactic DM distribution with our benchmark NFW profile with a scale radius of 20 kpc normalized to 0.4 GeV cm^{-3} at the solar radius. This model is consistent with all current observational constraints on the Galactic DM halo in the absence of baryons. Because the annihilation signal is proportional to the square of the DM density, the projected limits for CTA depend strongly on the assumptions that are made on the shape and normalization of the Galactic DM halo profile, and the role of baryons in either washing out or enhancing the signal. The projected limits presented here could be reduced by as much as a factor of 10, or improved by an even larger factor given these uncertainties.

Figure 15 shows the distribution of the CTA boost factor versus LSP mass for all pMSSM models and the subset of models that have an LSP relic density consistent with 100% of the DM relic density. CTA can exclude ∼20% of the total model set and >50% of the models in the subset with the DM relic density. Here we see that ∼ 19% of the models would be excluded by CTA if no signal were to be observed.

4.5.3 HAWC

The High Altitude Water Cherenkov (HAWC) observatory, nearing completion at Sierra Negra in the state of Puebla, Mexico, consists of a 20,000 square meter area of water Cherenkov detectors: water tanks instrumented with light-sensitive photomultiplier tubes. The experiment is used to detect energetic

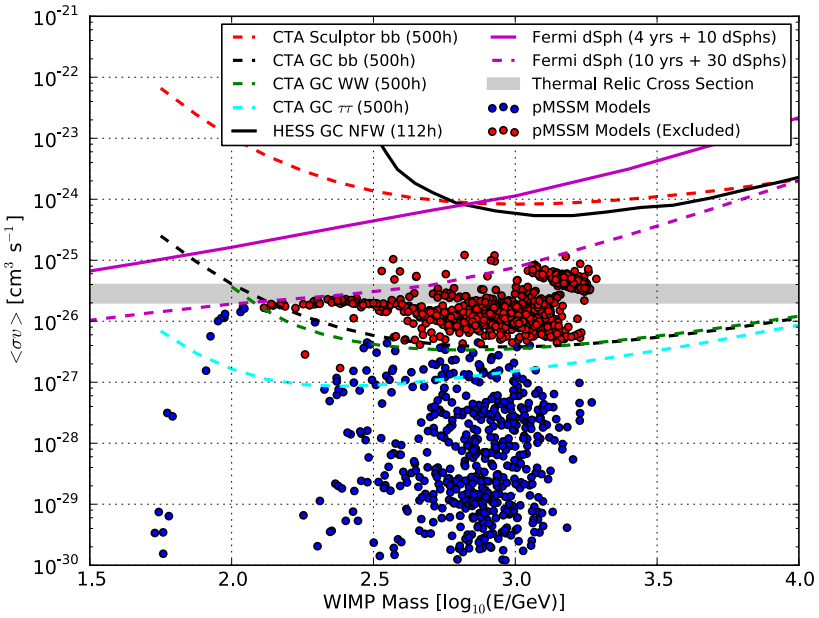

Figure 15: A comparison of pMSSM predictions and projected CTA, H.E.S.S. and *Fermi* sensitivities.

secondary particles reaching the ground when a 100 GeV to 100 TeV cosmic ray or gamma ray interacts in the atmosphere above the experiment. Gamma-ray primaries may be distinguished from cosmic-ray background by identifying the penetrating particles characteristic of a hadronic particle shower. As of summer 2013, the instrument is over 30% complete and is performing as designed. The full instrument will be completed in summer 2014.

HAWC will complement existing Imaging Atmospheric Cherenkov Telescopes and the space-based gamma-ray telescopes with its extreme high-energy sensitivity and its large field-of-view. The instrument has peak sensitivity to annihilation photons from dark matter with masses between about 10 and 100 TeV. Much like *Fermi*, HAWC will survey the entire Northern sky with sensitivity roughly comparable to existing IACTs and will search for annihilation from candidates that are not known a priori, such as baryon-poor dwarf galaxies. Furthermore, HAWC can search for sources of gamma rays that are extended by 10 degrees or more and can constrain even nearby sub halos of dark matter.

4.6 Constraints on Dark Matter Decay from Gamma-Ray observations

While this discussion is somewhat beyond the scope of the present work, in some dark matter particles it is possible that the dark matter is in the form of an unstable, but very long-lived particle. Example of decaying dark matter include neutralinos with slight R-parity violation as predicted by models when the gaugino masses are dominated by anomaly mediated supersymmetry breaking. [216, 217]. One such candidate of some recent interest is the TeV-scale decaying Wino that could explain the PAMELA/AMS excess [218]. Figure 17 gives some examples of constraints on decaying dark matter from indirect detection experiments.

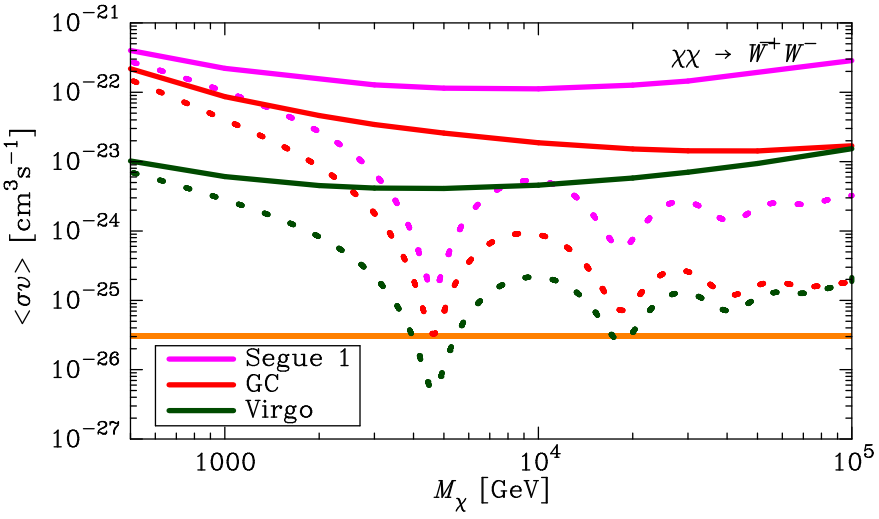

Figure 16: HAWC sensitivity to the W$^+$W$-$ annihilation channel (solid lines) and the same including nonperturbative effects (a Sommerfeld enhancement from W exchange)

We note that *Fermi* observations of galaxy clusters give comparable to or better limits on the dark matter particle lifetime to those shown for the *Fermi* Milky Way halo analysis [124, 125].

4.7 Neutrino Experiments

Like their gamma-ray counterparts, neutrino telescopes have sensitivity to WIMP annihilations in the Galactic Center, Halo, from galaxy clusters and from dSph galaxies. In addition, neutrino telescopes are sensitive to WIMP annihilations in the core of the earth or sun, regions that are inaccessible to gamma-ray telescopes. In fact, searches for WIMP annihilations in the solar core avoid many of the model dependencies suffered by searches from other candidate locations using neutrinos or photons. The WIMP source in the sun has built up over solar time, averaging over the galactic dark matter distribution as those WIMPs that scattered elastically with solar nuclei and lost enough momentum became gravitationally trapped. The main assumption one needs to make is that a sufficient density of WIMPs has accumulated in the solar core that equilibrium now exists between WIMP capture and annihilation. Then, given a WIMP mass and decay branching ratios, one can predict the signal in a neutrino telescope unambiguously. As seen in Fig. 19, the results from neutrino experiments are and will continue to be very competitive with direct-detection results, especially for spin-independent scattering. At WIMP masses above about 1 TeV, large neutrino telescopes such as IceCube probe a region of parameter space that is inaccessible to the LHC [223].

4.7.1 Solar WIMP Model Uncertainties

In the scenarios for production of secondaries by annihilation of halo WIMPs, we assumed that the dark matter's distribution was determined by something that did not depend on any of its particle properties, so that the only particle properties that matter for the annihilation rate are the annihilation cross section, and indirectly, the mass (because the mass density, which we can measure or estimate with astronomical

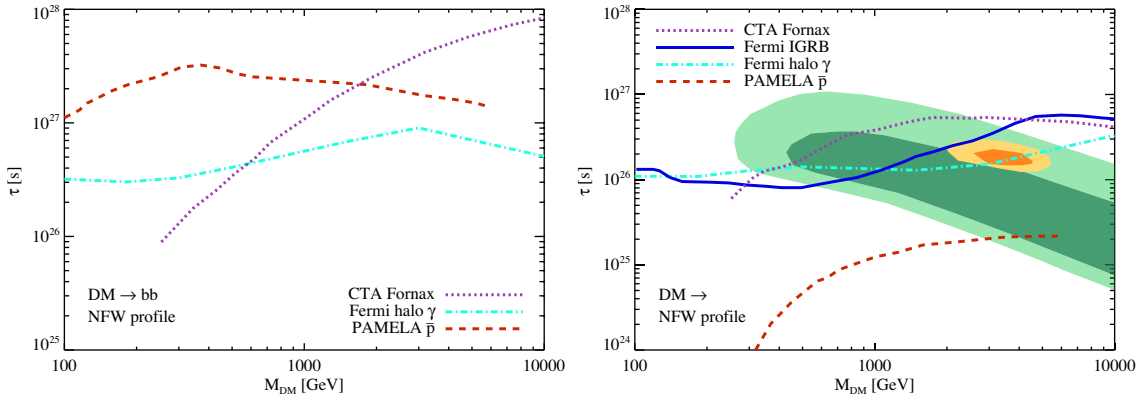

Figure 17: Top: Current and projected constraints on the $M_{\rm DM}$–τ parameter space for decay to $b\bar{b}$ from the *Fermi* LAT analysis of gamma-ray emission from the Milky Way halo [219], from PAMELA observations of the anti-proton flux [220], and projected sensitivity for CTA observations of the Fornax cluster in gamma rays [221]. The curves indicate lower limits on or projected sensitivity for CTA to the DM particle lifetime at 95% C.L. (99% C.L. for the *Fermi* Milky Way halo analysis), assuming a NFW density profile. Bottom: As in top panel, for decay to $\mu^+\mu^-$. Also shown are constraints from the *Fermi* LAT measurement of the Isotropic Gamma-ray Background (IGRB) published in [222] as derived in [221], and regions consistent with the positron fraction measurements by PAMELA and *Fermi*, and the PAMELA measurement of the antiproton flux, at 95.45% C.L. and 99.999% C.L. (dark and light green regions, respectively). Regions remaining consistent when the $e^+ + e^-$ fluxes measured by *Fermi*, H.E.S.S., and MAGIC are included in the fit are also shown at 95.45% C.L. and 99.999% C.L. (orange and yellow regions, respectively) [221].

observations, has to be divided through by the particle mass to get a number density). For WIMP capture and annihilation in the Sun, the other particle properties of WIMPs matter in estimating the annihilation rate, and hence, the flux of neutrinos emerging from the annihilations.

Fundamentally, the annihilation rate depends on the capture rate of WIMPs by the Sun. WIMPs that scatter off nuclei in the Sun can lose energy to solar nuclei. Depending on the reduced mass of the WIMP-nuclear system and the typical initial speed of WIMPs, WIMPs are scattered to speeds below the escape velocity of the Sun. Captured WIMPs keep re-scattering off solar WIMPs in their ever-tightening orbit, until they come to equilibrium with solar nuclei at the center of the Sun. This implies a dense core of WIMPs at the center of the Sun, where WIMPs can thus efficiently annihilate. The equation that governs the relationship between WIMP creation and destruction processes is:

$$\dot{N} = C - C_A N^2 - C_E N, \tag{14}$$

where N is the number of WIMPs in the Sun, and

$$C = \sum_i \int d^3\mathbf{r}_\odot d^3\mathbf{v} d^3\mathbf{v}_i d\Omega f_i(\mathbf{r}_\odot, \mathbf{v}_i) f(\mathbf{r}_\odot, \mathbf{v}|\mathbf{v} - \mathbf{v_i}|\frac{d\sigma_i}{d\Omega}\|_{v_f < v_{esc}} \tag{15}$$

is the capture rate of WIMPs in the Sun from elastic WIMP-nuclear scattering. Here i denotes a nuclear species, $d\sigma_i/d\Omega$ is the elastic scattering cross section, and the f's are the phase-space densities of nuclei (i) and the local WIMP population. The final WIMP speed v_f must be less than the escape velocity from the Sun v_{esc} for the WIMP to be trapped. The capture rate is quite sensitive to the WIMP mass, because for WIMPs with $m_\chi \gg m_i$, WIMPs only lose a small bit of kinetic energy to nuclei. Thus, for heavy WIMPs,

only particles initially moving slowly with respect to the Sun may be captured. Note that this quantity is independent of N, the number of captured WIMPs in the Sun, since we are considering the process by which WIMPs are gathered within the Sun from the local Galactic population. In addition, C_A is the annihilation term, defined such that the annihilation rate is:

$$\Gamma = \frac{1}{2} C_A N^2, \tag{16}$$

and

$$C_A = \langle \sigma v_{rel} \rangle \int d^3 \mathrm{r}_\odot n^2(r)/N^2. \tag{17}$$

Here, $\mathbf{r}_\odot$ denotes the position of the WIMPs or nuclei with respect to the center of the Sun. Note that we have implicitly assumed self-annihilation in this equation. If the WIMP mass $m_\chi < m_i$, then WIMPs can *gain* energy by elastic scattering off nuclei in the Sun. In fact, they can scatter above v_{esc} and hence "evaporate" from the Sun. See [224] for a detailed calculation of C_E. In brief, we see that $\dot{N} \propto N$ for evaporation because the evaporation depends on the WIMP-nuclear scattering rate, and hence on one power of the number of WIMPs in the Sun. For spin-independent scattering, the evaporation term is only relevant for WIMPs below $m_\chi \lesssim 3.3$ GeV (slightly less than the mass of helium); solar WIMP searches have no sensitivity below that mass. (This sensitivity is bracketed from above at $m_\chi \sim 1$ TeV because the daughter neutrinos of such massive WIMPs experience absorption as they pass through the solar interior.)

For typical values of the WIMP annihilation cross section ($\langle \sigma_A v_{rel} \rangle \approx 3 \times 10^{-26}$ cm$^3 s^{-1}$) and WIMP-nuclear elastic cross sections (that depend on the local Galactic WIMP velocity distribution) capture and annihilation are in equilibrium, and

$$\Gamma = \frac{1}{2} C_A. \tag{18}$$

Thus, in this special case, the annihilation rate grows only linearly with the local Galactic WIMP number density. (More detailed discussions of this process can be found in Refs. [225, 226, 227, 228, 229, 224, 230, 231, 232, 233]).

The velocity distributions also affect WIMP capture in the Sun, because WIMPs that are slow relative to the Sun are much more likely to scatter below the Sun's escape speed than will fast particles. In particular, if the Milky Way has a "dark disk" or any un-virialized dark-matter structures that approximately co-rotate with the Sun, the capture rate in the Sun will be dramatically enhanced [234].

For solar WIMP annihilation we need to know the local density structure (on scales of Astronomical Units, not the kpc scales that N-body simulations resolve). It is highly unlikely that we are sitting in a subhalo—the local volume filling factor of subhalos is at most 10^{-4} [235, 74, 236]. However, because of the long equilibrium time in the Sun, the annihilation rate depends on the time integral of the capture rate. In this case, small variations in the density structure of our local patch of the Milky Way could affect the WIMP annihilation rate in the Sun [237].

Of course, for dark-matter particles that have velocity-dependent annihilation cross sections, the velocity distribution matters as well. Velocity distributions tend to show large departures from the traditional Maxwell-Boltzmann distribution, and imprints of the accretion history of the host halo [74, 238, 239, 240]. It is anticipated that the hyper-local velocity distribution is highly streamy, but it is unclear how much that streaminess will affect solar WIMP searches—it is probably not enormously significant [241]. While these local anisotropies (in velocity and position space) are unlikely to affect this or other indirect searches, they may well have a significant effect on direct detection experiments. So while some of these uncertainties may have an impact on the reach of neutrino searches, they do not significantly change the great potential for

discovery for neutrino experiments, in the nearly unambiguous detection of a high-energy neutrino signal from the sun.

4.7.2 IceCube/DeepCore

IceCube has taken physics-quality data since 2006 and was completed in early 2010. Optimized for detecting neutrinos at TeV to PeV energies, IceCube has unparalleled sensitivity to neutrinos from WIMPs at masses of 1 TeV and above. Since 2009 IceCube has included DeepCore, an in-fill sub-array with increased module density providing improved sensitivity to low energy neutrinos and extending IceCube's reach to WIMP masses as low as roughly 20 GeV. The current configuration of the IceCube detector is illustrated in Fig. 18. The IceCube Collaboration continues to take data and has performed or is performing searches

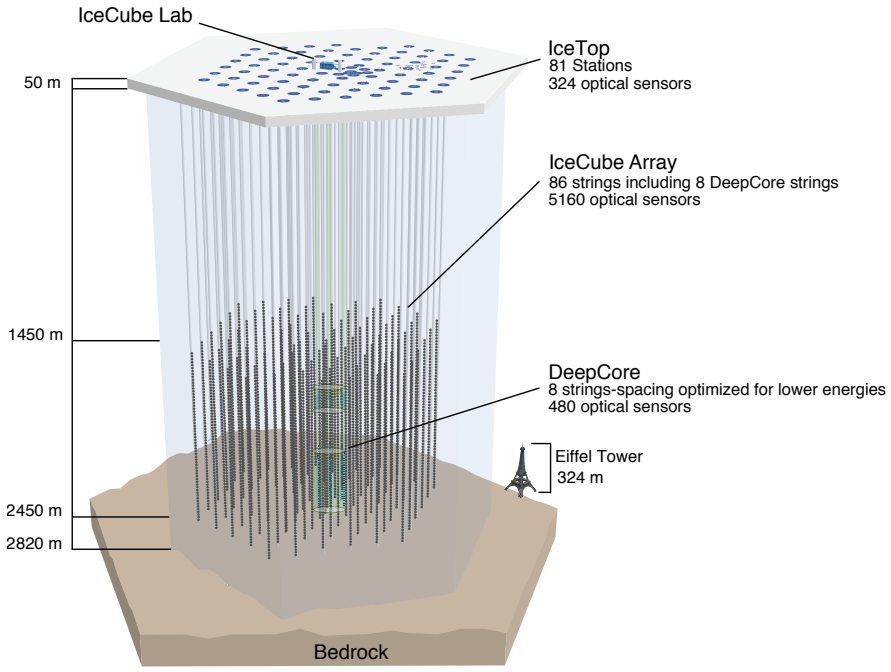

Figure 18: The IceCube neutrino telescope comprises 86 strings and 5,160 modules buried in the icecap at the South Pole, Antarctica. The modules have been deployed at depths ranging from 1450 m to 2450 m below the surface. DeepCore, at the bottom center of IceCube, has modules at higher density than the surrounding array for improved sensitivity to lower energy neutrinos and hence lower mass WIMPs.

for neutrino signals from WIMPs in the center of the earth [242], the solar core [243], the galactic halo [244] and center [245], galaxy clusters, and dwarf spheroidal galaxies [246] (see Fig. 19).

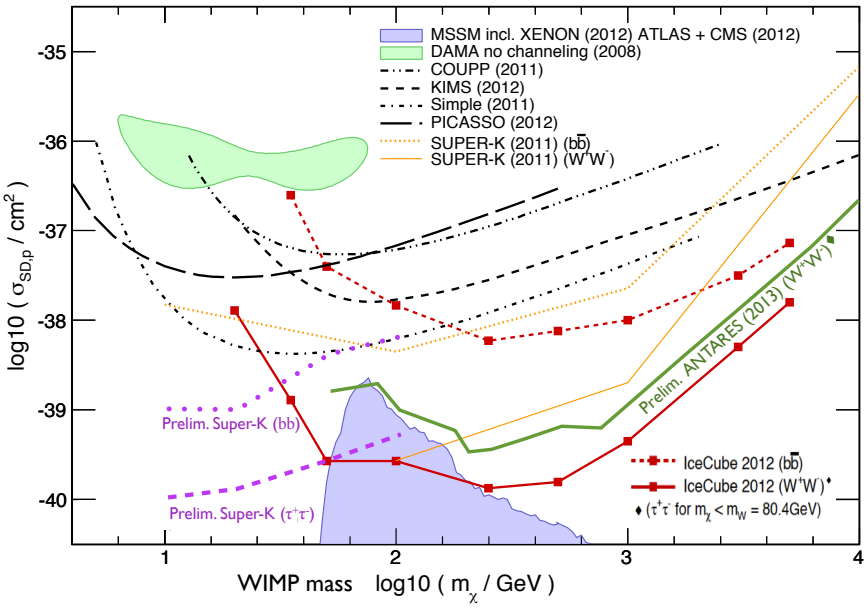

Figure 19: Constraints on the spin-dependent WIMP-proton scattering cross section.

As a specific example, we present predictions for an IceCube/DeepCore (IC/DC) search for neutralino dark matter. Our analysis closely follows that presented in [57]. In the results presented here we assume that each SUSY model results in a neutralino relic density given by the usual thermal calculation. We use DarkSUSY 5.0.6 [247] to simulate the (yearly-average) signal $\nu_\mu/\bar{\nu}_\mu$ neutrino flux spectra incident at the detector's position and convolve with preliminary $\nu_\mu/\bar{\nu}_\mu$ effective areas for muon events contained in DeepCore[3]. We consider a data set that includes $\sim$ 5yr of data that is taken during austral winters (the part of the year for which the sun is in the northern hemisphere) over a total period of $\sim$ 10yrs[4]. An irreducible background rate of $\sim$ 10 events/yr is expected from cosmic-ray interactions with nuclei in the sun. Here we will take (as discussed at greater length in [57]) a detected flux of $\Phi = 40$ events/yr as a conservative criterion for exclusion.

The basic results of this analysis are presented in Figure 20. In the figure we show all pMSSM models in our set using grey points, while highlighting WMAP-saturating models with mostly bino, wino, Higgsino or mixed ($\leq$80% of each) LSPs in red, blue, green and magenta, respectively. Detectability is tightly correlated with the elastic scattering cross-sections (σ_{SI} and σ_{SD}) while having little correlation with the annihilation cross-section $\langle\sigma v\rangle$, as expected.

The biggest difference between these results and those of the previous analysis [57], which used a set of pMSSM models that were chosen to have relatively light ($\leq$ 1TeV) sparticles, is that a much smaller percentage of the current pMSSM models are able to reach capture/annihilation equilibrium in the sun. This is due to the fact that so many of these models are nearly pure wino or Higgsino gauge eigenstates

[3]These are the same effective areas that were used in [57], referred to there as "SMT8/SMT4."

[4]In practice the IceCube/DeepCore treatment of data is more sophisticated, classifying events as through-going, contained and strongly-contained, and allowing for some contribution from data taken in the austral summer. We expect that inclusion of this data would affect our results at a quantitative, but not qualitative, level.

(which have both low relic density and small capture cross-sections) and that the LSPs in this model set tend to be much heavier than those in the previous set. If one defines out-of-equilibrium models as those with solar annihilation rates less than 90% of their capture rates, we find that no such models can be excluded by IceCube/DeepCore. In contrast, relatively light LSPs composed of a mixture of gaugino and Higgsino eigenstates have large scattering and annihilation cross sections and are highly detectable by IceCube/DeepCore. We observe that all such WMAP-saturating well-tempered neutralinos with masses $m_{LSP} \leq 500$GeV should be excluded by the IceCube/DeepCore search (*c.f.*, the magenta points in Fig. 20).

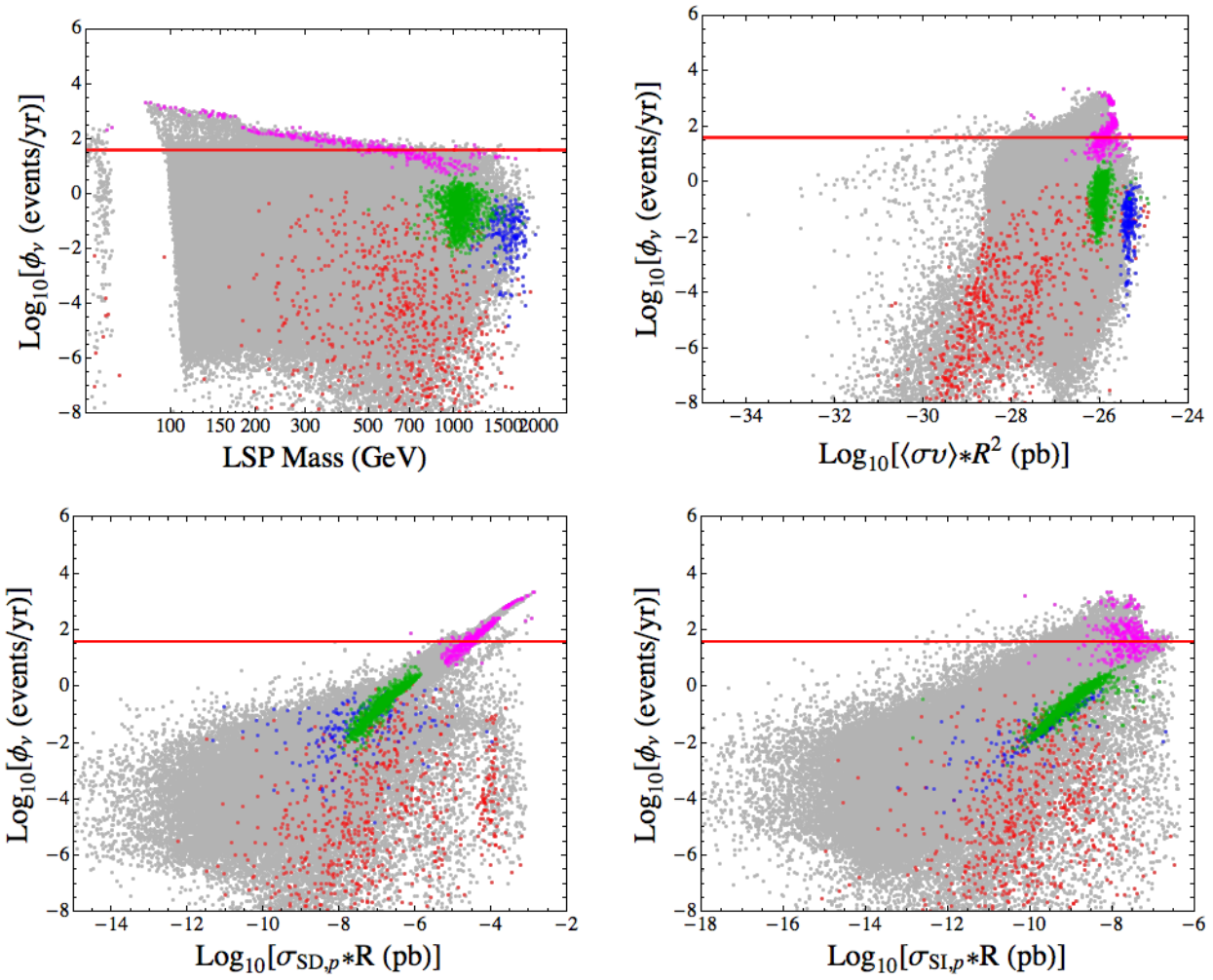

Figure 20: IceCube/DeepCore signal event rates as a function of LSP mass (upper-left), thermal annihilation cross-section $\langle\sigma v\rangle R^2$ (upper-right) and thermal elastic scattering cross-sections $\sigma_{SD,p}$ and $\sigma_{SI,p}$ (lower panels). In all panels the gray points represent generic models in our full pMSSM model set, while WMAP-saturating models with mostly bino, wino, Higgsino or mixed ($\leq$80% of each) LSPs in are highlighted in red, blue, green and magenta, respectively. The red line denotes a detected flux of 40 events/yr, our conservative estimate for exclusion.

4.7.3 Super-Kamiokande

The Super-Kamiokande detector began operation in 1996 and has consisted of up to 11,146 modules instrumenting a 22 kton fiducial volume of ultra-pure water. Super-K has performed searches for solar WIMPs using more than 3,000 live-days of data with sensitivity to WIMP masses between 10-100 GeV [248](see Fig. 19).

SuperK has sensitivity to low-energy neutrinos that have recently been identified as a complementary indirect detection probe of solar WIMP annihilations [249, 250]. Pions are produced abundantly by the hadronization of annihilation products and by subsequent inelastic interactions with the dense solar medium. Stopped positive pions decay, producing neutrinos at $\sim 25 - 50$ MeV with known spectra, an energy range covered by the currently-operating Super-K experiment and planned experiments including Hyper-K and large liquid scintillator detectors such as LENA. The advantages of this detection channel are high multiplicity of signal neutrinos (compared to the number of high-energy neutrinos from solar WIMP annihilation), relatively low backgrounds, insensitivity of the signal spectrum to the annihilation final states, and detection sensitivity that improves with decreasing WIMP mass until evaporation becomes important at ~ 4 GeV. The low-energy neutrino channel is complementary to direct searches and indirect searches with high-energy neutrinos, and is particularly valuable as an indirect probe of the WIMP-nucleon scattering cross-section at low WIMP masses.

4.8 Future Neutrino Experiments

4.8.1 HyperK

The Hyper-Kamiokande has been proposed as a next-generation underground water Cherenkov detector [251]. The design calls for a fiducial mass of 0.56 million metric tons, about 25 times larger than that of Super-K, viewed by 99,000 20-inch PMTs. This will give the detector 20% photo-cathode coverage, about half that of Super-K. A diagram of the Hyper-K detector is shown in Fig. 21.

Although focused primarily on other physics goals, the Hyper-Kamiokande detector will have sensitivity to neutrinos from solar, earth and galactic halo WIMP annihilations. For solar WIMPs annihilating in the soft-channel mode, Hyper-K's cross section sensitivity could reach down to 10^{-39} cm^2 at 10 GeV [251].

4.8.2 IceCube/PINGU

The Precision IceCube Next Generation Upgrade (PINGU) detector will be proposed as a new in-fill array for IceCube. The final geometry for the detector is still under study but will probably be comprised of between 20-40 new strings with 60-100 modules per string. PINGU will instrument an effective volume ranging from 2-4 million metric tons at energies from 5-15 GeV, respectively, with $\mathcal{O}(1000)$ modules.

Like Hyper-K, PINGU is focused on other physics goals but has sensitivity to neutrinos produced by WIMP annihilations. The two detectors will be able to probe a WIMP mass region that is of considerable interest due to intriguing results from other experiments that are consistent with a WIMP mass of a few GeV. WIMP properties motivated by DAMA's annual modulation signal [252] and isospin-violating scenarios [253] motivated by DAMA and CoGeNT signals would be testable by detectors with sensitivity to WIMP masses at the few GeV scale. The predicted sensitivity of Hyper-K and PINGU is shown in Fig. 22.

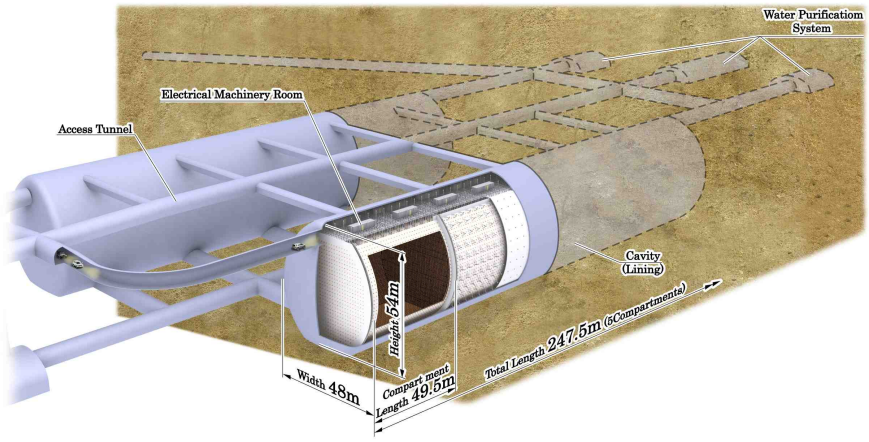

Figure 21: The Hyper-Kamiokande neutrino detector is planned to instrument 0.56 million metric tons of water with 99,000 PMTs. It will be housed in cavities with 1,750 m water equivalent overburden near Super-K in Gifu Prefecture, Japan.

4.9 Astrophysical Multiwavelength Constraints

The pair-annihilation of WIMPs yields gamma rays from the two photon decay of neutral pions, and, in the high energy end of the spectrum, from internal bremsstrahlung from charged particle final states. Concerning lower frequencies, a conspicuous non-thermal population of energetic electrons and positrons results from the decays of charged pions produced by the hadronization of strongly interacting particles in the final state, as well as from the decays of gauge bosons, Higgs bosons and charged leptons. This non-thermal $e^{\pm}$ population looses energy and produces secondary radiation through several processes: synchrotron in the presence of magnetic fields, inverse Compton scattering off starlight and cosmic microwave background photons and bremsstrahlung in the presence of ionized gas. This radiation can actually cover the whole electromagnetic spectrum between the radio band to the gamma-ray band.

The computation of the multi-wavelength emissions from WIMP-induced energetic $e^{\pm}$ involves several steps: (1) the assessment of the spectrum and production rate of electrons and positrons from dark matter pair annihilations; (2) the computation of the effects of propagation and energy losses, possibly leading to a steady state $e^{\pm}$ configuration; (3) the computation of the actual emissions from the mentioned equilibrium configuration; (4) the evaluation of eventual absorption of the emitted radiation along the line of sight to derive fluxes and intensities for a local observer.

The CF2 group recommends that benchmark models be adopted for the calculation of multi-wavelength emission from WIMP annihilation, at least in key astrophysical environments such as the Milky Way, selected nearby galaxy clusters and local dwarf spheroidal galaxies. The benchmark should include choices for diffusion, magnetic field intensity and spatial distribution, the background light spatial distribution and intensity.

Several recent studies have made it clear that radio [126] and X-ray frequencies [128] have the potential to reach a sensitivity to the relevant WIMP parameter space comparable, and in some instances broader than and complementary to, gamma-ray experiments. A detailed performance comparison however critically depends upon assumption on the propagation and energy losses and, generically, the astrophysical environ-

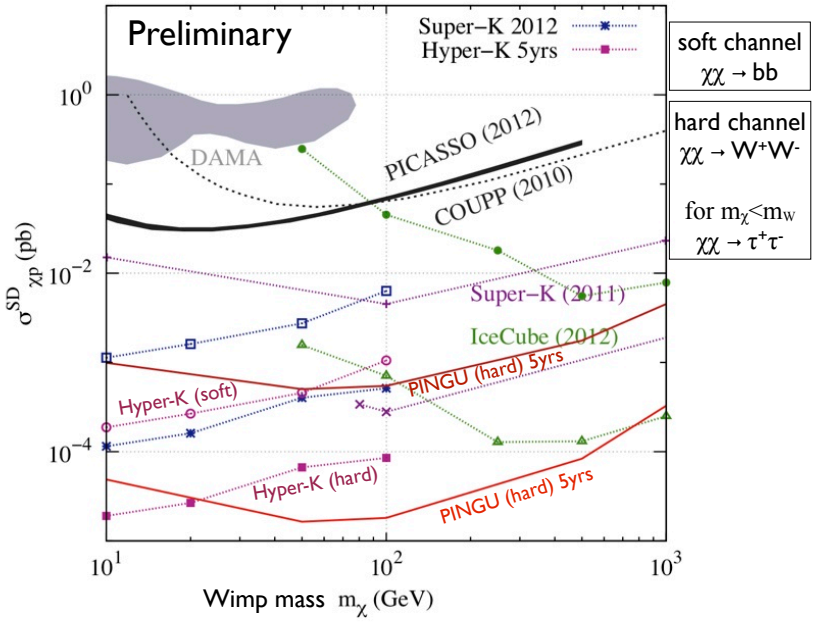

Figure 22: Constraints on the spin-dependent WIMP-proton scattering cross section from various current experiments and future sensitivities for Hyper-Kamiokande and PINGU with five years of data.

ment where the secondary radiation is emitted. This makes the accurate definition of benchmarks all the more important for this field. A detailed discussion of the uncertainties stemming from the magnetic field parameters is given for example in figures 7 and 8 of [126].

At radio frequencies, the DM-induced emission is dominated by the synchrotron radiation. The power for synchrotron emission takes the form [254]:

$$P_{syn}(x, E, \nu) = \frac{\sqrt{3}\, e^3}{m_e c^2}\, B(x) F(\nu/\nu_c)\ , \tag{19}$$

where m_e is the electron mass, the critical synchrotron frequency is defined as $\nu_c \equiv 3/(4\,\pi)\cdot c\, e/(m_e c^2)^3 B(x) E^2$, and $F(t) \equiv t \int_t^\infty dz K_{5/3}(z)$ is the standard function setting the spectral behavior of synchrotron radiation. Radio emission from dark matter was studied in a variety of recent works, including [255, 256, 257]. Near term and future radio facilities will give both large gains in low frequency capabilities (e.g. LOFAR, LWA) as well as increased sensitivity (e.g. ASKAP, MeerKAT, SKA).

The peak of the inverse-Compton emission from electrons and positrons produced by dark matter annihilation or decay for a large class of dark matter models falls in the hard X-ray band [128]. Future hard X-ray facilities will feature significantly better imaging capabilities. While in the observation of distant extragalactic objects the instrumental angular resolution is much less critical than the instrument field of view in the search for a signal from dark matter, there are other astrophysical environments where the opposite might be true. A clear example is the Galactic center, where source confusion plagues the possibility of a solid discrimination between a diffuse signal from dark matter versus multiple point sources with gamma-ray observations. Hard X-ray data on the Galactic center region will greatly help clarify the nature of the high-energy emission from that region, in particular in connection with a possible dark matter interpretation.

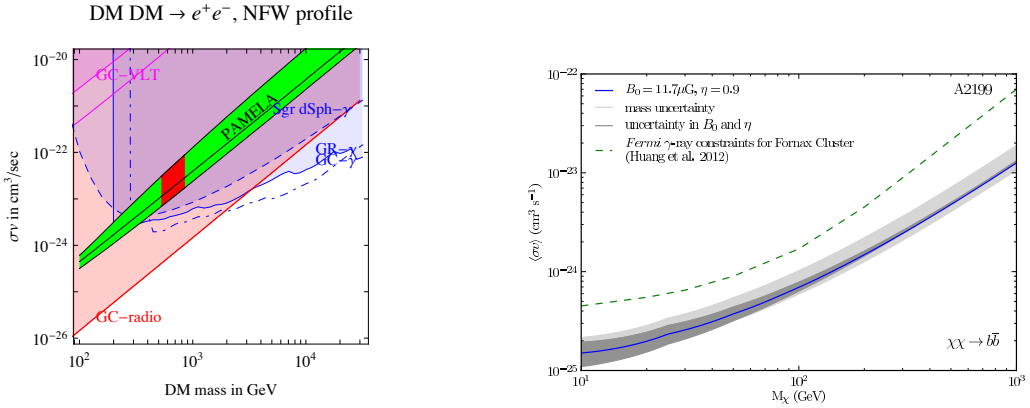

Figure 23: *Left:* Gamma-ray and radio constraints on leptophyllic dark matter from galactic center observations, from Ref. [25] *Right:* Example radio constraints on dark matter annihilation using the non-detection of diffuse radio emission in the A2199 cluster [126]. These are compared to the best current gamma-ray constraints from *Fermi* observations of clusters. In both cases, an NFW only profile is considered; the addition of substructure would improve the constraints in both cases. Effects of uncertainty in cluster mass and magnetic field parameters for A2199 are also shown.

The multi-wavelength emission from dark matter annihilation was studied in detail in the seminal works of [258] for galactic dark matter clumps, in [127] for the case of the Coma cluster and in [259] for the dwarf spheroidal galaxy Draco. Other recent studies include X-ray and radio observations of clusters of galaxies [126, 260, 261] and an analysis of the broad-band dark-matter annihilation spectrum expected from the galactic center region [262]. In addition, radio emission from e^+e^- produced in dark matter annihilation was considered as a possible source for the "WMAP haze" in the seminal paper of [263], and subsequently analyzed in detail in [264], [265] and [266]. Other studies have also previously addressed synchrotron radiation induced by dark matter annihilation (e.g., [255, 257, 256]).

Among the possible targets for mulit-wavelength searches for a signature of dark matter annihilation, clusters of galaxies stand out as excellent candidates for several reasons. They are both massive and dark matter dominated, and in terms of searches for secondary IC or synchrotron radiation signals the effect of spatial diffusion in clusters is typically negligible due to the fact that the high energy electrons and positrons produced in dark matter annihilation or decay events lose energy much faster than the time needed for them to diffuse through cluster scales [127]. Limits on dark matter annihilation were derived by [126] for a sample of nearby clusters using upper limits on the diffuse radio emission, low levels of observed diffuse emission, or detections of radio mini-haloes. It was found that the strongest limits on the annihilation cross section are better than limits derived from the non-detection of clusters in the gamma-ray band by a factor of ~ 3 or more when the same annihilation channel and substructure model, but different best-case clusters, are compared. The limits on the cross section depend on the assumed amount of substructure, varying by as much as 2 orders of magnitude for increasingly optimistic substructure models as compared to a smooth NFW profile.

Local dwarf spheroidal (dSph) galaxies are also potentially good targets for multi-wavelength searches; unlike the galactic center region or galaxy clusters, no significant diffuse radio, X-ray or gamma-ray emission is expected: the gravitational potential well of dSph galaxies is too shallow for them to host any sizable thermal bremsstrahlung emission at X-ray frequencies, and, more importantly, the gas densities appear to

be extremely low (e.g.,[267]). Constraints on particle dark matter models from observations of dSph with X-rays were given in [268]. The hard X-ray regime was analyzed more recently in [269].

Future studies and future observations hold much promise for even tighter constraints on dark matter from multi wavelength, and specifically radio, observations.

5 Experimental Methods and Key Enabling Technologies

5.1 Atmospheric Cherenkov Detectors

An Imaging Atmospheric Cherenkov Telescope (IACT) is essentially a wide-field optical telescope consisting of a large reflector (typically in a short focal-length f/0.6 to f/1.5 optical system) with a high-speed camera in the focal plane. To date, most ACT cameras use arrays of hundreds of photomultiplier tubes for their cameras, although new cameras are under development that make use of solid-state photomultipliers (SiPMs) where each pixel is made up of an array of small $\lesssim$100μm geiger-mode avalanche photodiode (APD) cells. Very large reflectors, and short exposures ($\lesssim$ 20nsec) are required to detect the faint flashes of Cherenkov light against the Poisson fluctuation in the night sky background. The signal to noise-ratio for detecting Cherenkov light flashes is proportional to the square root of the mirror area $A_{\rm m}$ times the reflectivity of the optics and quantum efficiency of the photodetectors ϵ and inversely proportional to the square root of the signal-integration timescale τ and solid angle of the pixels $\Omega_{\rm pix}$. Since the energy threshold is inversely proportional to the SNR it is advantageous to maximize the mirror area and throughput of the optical system to minimize the threshold. Operation at a dark site (and on moonless nights) is also important. Higher-speed photodetectors and electronics are required to minimize the integration time, ideally reducing this down to the shortest intrinsic timescale of the Cherenkov light wavefront (a few nanoseconds). Waveform digitizers are often employed in the camera electronics to handle the variation in the time profile of events with increasing impact parameter, and to buffer the event data for a long enough time to allow for the development of the trigger. The minimum angular size of the shower is determined by the angular extent of the core of the lateral distribution which is roughly 0.1° (full width) for a few-hundred GeV shower viewed at the zenith. To resolve the structure of a shower image, the angular resolution of the telescope, angular diameter of the pixels and the pointing accuracy of the telescope mount should all ideally be $\lesssim$0.1 deg. While the angular resolution requirement is considerably more relaxed than for an optical telescope (with $\lesssim$ arcsec optics), the field of view is substantially larger than most optical telescopes, with a $\gtrsim$ 3.5° FoV required to contain shower images from impact parameters $\sim$ 120m. Larger fields of view (up to 8° diameter) are being considered for the future CTA telescopes to provide a larger field of view for more efficient survey of the Galaxy, and better sensitivity to extended sources.

Images of the electromagnetic showers initiated by gamma rays have a compact elliptic shape, and the major axis of the ellipse indicates the shower axis projected onto the image plane. In contrast, the image of showers produced by cosmic-ray protons show complex structure due to hadronic interactions that produce neutral pions (and electromagnetic sub-showers initiated by the prompt decays of π^0s to gamma-rays) as well as penetrating muons from the decay of charged pions. The images of Cherenkov light observed by an individual IACT are typically analyzed by using a moment-analysis of the images to derive a set of quantities that characterize the roughly elliptical shape of the images. These are referred to as the *Hillas parameters* after Michael Hillas, who first proposed the present definition of these parameters [270]. Gamma rays are selected based on cuts on these parameters.

Arrays of telescopes provide stereoscopic imaging, with multiple images that better constrain the direction and energy of the gamma-ray shower. For analysis of data from multiple telescopes, one typically extends

the moment analysis approach and derives weighted combinations of the width and length parameters. A favored method is to calculate the mean-scaled-parameters (i.e., the mean-scaled-width MSW) and mean-scaled-length (MSL) from the Hillas parameters of the individual telescopes([271, 272]):

IACTs achieve their gamma/hadron separation based on intrinsic rejection of background at the trigger level, data selection based on the shape of the shower image (MSL and MSW) and on angular reconstruction and restriction of the point of origin of each candidate $\gamma-$rayevent to the source region. IACTs are triggered when several pixels in a camera exceed threshold, within some time coincidence window. By requiring a high multiplicity m for the coincidence, and a narrow time window τ the accidental trigger rate from the night sky background $R_{\rm acc}$ can be reduced well below the single pixel trigger rate R_1 according to the relation $R_{\rm acc} \propto R_1^m \tau^{m-1}$. Topological constraints (such as strict adjacency of triggering pixels, or requirements that the pixels lie within camera sectors) further reduce the accidentals rate from night-sky-background (and associated PMT after-pulsing). The local trigger signals from the individual telescopes are delayed (based on the position of the source) and brought into coincidence in an *array trigger* with a coincidence window ∼40-100 nsec. Cosmic-ray showers are also rejected at the trigger level due to their lower Cherenkov light yield than gamma-rays since for every neutral pion that gives rise to electromagnetic showers through $\pi^0 -> \gamma\gamma$ decay, roughly two thirds of the available energy goes into the formation of charged pions and penetrating muons and neutrinos that effectively reduce the available energy for the cascade.

Current generation experiments like VERITAS have typical data rates of about $50TB/year$. With an order of magnitude more pixels, lower energy thresholds, and at least an order of magnitude more telescopes, future ground-based gamma-ray experiments like CTA could easily result in several orders of magnitude higher data rates, if realtime (pipelined) compression and image processing is not done at the experiment.

Key enabling technologies for IACTs are high-quantum efficiency UV-blue photodetectors, low-cost large area mirrors, and high-speed waveform digitizers and data acquisition systems to handle the prodigious data rates.

5.2 Neutrino experiments

The IceCube neutrino observatory consists of 5160 optical sensors or Digital Optical Modules (DOMs) installed on 86 strings between 1450 m and 2450 m below the surface. Fifteen of the 86 strings were deployed at higher module density and comprise the sub-array DeepCore. DeepCore was designed to provide sensitivity to neutrinos at energies over an order of magnitude lower than initially envisioned for the original array, as low as about 10 GeV. The In-Ice array is complemented by a surface array, called IceTop. IceTop consists of 160 ice-tanks, in pairs, near the top of each string. Each tank has two DOMs for redundancy and extended dynamic range.

Each string is instrumented with 60 DOMs capable of detecting signals over a wide dynamic range, from a single photon to several thousands arriving within a few microseconds of each other. Strings are deployed in a triangular grid pattern with a characteristic spacing of 125 m (72 m for DeepCore) enclosing an area of 1 km^2. Each hole cable, which carries 60 DOMs, is connected to a surface junction box placed between the two IceTop tanks. The IceTop DOMs are also connected to the surface junction box. A cable from the surface junction box to the central counting house carries all DOM cables and service wires. Signals are digitized and time stamped in the modules. Times and waveforms from several modules are used to reconstruct events from the Cherenkov light emitted by charged particles in the deep ice and in the IceTop tanks.

5.3 Technology overlaps with other CF subgroups and Frontiers

The main instrumentation issue confronting the high energy gamma-ray and neutrino detector community is the cost of photon detection technology. Traditional PMTs have the requisite performance to extract the physics but their cost is prohibitive. A less expensive photon detection technology with comparable performance to PMTs would open up a number of highly interesting opportunities in fundamental neutrino physics, supernova neutrino burst detection, proton decay and indirect dark matter detection.

Development of UV-blue sensitive photodetectors is not only important for Atmospheric Cherenkov Telescopes (like CTA), but also for HEP detectors (Cherenkov and new high-yield scintillators), and liquid noble detectors. The wavelengths of interest are roughly 125nm for liquid Ar fluorescence, 175nm for Liquid Xe fluorescence, 320nm for ground-based instruments, and (as an example of a modern high-yield scintillator) 380nm for LaBr3. Despite progress in Silicon-based solid state detectors (e.g., Geiger-mode APDs) the surface of Silicon has a poor response in this regime. Development of photodetectors based on III-V (nitride) semiconductors (AlN, GaN - InN) offers potential for this wavelength regime.

Neutrino and gamma-ray DM-indirect detection (ID) detectors as well as liquid-Noble DM-Direct Detection experiments rely on high speed (¿100 Msps) waveform digitizers. Development in this area would be of broad benefit. For neutrino and gamma-ray experiments, analog pipeline ASICs with deep memory (up to $\sim$ several μsecs) are likely to be a key enabling technology. For DD, waveform digitizers with even deeper memory (up to millisec depth) and wider dynamic range (up to 14 bits) are desirable and currently only FADCs are viable. Outside of the Cosmic Frontier, other detector developments (e.g., psec-timing devices for particle ID) also rely on high-speed waveform digitizers (e.g, multi Gsps analog pipelines as developed for the LAPPD project) with similar architecture.

Microchannel plates (MCPs) and MCP based photodetectors also play a unique roll in photodetection, providing higher gain, lower electronic read noise than other solid state detectors- while still providing high resolution imaging. The LAPPD project has developed ALD coated detectors suitable for low counting rate applications. The Berkeley SSL group has demonstrated that cross-strip detectors can be used to achieve mega-pixel resolution by centroiding the MCP charge cloud, giving these devices the potential for combining single photon detection, essentially unlimited frame rates, but very high spatial resolution. However, current MCPs are not suitable many of the most interesting applications in the cosmic frontier (e.g, atmospheric Cherenkov detectors, widefield optical surveys) where the MCP is exposed to a high level of night-sky background. This results in the need for higher bias currents, resulting in thermal runaway or short lifetimes due to the limits of the MCP secondary emission coating. ALD offers a way to address these issues, making a new class of imaging, photoncounting, fast timing detectors possible. Efforts to produce MCP-based photodetectors with lower gains, and longer lifetimes are key advances needed to find broader applications of MCP photodetectors to CF experiments.

For detectors with megaton and larger fiducial volumes, like IceCube and the possible HyperK, KM3NeT, PINGU and MICA detectors, better than ns-scale timing resolution is not needed. The Cherenkov photons being detected have generally traveled through tens of meters of medium (ice or water) and experienced delays due to scattering. Their timing residuals–the difference in arrival time for a given photon undergoing scattering vs that same photon traveling in a straight line–easily reach ns-scales. Also, segmentation of the photosensitive element can improve the directionality these large detectors. For instance, instead of housing a single large PMT inside each pressure vessel, KM3NeT is likely to put dozens of much smaller (3") PMTs inside, each facing outward in a different direction. They can then determine from which direction a given photon came by using their knowledge of which PMT or PMTs got hit. Segmentation is thus readily achieved by adding more photosensitive elements, something that is feasible provided the cost of individual elements is low. For future neutrino telescopes, the key enabling technology would be low-cost blue-sensitive, large

area photodetectors. Preferably such devices would be available from a number of vendors to reduce risk (technical risk, budgetary risk and schedule risk) for this critical component of these experiments.

6 Tough Questions

As part of this planning process, tough questions were solicited from the particle physics community, and addressed to the various subgroups. Here, we explicitly answer two tough questions that were addressed to the CF2 subgoup.

(1) Tough question CF11 "*Can dark matter be convincingly discovered by indirect searches given astrophysical and propagation model uncertainties? Do indirect searches only serve a corroborating role?*"

As discussed extensively in §4.2 uncertainties in propagation models have a significant impact on the interpretation of the positron excess. However, a sharp spectral feature could stand out above the background, producing a strong indication of a dark matter signal. Some have argued for a dark matter interpretation in the AMS signal from the observed high level of spatial isotropy in the signal [10], the argument being that an astrophysical source (such as a nearby Pulsar) would reveal an observable anisotropy. However, this argument is problematic, since a secondary source of positrons (from cosmic-ray interactions) could also yield a high level of isotropy. In general, an observable positron signal (at the level of the current detection) would require a large astrophysical or particle physics boost. An astrophysical boost due to a nearby dark matter clump would result in an anisotropy similar to a pulsar or other point source.

However, the detection of a high energy neutrino signal from the sun, or a narrow gamma-ray line could provide a smoking-gun signal, and more than just a corroborating evidence. Even if the LHC or Direct Detection experiment sees a signal from dark matter, gamma-ray measurements would go further than just confirming such a detection: the observed spectrum would provide much better constraints on the dark matter particle mass, and details of the spectrum could help to identify the primary annihilation channels. Indirect detection, in this sense, is better described as *complementary* rather than *corroborating*.

(2) Tough Question CF12 "*Given large and unknown astrophysics uncertainties (for example, when observing the galactic center), what is the strategy to make progress in a project such as CTA which is in new territory as far as backgrounds go? How can we believe the limit projections until we have a better indication for backgrounds and how far does* Fermi *data go in terms of suggesting them? What would it take to convince ourselves we have a discovery of dark matter?*"

It should be emphasized that nearby dwarf satellite galaxies have no known high energy ($\gtrsim$GeV) backgrounds, and predictions for the annihilation signals are robust and relatively insensitive to astrophysical uncertainties. However, it is true that the astrophysical backgrounds for the Galactic center (GC) are quite large and uncertain. Similarly, models for the halo profile in the inner Galaxy have large uncertainties: as discussed in this report, baryonic matter could erase the central cusp leaving a cored halo, or adiabatic growth of the central black hole could result in a very steep inner halo profile that leads to a very large enhancement in the gamma-ray signal. The dominant gamma-ray background at the GC comes from the bright point source at the position of Sgr A*. Since the diffuse gamma-ray background falls as a fairly steep function of energy, the confusion from the strong diffuse gamma-ray backgrounds that makes measurements at GeV energies (with *Fermi*) very difficult are significantly reduced at energies above 100 GeV (as detected with ground-based gamma-ray instruments). Combined with the excellent angular resolution of ground based instruments $\lesssim 0.1^\circ$, it is possible to show that the GC source is consistent with a point source to within this resolution. It is also possible to determine the distribution of other sources along the galactic plane. Sensitivity estimates for the Galactic center region take this knowledge of source locations and create exclusion regions. DM

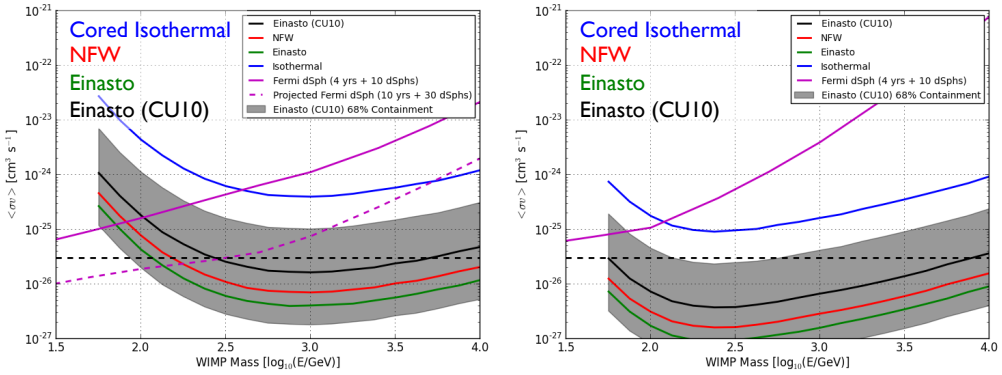

Figure 24: Estimated sensitivity of the enhanced CTA experiment to dark matter for Galactic center observations, taking into account the most likely and most conservative halo models.

upper limits produced with H.E.S.S., e.g., [199] exclude these regions but do not make any further attempt to subtract (or perform a joint fit) with other diffuse backgrounds, and hence are robust. These upper limits already reach a level only an order of magnitude above the GC. Even with the diffuse backgrounds present in the *Fermi* data, one can estimate that *with no background subtraction* the integral *Fermi* flux between 1-3 GeV and within 1° or the GC ($F \approx 1 \times 10^{-7}\mathrm{cm}^{-2}\mathrm{s}^{-1}$) gives an upper limit of $\langle \sigma\, v \rangle \approx 1.6 \times 10^{-25}\mathrm{cm}^{3}\mathrm{s}^{-1}$ less than an order of magnitude above the natural cross-section (T. Linden, private communication).

The best information about the extent of this point source and other sources actually comes from ground-based observatories, not *Fermi*. It is true that there is some uncertainty in the GC fluxes resulting from assumptions about the halo profile in the inner Galaxy. Moreover, neither N-body simulations or dynamical measurements (the rotation curve of the Galaxy) *directly* constrain the Galactic halo profile on scales much less than 1kpc. But given the bright point source at the GC, estimates already exclude the innermost part of the halo profile and rely on an annulus around the galactic center, somewhat mitigating this error. To quantitatively address this real systematic error, in Fig. 24 we show the effect of uncertainties in the GC halo model on the dark matter constraints. This figure clearly indicates that the GC measurements with an augmented CTA instrument are still sensitive enough to constrain the all but the most conservative (and physically unrealistic) isothermal distribution.

7 Complementarity

While a much more detailed study of complementarity of Dark Matter detection techniques is given in the CF4 report, here we summarize some of the most important observations made from our scans using the pMSSM benchmark models. Fig. 25 shows the survival and exclusion rates resulting from the various dark matter searches and their combinations in the LSP mass-scaled SI cross section plane (coordinates most relevant for direct detection experiments, but illustrative of the overall complementarity of techniques). In the upper left panel we compare these for the combined direct detection (DD = XENON1T + COUPP500) and indirect detection (ID = *Fermi*+ CTA) DM searches. While the distribution of model points, and priors for these distributions are a subject for religion rather than science, these scans provide some sense of how the different experimental techniques constrain the model space. For example, we see that 11% (15%) of the models are excluded by ID but not DD (excluded by DD but not ID) while 8% are excluded by both searches.

On the other hand, we also see that 66% of the models survive both sets of DM searches; 41% of this subset of models, in turn, are excluded by the LHC searches. Note that the DD- and ID-excluded regions are all relatively well separated in terms of mass and cross section although there is some overlap between the sets of models excluded by the different experiments. In particular we see that the ID searches (here almost entirely CTA) are covering the heavy LSP region even in cases where the SI cross section is very low and likely beyond the reach of any potential DD experiment. Similarly, in the upper right panel we see that 22% (0%) of the models are excluded uniquely by DD (IceCube) only while 1% can be simultaneously excluded by both sets of searches and 77% would be missed by either search set. In the lower left panel, ID and LHC searches are compared and we see that 17% (32%) of the models would be excluded only by the ID (LHC) searches. However, 2% (50%) of the models are seen to be excluded by (or would survive) both searches. The strong complementarity between the LHC, CTA and XENON1T experiments is evident here as CTA probes the high LSP mass region very well where winos and Higgsinos dominate, a 1T Xenon detector chops off the top of the distribution where the well-tempered neutralino LSP states dominate, while the LHC covers the relatively light LSP region (independent of LSP type) rather well. Of course the strength of the LHC coverage will significantly improve in the future as here only 7 and partial 8 TeV analysis results have been employed. In the lower right panel the relative contributions arising from the LHC and CTA searches to the model survival/exclusion are shown. Here the intensity of a given bin indicates the fraction of models excluded there by the combination of both CTA and the LHC while the color itself indicates the weighting from CTA (blue) and LHC (red). It is again quite clear that CTA completely dominates for large LSP masses (which correspond to the mostly wino and Higgsino LSPs) and also competes with the LHC throughout the band along the top of the distribution where the LSP thermal relic density is approximately saturating WMAP/Planck. The LHC covers the rest of the region but is not yet as effective as CTA (excluding a smaller fraction of models in the relevant bins). In the future we will examine how including the new 8 TeV LHC analyses and our extrapolation to 14 TeV will enhance the effectiveness of the LHC searches; we expect these improvements to be substantial.

8 Conclusions

We have described the primary methods of Indirect Detection including observation of charged cosmic-ray antimatter, searches for high energy neutrinos from annihilation in the sun, astrophysical signatures such as radio and hard X-ray emission and gamma-ray measurements in the center of our own Galactic halo, in nearby Dwarf galaxies and in clusters. Just as the next generation of direct detection experiments is approaching the natural cross-section range, and reaching the limit of the technique (from the irreducible background of pp and atmospheric neutrinos), the light (or perhaps dark) at the end of the tunnel is now clearly in view for gamma-ray searches as well. Given the close relation of the gamma-ray production cross-section to the total annihilation cross section, the bulk of the likely parameter space for SUSY WIMPs (or, in fact, any weakly interacting massive thermal relic) is within reach. A future experiment like CTA, with the U.S. enhancement (to increase sensitivity by a factor of 3, increase the field of view and enhance angular resolution) could reach most of the majority of the parameter space through observations of the GC for all but the most pessimistic assumptions about the halo profile, or new astrophysical backgrounds. While the most conservative estimates of sensitivity to Dwarf galaxies (assuming a boost of one) will still fall short for the most conservative halo models, a small boost in any one of these objects leads to the potential for discovery of a clean signal. If SUSY is not to be, and if some other model for low-mass WIMPs prevails, antideuteron experiments or hard X-ray measurements may provide another avenue for discovery. The best future space-based instrument for these searches is the continued operation of *Fermi* for at least 5 more years. An extension of *Fermi* leads to a linear (not square-root) improvement in the DM limits with time, since the observations are currently signal not background limited.

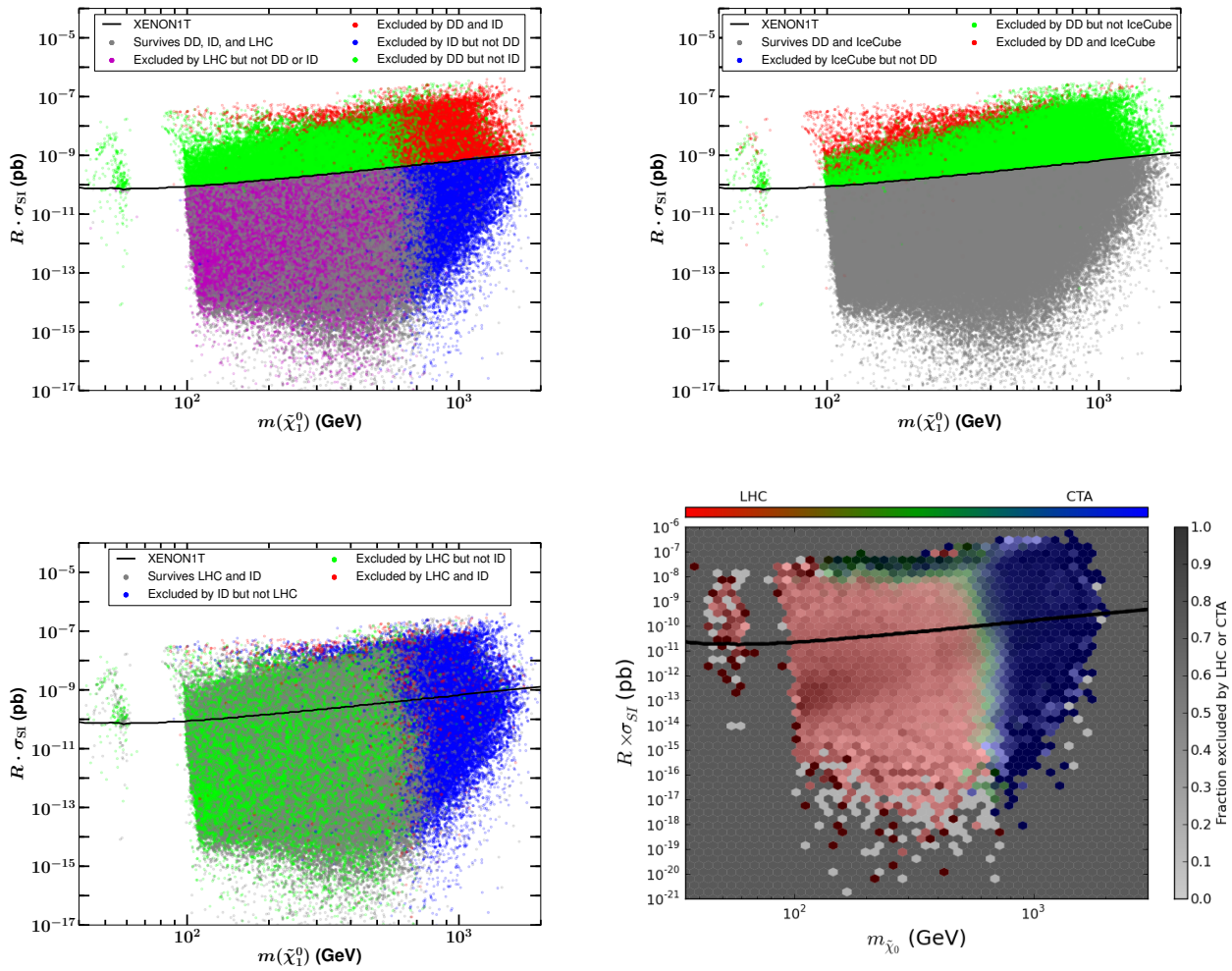

Figure 25: Comparisons of the models surviving or being excluded by the various searches in the LSP mass-scaled SI cross section plane as discussed in the text. The SI XENON1T line is shown as a guide to the eye.

Clearly, without indirect detection we are missing a key component of a comprehensive dark matter program. Perhaps it is important to consider various scenarios for how we might finally solve the dark matter problem to see just what we might be missing: Say that the G2 (or even G3) detectors (now limited by irreducible backgrounds from diffuse neutrinos) see a hint of a signal in the form of an exponential tail of events, suggesting a WIMP with a mass greater than that of the recoil nucleus, but little more information. And say that the LHC continues to find no evidence for dark matter up to energies of 1 TeV. Would we have a discovery of dark matter? But perhaps a future gamma-ray experiment could observe a peculiar hard spectrum that cuts off at several TeV both in the Galactic center, and in one of a few of the most promising dwarf spheroidal galaxies (at precisely the same energy, with the same spectral shape). If this would not provide the smoking gun detection of dark matter, wouldn't this provide a great motivation to push the energy frontier to still higher energies, and build a larger accelerator to definitively measure DM properties in the lab? Or, in another scenario, say that the LHC sees evidence for missing energy or missing momentum,

only weakly constraining the mass of the new particle and with no clear link of this with the dark matter - wouldn't it be desirable to build the biggest, most capable gamma-ray experiment to identify this particle on the sky, improve the mass measurement, and help identify the branching ratios through the spectral shape? Or perhaps the future upgrades of IceCube will result in a highly significant signal of high energy neutrinos from the sun, with energy that corresponds to the cutoff in the gamma-ray spectrum of an extended halo around the galactic center. Clearly this would be both a solution to the dark matter problem, and would provide a number of key measurements necessary to identify the particle properties and to map out the inner halo, beyond the resolution limits of dynamical measurements or N-body simulations. One could go on, but the message should be clear; indirect detection stands as one of the key pillars on which the U.S. dark matter program should be constructed.

Solar WIMP searches are quite competitive with direct searches [273, 274, 275, 276], currently beating out direct searches by orders of magnitude for spin-dependent WIMP-proton interactions and $m_\chi \gtrsim 10$ GeV. If large direct experiments like COUPP go forward, solar WIMP neutrino searches will cede some ground in the near term, but future upgrades to neutrino experiments (like PINGU) may once agian make these indirect searches the most sensitive for probing spin-dependent cross sections. Stacked Milky Way dwarf searches are already excluding highly interesting regions of WIMP parameter space—in particular, at small WIMP masses ($m_\chi \lesssim 30$ GeV but above a few GeV, driven by *Fermi*-LAT sensitivity). Limits are likely to improve as *Fermi* runs longer and more Milky Way dwarf galaxies are discovered in the southern hemisphere with the Dark Energy Survey. These analyses typically assume a boost factor of 1, which is generically a conservative choice.

ACKNOWLEDGEMENTS

We are grateful to Jonathan Feng and Steve Ritz for coordinating the Cosmic Frontier working group, and for all of the contributions from individuals and Collaborations in the indirect detection community.

References

[1] D. Bauer, J. Buckley, M. Cahill-Rowley, R. Cotta, A. Drlica-Wagner, J. Feng, S. Funk, J. Hewett, D. Hooper, A. Ismail, M. Kaplinghat, A. Kusenko, K. Matchev, D. McKinsey, T. Rizzo, W. Shepherd, T. M. P. Tait, A. M. Wijangco, and M. Wood, "Dark Matter in the Coming Decade: Complementary Paths to Discovery and Beyond," *ArXiv e-prints* (May, 2013) , arXiv:1305.1605 [hep-ph].

[2] E. Komatsu, K. M. Smith, J. Dunkley, C. L. Bennett, B. Gold, G. Hinshaw, N. Jarosik, D. Larson, M. R. Nolta, L. Page, D. N. Spergel, M. Halpern, R. S. Hill, A. Kogut, M. Limon, S. S. Meyer, N. Odegard, G. S. Tucker, J. L. Weiland, E. Wollack, and E. L. Wright, "Seven-year Wilkinson Microwave Anisotropy Probe (WMAP) Observations: Cosmological Interpretation," *ApJS* **192** (Feb., 2011) 18, arXiv:1001.4538 [astro-ph.CO].

[3] Planck Collaboration, P. A. R. Ade, N. Aghanim, C. Armitage-Caplan, M. Arnaud, M. Ashdown, F. Atrio-Barandela, J. Aumont, C. Baccigalupi, A. J. Banday, and et al., "Planck 2013 results. XVI. Cosmological parameters," *ArXiv e-prints* (Mar., 2013) , arXiv:1303.5076 [astro-ph.CO].

[4] G. Jungman, M. Kamionkowski, and K. Griest, "Supersymmetric dark matter," *Phys.Rept.* **267** (1996) 195–373, arXiv:hep-ph/9506380 [hep-ph].

[5] J. Knodlseder, V. Lonjou, P. Jean, M. Allain, P. Mandrou, *et al.*, "Early SPI / INTEGRAL contraints on the morphology of the 511 keV line emission in the 4th galactic quadrant," *Astron.Astrophys.* **411** (2003) L457–L460, arXiv:astro-ph/0309442 [astro-ph].

[6] M. Su, T. R. Slatyer, and D. P. Finkbeiner, "Giant Gamma-ray Bubbles from Fermi-LAT: AGN Activity or Bipolar Galactic Wind?," *Astrophys.J.* **724** (2010) 1044–1082, arXiv:1005.5480 [astro-ph.HE].

[7] T. Bringmann, X. Huang, A. Ibarra, S. Vogl, and C. Weniger, "Fermi LAT Search for Internal Bremsstrahlung Signatures from Dark Matter Annihilation," *JCAP* **1207** (2012) 054, arXiv:1203.1312 [hep-ph].

[8] C. Weniger, "A Tentative Gamma-Ray Line from Dark Matter Annihilation at the Fermi Large Area Telescope," *JCAP* **1208** (2012) 007, arXiv:1204.2797 [hep-ph].

[9] **PAMELA Collaboration** Collaboration, O. Adriani *et al.*, "An anomalous positron abundance in cosmic rays with energies 1.5-100 GeV," *Nature* **458** (2009) 607–609, arXiv:0810.4995 [astro-ph].

[10] **AMS Collaboration** Collaboration, M. Aguilar *et al.*, "First Result from the Alpha Magnetic Spectrometer on the International Space Station: Precision Measurement of the Positron Fraction in Primary Cosmic Rays of 0.5 - 350 GeV," *Phys.Rev.Lett.* **110** no. 14, (2013) 141102.

[11] C. Boehm, D. Hooper, J. Silk, M. Casse, and J. Paul, "MeV dark matter: Has it been detected?," *Phys.Rev.Lett.* **92** (2004) 101301, arXiv:astro-ph/0309686 [astro-ph].

[12] D. Hooper, F. Ferrer, C. Boehm, J. Silk, J. Paul, *et al.*, "Possible evidence for MeV dark matter in dwarf spheroidals," *Phys.Rev.Lett.* **93** (2004) 161302, arXiv:astro-ph/0311150 [astro-ph].

[13] D. Hooper and T. R. Slatyer, "Two Emission Mechanisms in the Fermi Bubbles: A Possible Signal of Annihilating Dark Matter," arXiv:1302.6589 [astro-ph.HE].

[14] D. Hooper and T. Linden, "On The Origin Of The Gamma Rays From The Galactic Center," *Phys.Rev.* **D84** (2011) 123005, arXiv:1110.0006 [astro-ph.HE].

[15] K. N. Abazajian and M. Kaplinghat, "Detection of a Gamma-Ray Source in the Galactic Center Consistent with Extended Emission from Dark Matter Annihilation and Concentrated Astrophysical Emission," *Phys.Rev.* **D86** (2012) 083511, arXiv:1207.6047 [astro-ph.HE].

[16] C. Boehm, T. Ensslin, and J. Silk, "Can Annihilating dark matter be lighter than a few GeVs?," *J.Phys.* **G30** (2004) 279–286, arXiv:astro-ph/0208458 [astro-ph].

[17] C. Boehm and P. Fayet, "Scalar dark matter candidates," *Nucl.Phys.* **B683** (2004) 219–263, arXiv:hep-ph/0305261 [hep-ph].

[18] D. Hooper, A. Stebbins, and K. M. Zurek, "Excesses in cosmic ray positron and electron spectra from a nearby clump of neutralino dark matter," *Phys.Rev.* **D79** (2009) 103513, arXiv:0812.3202 [hep-ph].

[19] L. Pieri, J. Lavalle, G. Bertone, and E. Branchini, "Implications of High-Resolution Simulations on Indirect Dark Matter Searches," *Phys.Rev.* **D83** (2011) 023518, arXiv:0908.0195 [astro-ph.HE].

[20] J. Hisano, S. Matsumoto, M. M. Nojiri, and O. Saito, "Non-perturbative effect on dark matter annihilation and gamma ray signature from galactic center," *Phys.Rev.* **D71** (2005) 063528, arXiv:hep-ph/0412403 [hep-ph].

[21] N. Arkani-Hamed, D. P. Finkbeiner, T. R. Slatyer, and N. Weiner, "A theory of dark matter," *Physics Review D* **79** no. 1, (Jan., 2009) 015014–+, arXiv:0810.0713.

[22] M. Pospelov and A. Ritz, "Astrophysical Signatures of Secluded Dark Matter," *Phys.Lett.* **B671** (2009) 391–397, arXiv:0810.1502 [hep-ph].

[23] M. Cirelli, A. Strumia, and M. Tamburini, "Cosmology and Astrophysics of Minimal Dark Matter," *Nucl.Phys.* **B787** (2007) 152–175, arXiv:0706.4071 [hep-ph].

[24] F. Donato, D. Maurin, P. Brun, T. Delahaye, and P. Salati, "Constraints on WIMP Dark Matter from the High Energy PAMELA $\bar{p}/p$ data," *Phys.Rev.Lett.* **102** (2009) 071301, arXiv:0810.5292 [astro-ph].

[25] G. Bertone, M. Cirelli, A. Strumia, and M. Taoso, "Gamma-ray and radio tests of the e+e- excess from DM annihilations," *JCAP* **0903** (2009) 009, arXiv:0811.3744 [astro-ph].

[26] L. Bergstrom, G. Bertone, T. Bringmann, J. Edsjo, and M. Taoso, "Gamma-ray and Radio Constraints of High Positron Rate Dark Matter Models Annihilating into New Light Particles," *Phys.Rev.* **D79** (2009) 081303, arXiv:0812.3895 [astro-ph].

[27] M. Cirelli, P. Panci, and P. D. Serpico, "Diffuse gamma ray constraints on annihilating or decaying Dark Matter after Fermi," *Nucl.Phys.* **B840** (2010) 284–303, arXiv:0912.0663 [astro-ph.CO].

[28] A. De Simone, A. Riotto, and W. Xue, "Interpretation of AMS-02 Results: Correlations among Dark Matter Signals," *JCAP* **1305** (2013) 003, arXiv:1304.1336 [hep-ph].

[29] C. Weniger, "A tentative gamma-ray line from Dark Matter annihilation at the Fermi Large Area Telescope," *JCAP* **8** (Aug., 2012) 7, arXiv:1204.2797 [hep-ph].

[30] D. Hooper and L. Goodenough, "Dark matter annihilation in the Galactic Center as seen by the Fermi Gamma Ray Space Telescope," *Physics Letters B* **697** (Mar., 2011) 412–428, arXiv:1010.2752 [hep-ph].

[31] M. Ackermann, M. Ajello, A. Albert, W. B. Atwood, L. Baldini, J. Ballet, G. Barbiellini, D. Bastieri, K. Bechtol, R. Bellazzini, B. Berenji, R. D. Blandford, E. D. Bloom, E. Bonamente, A. W. Borgland, J. Bregeon, M. Brigida, P. Bruel, R. Buehler, T. H. Burnett, S. Buson, G. A. Caliandro, R. A. Cameron, B. Cañadas, P. A. Caraveo, J. M. Casandjian, C. Cecchi, E. Charles, A. Chekhtman, J. Chiang, S. Ciprini, R. Claus, J. Cohen-Tanugi, J. Conrad, S. Cutini, A. de Angelis, F. de Palma, C. D. Dermer, S. W. Digel, E. Do Couto E Silva, P. S. Drell, A. Drlica-Wagner, L. Falletti, C. Favuzzi, S. J. Fegan, E. C. Ferrara, Y. Fukazawa, S. Funk, P. Fusco, F. Gargano, D. Gasparrini, N. Gehrels, S. Germani, N. Giglietto, F. Giordano, M. Giroletti, T. Glanzman, G. Godfrey, I. A. Grenier, S. Guiriec, M. Gustafsson, D. Hadasch, M. Hayashida, E. Hays, R. E. Hughes, T. E. Jeltema, G. Jóhannesson, R. P. Johnson, A. S. Johnson, T. Kamae, H. Katagiri, J. Kataoka, J. Knödlseder, M. Kuss, J. Lande, L. Latronico, A. M. Lionetto, M. Llena Garde, F. Longo, F. Loparco, B. Lott, M. N. Lovellette, P. Lubrano, G. M. Madejski, M. N. Mazziotta, J. E. McEnery, J. Mehault, P. F. Michelson, W. Mitthumsiri, T. Mizuno, C. Monte, M. E. Monzani, A. Morselli, I. V. Moskalenko, S. Murgia, M. Naumann-Godo, J. P. Norris, E. Nuss, T. Ohsugi, A. Okumura, N. Omodei, E. Orlando, J. F. Ormes, M. Ozaki, D. Paneque, D. Parent, M. Pesce-Rollins, M. Pierbattista, F. Piron, G. Pivato, T. A. Porter, S. Profumo, S. Rainò, M. Razzano, A. Reimer, O. Reimer, S. Ritz, M. Roth, H. F.-W. Sadrozinski, C. Sbarra, J. D. Scargle, T. L. Schalk, C. Sgrò, E. J. Siskind, G. Spandre, P. Spinelli, L. Strigari, D. J. Suson, H. Tajima, H. Takahashi, T. Tanaka, J. G. Thayer, J. B. Thayer, D. J. Thompson, L. Tibaldo, M. Tinivella, D. F. Torres, E. Troja, Y. Uchiyama, J. Vandenbroucke, V. Vasileiou, G. Vianello, V. Vitale, A. P. Waite, P. Wang, B. L. Winer, K. S. Wood, M. Wood, Z. Yang, S. Zimmer, M. Kaplinghat, and G. D. Martinez, "Constraining Dark Matter Models from a Combined Analysis of Milky Way Satellites with the Fermi Large Area Telescope," *Physical Review Letters* **107** no. 24, (Dec., 2011) 241302, `arXiv:1108.3546 [astro-ph.HE]`.

[32] R. Cowsik, B. Burch, and T. Madziwa-Nussinov, "The origin of the spectral intensities of cosmic-ray positrons," *ArXiv e-prints* (May, 2013) , `arXiv:1305.1242 [astro-ph.HE]`.

[33] R. Cowsik and B. Burch, "Positron fraction in cosmic rays and models of cosmic-ray propagation," *Physics Review D* **82** no. 2, (July, 2010) 023009.

[34] V. L. Ginzburg and S. I. Syrovatskii, *The Origin of Cosmic Rays*. 1964.

[35] I. V. Moskalenko and A. W. Strong, "Production and Propagation of Cosmic-Ray Positrons and Electrons," *Astrophysical Journal* **493** (Jan., 1998) 694, `arXiv:astro-ph/9710124`.

[36] G. Servant and T. M. P. Tait, "Is the lightest Kaluza-Klein particle a viable dark matter candidate?," *Nuclear Physics B* **650** (Feb., 2003) 391–419, `arXiv:hep-ph/0206071`.

[37] D. Hooper and S. Profumo, "Dark matter and collider phenomenology of universal extra dimensions," *Phys. Rep.* **453** (Dec., 2007) 29–115, `arXiv:hep-ph/0701197`.

[38] K. Griest and M. Kamionkowski, "Unitarity limits on the mass and radius of dark-matter particles," *Physical Review Letters* **64** (Feb., 1990) 615–618.

[39] S. Profumo, "TeV γ-rays and the largest masses and annihilation cross sections of neutralino dark matter," *Physics Review D* **72** no. 10, (Nov., 2005) 103521, `arXiv:astro-ph/0508628`.

[40] S. P. Martin, "A Supersymmetry primer," `arXiv:hep-ph/9709356 [hep-ph]`.

[41] T. Cohen and J. G. Wacker, "Here be Dragons: The Unexplored Continents of the CMSSM," *ArXiv e-prints* (May, 2013) , `arXiv:1305.2914 [hep-ph]`.

[42] G. ATLAS Collaboration Aad, T. Abajyan, B. Abbott, J. Abdallah, S. Abdel Khalek, A. A. Abdelalim, O. Abdinov, R. Aben, B. Abi, M. Abolins, and et al., "Observation of a new particle in the search for the Standard Model Higgs boson with the ATLAS detector at the LHC," *Physics Letters B* **716** (Sept., 2012) 1–29, arXiv:1207.7214 [hep-ex].

[43] S. CMS Collaboration Chatrchyan, V. Khachatryan, A. M. Sirunyan, A. Tumasyan, W. Adam, E. Aguilo, T. Bergauer, M. Dragicevic, J. Erö, C. Fabjan, and et al., "Observation of a new boson at a mass of 125 GeV with the CMS experiment at the LHC," *Physics Letters B* **716** (Sept., 2012) 30–61, arXiv:1207.7235 [hep-ex].

[44] A. Djouadi, S. Rosier-Lees, M. Bezouh, M. A. Bizouard, C. Boehm, F. Borzumati, C. Briot, J. Carr, M. B. Causse, F. Charles, X. Chereau, P. Colas, L. Duflot, A. Dupperin, A. Ealet, H. El-Mamouni, N. Ghodbane, F. Gieres, B. Gonzalez-Pineiro, S. Gourmelen, G. Grenier, P. Gris, J. . Grivaz, C. Hebrard, B. Ille, J. . Kneur, N. Kostantinidis, J. Layssac, P. Lebrun, R. Ledu, M. . Lemaire, C. LeMouel, L. Lugnier, Y. Mambrini, J. P. Martin, G. Montarou, G. Moultaka, S. Muanza, E. Nuss, E. Perez, F. M. Renard, D. Reynaud, L. Serin, C. Thevenet, A. Trabelsi, F. Zach, and D. Zerwas, "The Minimal Supersymmetric Standard Model: Group Summary Report," *ArXiv High Energy Physics - Phenomenology e-prints* (Jan., 1999) , arXiv:hep-ph/9901246.

[45] M. Loewenstein and A. Kusenko, "Dark Matter Search Using XMM-Newton Observations of Willman 1," *Astrophysical Journal* **751** (June, 2012) 82, arXiv:1203.5229 [astro-ph.CO].

[46] S. Chang and L. Goodenough, "Charge asymmetric cosmic ray signals from dark matter decay," *Physics Review D* **84** no. 2, (July, 2011) 023524, arXiv:1105.3976 [hep-ph].

[47] P. Bhattacharjee, "Origin and propagation of extremely high energy cosmic rays," *Phys. Rep.* **327** (Mar., 2000) 109–247, arXiv:astro-ph/9811011.

[48] M. Cahill-Rowley, J. L. Hewett, A. Ismail, and T. G. Rizzo, "pMSSM Studies at the 7, 8 and 14 TeV LHC," *ArXiv e-prints* (July, 2013) , arXiv:1307.8444 [hep-ph].

[49] M. W. Cahill-Rowley, J. L. Hewett, A. Ismail, and T. G. Rizzo, "More energy, more searches, but the phenomenological MSSM lives on," *Physics Review D* **88** no. 3, (Aug., 2013) 035002, arXiv:1211.1981 [hep-ph].

[50] M. W. Cahill-Rowley, J. L. Hewett, A. Ismail, and T. G. Rizzo, "Higgs sector and fine-tuning in the phenomenological MSSM," *Physics Review D* **86** no. 7, (Oct., 2012) 075015, arXiv:1206.5800 [hep-ph].

[51] E. Komatsu *et al.*, "Seven-Year Wilkinson Microwave Anisotropy Probe (WMAP) Observations: Cosmological Interpretation," arXiv:1001.4538 [astro-ph.CO].

[52] B. C. Allanach, "SOFTSUSY: A program for calculating supersymmetric spectra," *Computer Physics Communications* **143** (Mar., 2002) 305–331, arXiv:hep-ph/0104145.

[53] A. Djouadi, J.-L. Kneur, and G. Moultaka, "SuSpect: A Fortran code for the Supersymmetric and Higgs particle spectrum in the MSSM," *Computer Physics Communications* **176** (Mar., 2007) 426–455, arXiv:hep-ph/0211331.

[54] M. M. Muehlleitner, A. Djouadi, and M. Spira, "Decays of Supersymmetric Particles — the Program SUSY-HIT," *Acta Physica Polonica B* **38** (Feb., 2007) 635, arXiv:hep-ph/0609292.

[55] J. Ellis, K. Enqvist, D. V. Nanopoulos, and F. Zwirner, "Observables in Low-Energy Superstring Models," *Modern Physics Letters A* **1** (1986) 57–69.

[56] R. Barbieri and G. Giudice, "Upper Bounds on Supersymmetric Particle Masses," *Nucl.Phys.* **B306** (1988) 63.

[57]

[58] J. Diemand and B. Moore, "The structure and evolution of cold dark matter halos," *Adv.Sci.Lett.* **4** (2011) 297–310, arXiv:0906.4340 [astro-ph.CO].

[59] C. S. Frenk and S. D. White, "Dark matter and cosmic structure," *Annalen Phys.* **524** (2012) 507–534, arXiv:1210.0544 [astro-ph.CO].

[60] M. Kuhlen, M. Vogelsberger, and R. Angulo, "Numerical simulations of the dark universe: State of the art and the next decade," *Physics of the Dark Universe* **1** (Nov., 2012) 50–93, arXiv:1209.5745 [astro-ph.CO].

[61] J. F. Navarro, C. S. Frenk, and S. D. M. White, "A Universal Density Profile from Hierarchical Clustering," *Astrophysical Journal* **490** (Dec., 1997) 493–+, astro-ph/9611107.

[62] J. F. Navarro, E. Hayashi, C. Power, A. R. Jenkins, C. S. Frenk, S. D. M. White, V. Springel, J. Stadel, and T. R. Quinn, "The inner structure of ΛCDM haloes - III. Universality and asymptotic slopes," *Monthly Notices of the Royal Astronomical Society* **349** (Apr., 2004) 1039–1051, arXiv:astro-ph/0311231.

[63] J. F. Navarro, A. Ludlow, V. Springel, J. Wang, M. Vogelsberger, S. D. M. White, A. Jenkins, C. S. Frenk, and A. Helmi, "The diversity and similarity of simulated cold dark matter haloes," *Monthly Notices of the Royal Astronomical Society* **402** (Feb., 2010) 21–34, arXiv:0810.1522.

[64] J. S. Bullock, T. S. Kolatt, Y. Sigad, R. S. Somerville, A. V. Kravtsov, A. A. Klypin, J. R. Primack, and A. Dekel, "Profiles of dark haloes: evolution, scatter and environment," *Monthly Notices of the Royal Astronomical Society* **321** (Mar., 2001) 559–575, arXiv:astro-ph/9908159.

[65] R. H. Wechsler, J. S. Bullock, J. R. Primack, A. V. Kravtsov, and A. Dekel, "Concentrations of Dark Halos from Their Assembly Histories," *Astrophysical Journal* **568** (Mar., 2002) 52–70, arXiv:astro-ph/0108151.

[66] B. Allgood, R. A. Flores, J. R. Primack, A. V. Kravtsov, R. H. Wechsler, A. Faltenbacher, and J. S. Bullock, "The shape of dark matter haloes: dependence on mass, redshift, radius and formation," *Monthly Notices of the Royal Astronomical Society* **367** (Apr., 2006) 1781–1796, arXiv:astro-ph/0508497.

[67] G. R. Blumenthal, S. M. Faber, J. R. Primack, and M. J. Rees, "Formation of galaxies and large-scale structure with cold dark matter," *Nature* **311** (Oct., 1984) 517–525.

[68] O. Y. Gnedin, A. V. Kravtsov, A. A. Klypin, and D. Nagai, "Response of Dark Matter Halos to Condensation of Baryons: Cosmological Simulations and Improved Adiabatic Contraction Model," *Astrophys. J.* **616** (Nov., 2004) 16–26, arXiv:astro-ph/0406247.

[69] P. B. Tissera, S. D. M. White, S. Pedrosa, and C. Scannapieco, "Dark matter response to galaxy formation," *Monthly Notices of the Royal Astronomical Society* **406** (Aug., 2010) 922–935, arXiv:0911.2316 [astro-ph.CO].

[70] D. Martizzi, R. Teyssier, and B. Moore, "Cusp-core transformations induced by AGN feedback in the progenitors of cluster galaxies." arXiv:1211.2648, 2012.

[71] F. Governato, A. Zolotov, A. Pontzen, C. Christensen, S. H. Oh, A. M. Brooks, T. Quinn, S. Shen, and J. Wadsley, "Cuspy no more: how outflows affect the central dark matter and baryon distribution in Λ cold dark matter galaxies," *Monthly Notices of the Royal Astronomical Society* (Mar., 2012) 2697, arXiv:1202.0554 [astro-ph.CO].

[72] A. Pontzen and F. Governato, "How supernova feedback turns dark matter cusps into cores," *Monthly Notices of the Royal Astronomical Society* **421** (Apr., 2012) 3464–3471, arXiv:1106.0499 [astro-ph.CO].

[73] C. Scannapieco, M. Wadepuhl, O. H. Parry, J. F. Navarro, A. Jenkins, V. Springel, R. Teyssier, E. Carlson, H. M. P. Couchman, R. A. Crain, C. D. Vecchia, C. S. Frenk, C. Kobayashi, P. Monaco, G. Murante, T. Okamoto, T. Quinn, J. Schaye, G. S. Stinson, T. Theuns, J. Wadsley, S. D. M. White, and R. Woods, "The Aquila comparison project: the effects of feedback and numerical methods on simulations of galaxy formation," *Monthly Notices of the Royal Astronomical Society* **423** (June, 2012) 1726–1749, arXiv:1112.0315 [astro-ph.GA].

[74] M. Vogelsberger, A. Helmi, V. Springel, S. D. M. White, J. Wang, C. S. Frenk, A. Jenkins, A. Ludlow, and J. F. Navarro, "Phase-space structure in the local dark matter distribution and its signature in direct detection experiments," *Monthly Notices of the Royal Astronomical Society* **395** (May, 2009) 797–811, arXiv:0812.0362.

[75] V. Springel, J. Wang, M. Vogelsberger, A. Ludlow, A. Jenkins, A. Helmi, J. F. Navarro, C. S. Frenk, and S. D. M. White, "The Aquarius Project: the subhaloes of galactic haloes," *Mon. Not. R. Astron. Soc.* **391** (Dec., 2008) 1685–1711, arXiv:0809.0898.

[76] M. Kuhlen, J. Diemand, and P. Madau, "The Dark Matter Annihilation Signal from Galactic Substructure: Predictions for GLAST," *Astrophysical Journal* **686** (Oct., 2008) 262–278, arXiv:arXiv:0805.4416.

[77] G. D. Martinez, J. S. Bullock, M. Kaplinghat, L. E. Strigari, and R. Trotta, "Indirect Dark Matter detection from Dwarf satellites: joint expectations from astrophysics and supersymmetry," *Journal of Cosmology and Astro-Particle Physics* **6** (June, 2009) 14–+, arXiv:0902.4715.

[78] L. Gao, C. S. Frenk, M. Boylan-Kolchin, A. Jenkins, V. Springel, and S. D. M. White, "The statistics of the subhalo abundance of dark matter haloes," *Monthly Notices of the Royal Astronomical Society* **410** (Feb., 2011) 2309–2314, arXiv:1006.2882 [astro-ph.CO].

[79] L. Gao, C. S. Frenk, A. Jenkins, V. Springel, and S. D. M. White, "Where will supersymmetric dark matter first be seen?," *Monthly Notices of the Royal Astronomical Society* **419** (Jan., 2012) 1721–1726, arXiv:1107.1916 [astro-ph.CO].

[80] A. Pinzke, C. Pfrommer, and L. Bergström, "Prospects of detecting gamma-ray emission from galaxy clusters: Cosmic rays and dark matter annihilations," *Physics Review D* **84** no. 12, (Dec., 2011) 123509, arXiv:1105.3240 [astro-ph.HE].

[81] O. Y. Gnedin, L. Hernquist, and J. P. Ostriker, "Tidal Shocking by Extended Mass Distributions," *Astrophysical Journal* **514** (Mar., 1999) 109–118.

[82] E. D'Onghia, V. Springel, L. Hernquist, and D. Keres, "Substructure depletion in the Milky Way halo by the disk," *ArXiv e-prints* (July, 2009) , arXiv:0907.3482.

[83] A. Zolotov, A. M. Brooks, B. Willman, F. Governato, A. Pontzen, C. Christensen, A. Dekel, T. Quinn, S. Shen, and J. Wadsley, "Baryons Matter: Why Luminous Satellite Galaxies have Reduced Central Masses," *Astrophysical Journal* **761** (Dec., 2012) 71, arXiv:1207.0007 [astro-ph.CO].

[84] A. M. Brooks, M. Kuhlen, A. Zolotov, and D. Hooper, "A Baryonic Solution to the Missing Satellites Problem," *Astrophysical Journal* **765** (Mar., 2013) 22, arXiv:1209.5394 [astro-ph.CO].

[85] G. Lake, "Must the disk and halo dark matter be different?," *Astron. J.* **98** (Nov., 1989) 1554–1556.

[86] J. I. Read, G. Lake, O. Agertz, and V. P. Debattista, "Thin, thick and dark discs in ΛCDM," *Mon. Not. R. Astron. Soc.* **389** (Sept., 2008) 1041–1057, arXiv:arXiv:0803.2714.

[87] M. Rocha, A. H. G. Peter, J. S. Bullock, M. Kaplinghat, S. Garrison-Kimmel, J. Oñorbe, and L. A. Moustakas, "Cosmological simulations with self-interacting dark matter - I. Constant-density cores and substructure," *Monthly Notices of the Royal Astronomical Society* **430** (Mar., 2013) 81–104, arXiv:1208.3025 [astro-ph.CO].

[88] M. Vogelsberger and J. Zavala, "Direct detection of self-interacting dark matter," *Monthly Notices of the Royal Astronomical Society* **430** (Apr., 2013) 1722–1735, arXiv:1211.1377 [astro-ph.CO].

[89] N. Evans, F. Ferrer, and S. Sarkar, "A 'Baedecker' for the dark matter annihilation signal," *Phys.Rev.* **D69** (2004) 123501, arXiv:astro-ph/0311145 [astro-ph].

[90] Y. Ascasibar, P. Jean, C. Boehm, and J. Knoedlseder, "Constraints on dark matter and the shape of the Milky Way dark halo from the 511-keV line," *Mon.Not.Roy.Astron.Soc.* **368** (2006) 1695–1705, arXiv:astro-ph/0507142 [astro-ph].

[91] S. Campbell and B. Dutta, "Effects of P-wave Annihilation on the Angular Power Spectrum of Extragalactic Gamma-rays from Dark Matter Annihilation," *Phys.Rev.* **D84** (2011) 075004, arXiv:1106.4621 [astro-ph.HE].

[92] B. Robertson and A. Zentner, "Dark Matter Annihilation Rates with Velocity-Dependent Annihilation Cross Sections," *Phys.Rev.* **D79** (2009) 083525, arXiv:0902.0362 [astro-ph.CO].

[93] M. Kuhlen, N. Weiner, J. Diemand, P. Madau, B. Moore, *et al.*, "Dark Matter Direct Detection with Non-Maxwellian Velocity Structure," *JCAP* **1002** (2010) 030, arXiv:0912.2358 [astro-ph.GA].

[94] Y.-Y. Mao, L. E. Strigari, R. H. Wechsler, H.-Y. Wu, and O. Hahn, "Halo-to-Halo Similarity and Scatter in the Velocity Distribution of Dark Matter," *Astrophys.J.* **764** (2013) 35, arXiv:1210.2721 [astro-ph.CO].

[95] Y.-Y. Mao, L. E. Strigari, and R. H. Wechsler, "Connecting Direct Dark Matter Detection Experiments to Cosmologically Motivated Halo Models," *ArXiv e-prints* (Apr., 2013) , arXiv:1304.6401 [astro-ph.CO].

[96] M. T. Frandsen, F. Kahlhoefer, C. McCabe, S. Sarkar, and K. Schmidt-Hoberg, "Resolving astrophysical uncertainties in dark matter direct detection," *JCAP* **1201** (2012) 024, arXiv:1111.0292 [hep-ph].

[97] P. J. Fox, G. D. Kribs, and T. M. Tait, "Interpreting Dark Matter Direct Detection Independently of the Local Velocity and Density Distribution," *Phys.Rev.* **D83** (2011) 034007, arXiv:1011.1910 [hep-ph].

[98] B. Willman, J. J. Dalcanton, D. Martinez-Delgado, A. A. West, M. R. Blanton, D. W. Hogg, J. C. Barentine, H. J. Brewington, M. Harvanek, S. J. Kleinman, J. Krzesinski, D. Long, E. H. Neilsen, Jr., A. Nitta, and S. A. Snedden, "A New Milky Way Dwarf Galaxy in Ursa Major," *Astrophysical Journal, Letters* **626** (June, 2005) L85–L88, arXiv:astro-ph/0503552.

[99] V. Belokurov, D. B. Zucker, N. W. Evans, J. T. Kleyna, S. Koposov, S. T. Hodgkin, M. J. Irwin, G. Gilmore, M. I. Wilkinson, M. Fellhauer, D. M. Bramich, P. C. Hewett, S. Vidrih, J. T. A. De Jong, J. A. Smith, H. Rix, E. F. Bell, R. F. G. Wyse, H. J. Newberg, P. A. Mayeur, B. Yanny, C. M. Rockosi, O. Y. Gnedin, D. P. Schneider, T. C. Beers, J. C. Barentine, H. Brewington, J. Brinkmann, M. Harvanek, S. J. Kleinman, J. Krzesinski, D. Long, A. Nitta, and S. A. Snedden, "Cats and Dogs, Hair and a Hero: A Quintet of New Milky Way Companions," *Astrophysical Journal* **654** (Jan., 2007) 897–906, arXiv:astro-ph/0608448.

[100] S. M. Walsh, B. Willman, and H. Jerjen, "The Invisibles: A Detection Algorithm to Trace the Faintest Milky Way Satellites," *Astron. J.* **137** (Jan., 2009) 450–469, arXiv:0807.3345.

[101] D. B. Zucker, V. Belokurov, N. W. Evans, M. I. Wilkinson, M. J. Irwin, T. Sivarani, S. Hodgkin, D. M. Bramich, J. M. Irwin, G. Gilmore, B. Willman, S. Vidrih, M. Fellhauer, P. C. Hewett, T. C. Beers, E. F. Bell, E. K. Grebel, D. P. Schneider, H. J. Newberg, R. F. G. Wyse, C. M. Rockosi, B. Yanny, R. Lupton, J. A. Smith, J. C. Barentine, H. Brewington, J. Brinkmann, M. Harvanek, S. J. Kleinman, J. Krzesinski, D. Long, A. Nitta, and S. A. Snedden, "A New Milky Way Dwarf Satellite in Canes Venatici," *Astrophysical Journal* **643** (June, 2006) L103–L106, arXiv:astro-ph/0604354.

[102] S. Koposov, V. Belokurov, N. W. Evans, P. C. Hewett, M. J. Irwin, G. Gilmore, D. B. Zucker, H. Rix, M. Fellhauer, E. F. Bell, and E. V. Glushkova, "The Luminosity Function of the Milky Way Satellites," *Astrophysical Journal* **686** (Oct., 2008) 279–291, arXiv:0706.2687.

[103] E. J. Tollerud, J. S. Bullock, L. E. Strigari, and B. Willman, "Hundreds of Milky Way Satellites? Luminosity Bias in the Satellite Luminosity Function," *Astrophysical Journal* **688** (Nov., 2008) 277–289, arXiv:0806.4381.

[104] A. Geringer-Sameth and S. M. Koushiappas, "Exclusion of canonical WIMPs by the joint analysis of Milky Way dwarfs with Fermi," *Phys.Rev.Lett.* **107** (2011) 241303, arXiv:1108.2914 [astro-ph.CO].

[105] M. Ackermann, M. Ajello, A. Albert, W. B. Atwood, L. Baldini, J. Ballet, G. Barbiellini, D. Bastieri, K. Bechtol, R. Bellazzini, B. Berenji, R. D. Blandford, E. D. Bloom, E. Bonamente, A. W. Borgland, J. Bregeon, M. Brigida, P. Bruel, R. Buehler, T. H. Burnett, S. Buson, G. A. Caliandro, R. A. Cameron, B. Cañadas, P. A. Caraveo, J. M. Casandjian, C. Cecchi, E. Charles, A. Chekhtman, J. Chiang, S. Ciprini, R. Claus, J. Cohen-Tanugi, J. Conrad, S. Cutini, A. de Angelis, F. de Palma, C. D. Dermer, S. W. Digel, E. Do Couto E Silva, P. S. Drell, A. Drlica-Wagner, L. Falletti, C. Favuzzi, S. J. Fegan, E. C. Ferrara, Y. Fukazawa, S. Funk, P. Fusco, F. Gargano, D. Gasparrini, N. Gehrels, S. Germani, N. Giglietto, F. Giordano, M. Giroletti, T. Glanzman, G. Godfrey, I. A. Grenier, S. Guiriec, M. Gustafsson, D. Hadasch, M. Hayashida, E. Hays, R. E. Hughes, T. E. Jeltema, G. Jóhannesson, R. P. Johnson, A. S. Johnson, T. Kamae, H. Katagiri, J. Kataoka, J. Knödlseder, M. Kuss, J. Lande, L. Latronico, A. M. Lionetto, M. Llena Garde, F. Longo, F. Loparco, B. Lott, M. N. Lovellette, P. Lubrano, G. M. Madejski, M. N. Mazziotta, J. E. McEnery, J. Mehault, P. F. Michelson, W. Mitthumsiri, T. Mizuno, C. Monte, M. E. Monzani, A. Morselli, I. V. Moskalenko, S. Murgia, M. Naumann-Godo, J. P. Norris, E. Nuss, T. Ohsugi, A. Okumura, N. Omodei, E. Orlando, J. F. Ormes, M. Ozaki, D. Paneque, D. Parent, M. Pesce-Rollins, M. Pierbattista, F. Piron, G. Pivato, T. A. Porter, S. Profumo, S. Rainò, M. Razzano, A. Reimer, O. Reimer, S. Ritz, M. Roth, H. F.-W. Sadrozinski, C. Sbarra, J. D. Scargle, T. L. Schalk, C. Sgrò, E. J. Siskind, G. Spandre, P. Spinelli, L. Strigari, D. J. Suson, H. Tajima, H. Takahashi, T. Tanaka, J. G. Thayer, J. B. Thayer, D. J. Thompson, L. Tibaldo, M. Tinivella, D. F. Torres, E. Troja, Y. Uchiyama, J. Vandenbroucke, V. Vasileiou, G. Vianello, V. Vitale, A. P. Waite, P. Wang, B. L. Winer, K. S. Wood, M. Wood, Z. Yang, S. Zimmer, M. Kaplinghat, and G. D. Martinez, "Constraining Dark Matter Models from a Combined Analysis of Milky Way Satellites with the Fermi Large Area Telescope," *Phys. Rev. Lett.* **107** no. 24, (Dec., 2011) 241302, arXiv:1108.3546 [astro-ph.HE].

[106] L. E. Strigari, S. M. Koushiappas, J. S. Bullock, M. Kaplinghat, J. D. Simon, M. Geha, and B. Willman, "The Most Dark-Matter-dominated Galaxies: Predicted Gamma-Ray Signals from the Faintest Milky Way Dwarfs," *Astrophysical Journal* **678** (May, 2008) 614–620, arXiv:0709.1510.

[107] M. G. Walker and J. Peñarrubia, "A Method for Measuring (Slopes of) the Mass Profiles of Dwarf Spheroidal Galaxies," *ArXiv e-prints* (Aug., 2011) , arXiv:1108.2404 [astro-ph.CO].

[108] J. Wolf, G. D. Martinez, J. S. Bullock, M. Kaplinghat, M. Geha, R. R. Muñoz, J. D. Simon, and F. F. Avedo, "Accurate masses for dispersion-supported galaxies," *Mon. Not. R. Astron. Soc.* **406** (Aug., 2010) 1220–1237, arXiv:0908.2995 [astro-ph.CO].

[109] J. Wolf and J. S. Bullock, "Dark matter concentrations and a search for cores in Milky Way dwarf satellites," *ArXiv e-prints* (Mar., 2012) , arXiv:1203.4240 [astro-ph.CO].

[110] M. A. Breddels, A. Helmi, R. C. E. van den Bosch, G. van de Ven, and G. Battaglia, "Orbit-based dynamical models of the Sculptor dSph galaxy," *Monthly Notices of the Royal Astronomical Society* (July, 2013) , arXiv:1205.4712 [astro-ph.CO].

[111] N. C. Amorisco and N. W. Evans, "Phase-space models of the dwarf spheroidals," *Monthly Notices of the Royal Astronomical Society* **411** (Mar., 2011) 2118–2136, arXiv:1009.1813 [astro-ph.GA].

[112] G. Battaglia, A. Helmi, and M. Breddels, "Internal kinematics and dynamical models of dwarf spheroidal galaxies around the Milky Way," *ArXiv e-prints* (May, 2013) , arXiv:1305.5965 [astro-ph.CO].

[113] V. Springel, S. D. M. White, C. S. Frenk, J. F. Navarro, A. Jenkins, M. Vogelsberger, J. Wang, A. Ludlow, and A. Helmi, "Prospects for detecting supersymmetric dark matter in the Galactic halo," *Nature* **456** (Nov., 2008) 73–76, arXiv:0809.0894.

[114] S. Profumo, "Dissecting Pamela (and ATIC) with Occam's Razor: existing, well-known Pulsars naturally account for the "anomalous" Cosmic-Ray Electron and Positron Data." Dec., 2008.

[115] C.-A. Faucher-Giguère and A. Loeb, "The pulsar contribution to the gamma-ray background," *JCAP* **1** (Jan., 2010) 5, arXiv:0904.3102 [astro-ph.HE].

[116] L. E. Strigari, "Galactic Searches for Dark Matter," *ArXiv e-prints* (Nov., 2012) , arXiv:1211.7090 [astro-ph.CO].

[117] K. Umetsu, E. Medezinski, M. Nonino, J. Merten, A. Zitrin, A. Molino, C. Grillo, M. Carrasco, M. Donahue, A. Mahdavi, D. Coe, M. Postman, A. Koekemoer, N. Czakon, J. Sayers, T. Mroczkowski, S. Golwala, P. M. Koch, K.-Y. Lin, S. M. Molnar, P. Rosati, I. Balestra, A. Mercurio, M. Scodeggio, A. Biviano, T. Anguita, L. Infante, G. Seidel, I. Sendra, S. Jouvel, O. Host, D. Lemze, T. Broadhurst, M. Meneghetti, L. Moustakas, M. Bartelmann, N. Benítez, R. Bouwens, L. Bradley, H. Ford, Y. Jiménez-Teja, D. Kelson, O. Lahav, P. Melchior, J. Moustakas, S. Ogaz, S. Seitz, and W. Zheng, "CLASH: Mass Distribution in and around MACS J1206.2-0847 from a Full Cluster Lensing Analysis," *Astrophysical Journal* **755** (Aug., 2012) 56, arXiv:1204.3630 [astro-ph.CO].

[118] D. Coe, K. Umetsu, A. Zitrin, M. Donahue, E. Medezinski, M. Postman, M. Carrasco, T. Anguita, M. J. Geller, K. J. Rines, A. Diaferio, M. J. Kurtz, L. Bradley, A. Koekemoer, W. Zheng, M. Nonino, A. Molino, A. Mahdavi, D. Lemze, L. Infante, S. Ogaz, P. Melchior, O. Host, H. Ford, C. Grillo, P. Rosati, Y. Jiménez-Teja, J. Moustakas, T. Broadhurst, B. Ascaso, O. Lahav, M. Bartelmann, N. Benítez, R. Bouwens, O. Graur, G. Graves, S. Jha, S. Jouvel, D. Kelson, L. Moustakas, D. Maoz, M. Meneghetti, J. Merten, A. Riess, S. Rodney, and S. Seitz, "CLASH: Precise New Constraints on the Mass Profile of the Galaxy Cluster A2261," *Astrophysical Journal* **757** (Sept., 2012) 22, arXiv:1201.1616 [astro-ph.CO].

[119] A. B. Newman, T. Treu, R. S. Ellis, D. J. Sand, C. Nipoti, J. Richard, and E. Jullo, "The Density Profiles of Massive, Relaxed Galaxy Clusters. I. The Total Density Over Three Decades in Radius," *Astrophysical Journal* **765** (Mar., 2013) 24, arXiv:1209.1391 [astro-ph.CO].

[120] A. B. Newman, T. Treu, R. S. Ellis, and D. J. Sand, "The Density Profiles of Massive, Relaxed Galaxy Clusters. II. Separating Luminous and Dark Matter in Cluster Cores," *Astrophysical Journal* **765** (Mar., 2013) 25, arXiv:1209.1392 [astro-ph.CO].

[121] P. Natarajan, G. De Lucia, and V. Springel, "Substructure in lensing clusters and simulations," *Monthly Notices of the Royal Astronomical Society* **376** (Mar., 2007) 180–192, arXiv:astro-ph/0604414.

[122] M. Limousin, J. P. Kneib, S. Bardeau, P. Natarajan, O. Czoske, I. Smail, H. Ebeling, and G. P. Smith, "Truncation of galaxy dark matter halos in high density environments," *Astronomy and Astrophysics* **461** (Jan., 2007) 881–891, arXiv:astro-ph/0609782.

[123] M. Ackermann, M. Ajello, A. Allafort, L. Baldini, J. Ballet, G. Barbiellini, D. Bastieri, K. Bechtol, R. Bellazzini, R. D. Blandford, P. Blasi, E. D. Bloom, E. Bonamente, A. W. Borgland, A. Bouvier, T. J. Brandt, J. Bregeon, M. Brigida, P. Bruel, R. Buehler, S. Buson, G. A. Caliandro, R. A. Cameron, P. A. Caraveo, S. Carrigan, J. M. Casandjian, E. Cavazzuti, C. Cecchi, Ö. Çelik, E. Charles, A. Chekhtman, C. C. Cheung, J. Chiang, S. Ciprini, R. Claus, J. Cohen-Tanugi, S. Colafrancesco, L. R. Cominsky, J. Conrad, C. D. Dermer, F. de Palma, E. d. C. e. Silva, P. S. Drell, R. Dubois, D. Dumora, Y. Edmonds, C. Farnier, C. Favuzzi, M. Frailis, Y. Fukazawa, S. Funk, P. Fusco, F. Gargano, D. Gasparrini, N. Gehrels, S. Germani, N. Giglietto, F. Giordano, M. Giroletti, T. Glanzman, G. Godfrey, I. A. Grenier, M. Hayashida, E. Hays, D. Horan, R. E. Hughes, T. E. Jeltema, G. Jóhannesson, A. S. Johnson, T. J. Johnson, W. N. Johnson, T. Kamae, H. Katagiri, J. Kataoka, M. Kerr, J. Knödlseder, M. Kuss, J. Lande, L. Latronico, S.-H. Lee, M. Lemoine-Goumard, F. Longo, F. Loparco, B. Lott, M. N. Lovellette, P. Lubrano, G. M. Madejski, A. Makeev, M. N. Mazziotta, P. F. Michelson, W. Mitthumsiri, T. Mizuno, A. A. Moiseev, C. Monte, M. E. Monzani, A. Morselli, I. V. Moskalenko, S. Murgia, M. Naumann-Godo, P. L. Nolan, J. P. Norris, E. Nuss, T. Ohsugi, N. Omodei, E. Orlando, J. F. Ormes, M. Ozaki, D. Paneque, J. H. Panetta, M. Pepe, M. Pesce-Rollins, V. Petrosian, C. Pfrommer, F. Piron, T. A. Porter, S. Profumo, S. Rainò, R. Rando, M. Razzano, A. Reimer, O. Reimer, T. Reposeur, J. Ripken, S. Ritz, A. Y. Rodriguez, R. W. Romani, M. Roth, H. F.-W. Sadrozinski, A. Sander, P. M. Saz Parkinson, J. D. Scargle, C. Sgrò, E. J. Siskind, P. D. Smith, G. Spandre, P. Spinelli, J.-L. Starck, L. Stawarz, M. S. Strickman, A. W. Strong, D. J. Suson, H. Tajima, H. Takahashi, T. Takahashi, T. Tanaka, J. B. Thayer, J. G. Thayer, L. Tibaldo, O. Tibolla, D. F. Torres, G. Tosti, A. Tramacere, Y. Uchiyama, T. L. Usher, J. Vandenbroucke, V. Vasileiou, N. Vilchez, V. Vitale, A. P. Waite, P. Wang, B. L. Winer, K. S. Wood, Z. Yang, T. Ylinen, and M. Ziegler, "GeV Gamma-ray Flux Upper Limits from Clusters of Galaxies," *Astrophysical Journal, Letters* **717** (July, 2010) L71–L78, arXiv:1006.0748 [astro-ph.HE].

[124] L. Dugger, T. E. Jeltema, and S. Profumo, "Constraints on Decaying Dark Matter from Fermi Observations of Nearby Galaxies and Clusters," *JCAP* **1012** (2010) 015, arXiv:1009.5988 [astro-ph.HE].

[125] X. Huang, G. Vertongen, and C. Weniger, "Probing Dark Matter Decay and Annihilation with Fermi LAT Observations of Nearby Galaxy Clusters," *JCAP* **1201** (2012) 042, arXiv:1110.1529 [hep-ph].

[126] E. Storm, T. E. Jeltema, S. Profumo, and L. Rudnick, "Constraints on Dark Matter Annihilation in Clusters of Galaxies from Diffuse Radio Emission," *Astrophys.J.* **768** (2013) 106, arXiv:1210.0872 [astro-ph.CO].

[127] S. Colafrancesco, S. Profumo, and P. Ullio, "Multi-frequency analysis of neutralino dark matter annihilations in the Coma cluster," *Astronomy and Astrophysics* **455** (Aug., 2006) 21–43, arXiv:astro-ph/0507575.

[128] T. E. Jeltema and S. Profumo, "Dark Matter Detection with Hard X-ray Telescopes," *Monthly Notices of the Royal Astronomical Society* **421** (Apr., 2012) 1215–1221, arXiv:1108.1407 [astro-ph.HE].

[129] S. Profumo, "Non-thermal X-rays from the Ophiuchus cluster and dark matter annihilation," *Phys.Rev.* **D77** (2008) 103510, arXiv:0801.0740 [astro-ph].

[130] A. Cuesta, T. Jeltema, F. Zandanel, S. Profumo, F. Prada, *et al.*, "Dark Matter decay and annihilation in the Local Universe: CLUES from Fermi," *Astrophys.J.* **726** (2011) L6, arXiv:1007.3469 [astro-ph.HE].

[131] J. F. Navarro, C. S. Frenk, and S. D. White, "A Universal density profile from hierarchical clustering," *Astrophys.J.* **490** (1997) 493–508, arXiv:astro-ph/9611107 [astro-ph].

[132] L. E. Strigari, J. S. Bullock, M. Kaplinghat, J. D. Simon, M. Geha, *et al.*, "A common mass scale for satellite galaxies of the Milky Way," *Nature* **454** (2008) 1096–1097, arXiv:0808.3772 [astro-ph].

[133] M. G. Walker, "Dark Matter in the Milky Way's Dwarf Spheroidal Satellites," arXiv:1205.0311 [astro-ph.CO].

[134] A. V. Macciò, A. A. Dutton, and F. C. van den Bosch, "Concentration, spin and shape of dark matter haloes as a function of the cosmological model: WMAP1, WMAP3 and WMAP5 results," *Monthly Notices of the Royal Astronomical Society* **391** (Dec., 2008) 1940–1954, arXiv:0805.1926.

[135] E. Aliu, S. Archambault, T. Arlen, T. Aune, M. Beilicke, W. Benbow, A. Bouvier, S. M. Bradbury, J. H. Buckley, V. Bugaev, K. Byrum, A. Cannon, A. Cesarini, J. L. Christiansen, L. Ciupik, E. Collins-Hughes, M. P. Connolly, W. Cui, G. Decerprit, R. Dickherber, J. Dumm, M. Errando, A. Falcone, Q. Feng, F. Ferrer, J. P. Finley, G. Finnegan, L. Fortson, A. Furniss, N. Galante, D. Gall, S. Godambe, S. Griffin, J. Grube, G. Gyuk, D. Hanna, J. Holder, H. Huan, G. Hughes, T. B. Humensky, P. Kaaret, N. Karlsson, M. Kertzman, Y. Khassen, D. Kieda, H. Krawczynski, F. Krennrich, K. Lee, A. S. Madhavan, G. Maier, P. Majumdar, S. McArthur, A. McCann, P. Moriarty, R. Mukherjee, R. A. Ong, M. Orr, A. N. Otte, N. Park, J. S. Perkins, M. Pohl, H. Prokoph, J. Quinn, K. Ragan, L. C. Reyes, P. T. Reynolds, E. Roache, H. J. Rose, J. Ruppel, D. B. Saxon, M. Schroedter, G. H. Sembroski, G. D. Şentürk, C. Skole, A. W. Smith, D. Staszak, I. Telezhinsky, G. Tešić, M. Theiling, S. Thibadeau, K. Tsurusaki, A. Varlotta, V. V. Vassiliev, S. Vincent, M. Vivier, R. G. Wagner, S. P. Wakely, J. E. Ward, T. C. Weekes, A. Weinstein, T. Weisgarber, D. A. Williams, and B. Zitzer, "VERITAS deep observations of the dwarf spheroidal galaxy Segue 1," *Physics Review D* **85** no. 6, (Mar., 2012) 062001, arXiv:1202.2144 [astro-ph.HE].

[136] M. G. Walker and J. Penarrubia, "A Method for Measuring (Slopes of) the Mass Profiles of Dwarf Spheroidal Galaxies," *Astrophys.J.* **742** (2011) 20, arXiv:1108.2404 [astro-ph.CO].

[137] N. Amorisco, A. Agnello, and N. Evans, "The core size of the Fornax dwarf Spheroidal," arXiv:1210.3157 [astro-ph.CO].

[138] A. Burkert, "The Structure of dark matter halos in dwarf galaxies," *IAU Symp.* **171** (1996) 175, arXiv:astro-ph/9504041 [astro-ph].

[139] P. Salucci, M. I. Wilkinson, M. G. Walker, G. F. Gilmore, E. K. Grebel, *et al.*, "Dwarf spheroidal galaxy kinematics and spiral galaxy scaling laws," arXiv:1111.1165 [astro-ph.CO].

[140] L. Bergström, J. Edsjö, and G. Zaharijas, "Dark Matter Interpretation of Recent Electron and Positron Data," *Physical Review Letters* **103** no. 3, (July, 2009) 031103, arXiv:0905.0333 [astro-ph.HE].

[141] A. Hektor, M. Raidal, A. Strumia, and E. Tempel, "The cosmic-ray positron excess from a local Dark Matter over-density," *ArXiv e-prints* (July, 2013) , arXiv:1307.2561 [hep-ph].

[142] D. Hooper, P. Blasi, and P. Dario Serpico, "Pulsars as the sources of high energy cosmic ray positrons," *JCAP* **1** (Jan., 2009) 25, arXiv:0810.1527.

[143] I. Cholis and D. Hooper, "Dark matter and pulsar origins of the rising cosmic ray positron fraction in light of new data from the AMS," *Physics Review D* **88** no. 2, (July, 2013) 023013, arXiv:1304.1840 [astro-ph.HE].

[144] P.-F. Yin, Z.-H. Yu, Q. Yuan, and X.-J. Bi, "Pulsar interpretation for the AMS-02 result," *Physics Review D* **88** no. 2, (July, 2013) 023001, arXiv:1304.4128 [astro-ph.HE].

[145] P. Blasi, "Origin of the Positron Excess in Cosmic Rays," *Physical Review Letters* **103** no. 5, (July, 2009) 051104, arXiv:0903.2794 [astro-ph.HE].

[146] B. Katz, K. Blum, J. Morag, and E. Waxman, "What can we really learn from positron flux 'anomalies'?," *Monthly Notices of the Royal Astronomical Society* **405** (July, 2010) 1458–1472, arXiv:0907.1686 [astro-ph.HE].

[147] K. Blum, B. Katz, and E. Waxman, "AMS02 results support the secondary origin of cosmic ray positrons," *ArXiv e-prints* (May, 2013) , arXiv:1305.1324 [astro-ph.HE].

[148] N. J. Shaviv, E. Nakar, and T. Piran, "Inhomogeneity in Cosmic Ray Sources as the Origin of the Electron Spectrum and the PAMELA Anomaly," *Physical Review Letters* **103** no. 11, (Sept., 2009) 111302, arXiv:0902.0376 [astro-ph.HE].

[149]

[150] R. Cowsik and B. Burch, "Positron fraction in cosmic rays and models of cosmic-ray propagation," *Physics Review D* **82** no. 2, (July, 2010) 023009.

[151] R. Cowsik, B. Burch, and T. Madziwa-Nussinov, "The origin of the spectral intensities of cosmic-ray positrons," *ArXiv e-prints* (May, 2013) , arXiv:1305.1242 [astro-ph.HE].

[152] M. D. Kistler, H. Yuksel, and A. Friedland, "Galactic Streams of Cosmic-ray Electrons and Positrons," *ArXiv e-prints* (Oct., 2012) , arXiv:1210.8180 [astro-ph.HE].

[153] T. Delahaye, J. Lavalle, R. Lineros, F. Donato, and N. Fornengo, "Galactic electrons and positrons at the Earth:new estimate of the primary and secondary fluxes," *Astron.Astrophys.* **524** (2010) A51, arXiv:1002.1910 [astro-ph.HE].

[154] T. Kobayashi, Y. Komori, K. Yoshida, and J. Nishimura, "The Most Likely Sources of High-Energy Cosmic-Ray Electrons in Supernova Remnants," *Astrophysical Journal* **601** (Jan., 2004) 340–351, arXiv:astro-ph/0308470.

[155] **H.E.S.S. Collaboration** Collaboration, F. Aharonian *et al.*, "The energy spectrum of cosmic-ray electrons at TeV energies," *Phys.Rev.Lett.* **101** (2008) 261104, arXiv:0811.3894 [astro-ph].

[156] M. Ackermann, M. Ajello, A. Allafort, W. B. Atwood, L. Baldini, G. Barbiellini, D. Bastieri, K. Bechtol, R. Bellazzini, B. Berenji, R. D. Blandford, E. D. Bloom, E. Bonamente, A. W. Borgland, A. Bouvier, J. Bregeon, M. Brigida, P. Bruel, R. Buehler, S. Buson, G. A. Caliandro, R. A. Cameron, P. A. Caraveo, J. M. Casandjian, C. Cecchi, E. Charles, A. Chekhtman, C. C. Cheung, J. Chiang, S. Ciprini, R. Claus, J. Cohen-Tanugi, J. Conrad, S. Cutini, A. de Angelis, F. de Palma, C. D. Dermer, S. W. Digel, E. Do Couto E Silva, P. S. Drell, A. Drlica-Wagner, C. Favuzzi, S. J. Fegan, E. C. Ferrara, W. B. Focke, P. Fortin, Y. Fukazawa, S. Funk, P. Fusco, F. Gargano, D. Gasparrini, S. Germani, N. Giglietto, P. Giommi, F. Giordano, M. Giroletti, T. Glanzman, G. Godfrey, I. A. Grenier, J. E. Grove, S. Guiriec, M. Gustafsson, D. Hadasch, A. K. Harding, M. Hayashida, R. E. Hughes, G. Jóhannesson, A. S. Johnson, T. Kamae, H. Katagiri, J. Kataoka, J. Knödlseder, M. Kuss, J. Lande, L. Latronico, M. Lemoine-Goumard, M. Llena Garde, F. Longo, F. Loparco, M. N. Lovellette, P. Lubrano, G. M. Madejski, M. N. Mazziotta, J. E. McEnery, P. F. Michelson, W. Mitthumsiri, T. Mizuno, A. A. Moiseev, C. Monte, M. E. Monzani, A. Morselli, I. V. Moskalenko, S. Murgia, T. Nakamori, P. L. Nolan, J. P. Norris, E. Nuss, M. Ohno, T. Ohsugi, A. Okumura, N. Omodei, E. Orlando, J. F. Ormes, M. Ozaki, D. Paneque, D. Parent, M. Pesce-Rollins, M. Pierbattista, F. Piron, G. Pivato, T. A. Porter, S. Rainò, R. Rando, M. Razzano, S. Razzaque, A. Reimer, O. Reimer, T. Reposeur, S. Ritz, R. W. Romani, M. Roth, H. F.-W. Sadrozinski, C. Sbarra, T. L. Schalk, C. Sgrò, E. J. Siskind, G. Spandre, P. Spinelli, A. W. Strong, H. Takahashi, T. Takahashi, T. Tanaka, J. G. Thayer, J. B. Thayer, L. Tibaldo, M. Tinivella, D. F. Torres, G. Tosti, E. Troja, Y. Uchiyama, T. L. Usher, J. Vandenbroucke, V. Vasileiou, G. Vianello, V. Vitale, A. P. Waite, B. L. Winer, K. S. Wood, M. Wood, Z. Yang, and S. Zimmer, "Measurement of Separate Cosmic-Ray Electron and Positron Spectra with the Fermi Large Area Telescope," *Physical Review Letters* **108** no. 1, (Jan., 2012) 011103, `arXiv:1109.0521 [astro-ph.HE]`.

[157] F. Aharonian, A. G. Akhperjanian, G. Anton, U. Barres de Almeida, A. R. Bazer-Bachi, Y. Becherini, B. Behera, K. Bernlöhr, A. Bochow, C. Boisson, J. Bolmont, V. Borrel, J. Brucker, F. Brun, P. Brun, R. Bühler, T. Bulik, I. Büsching, T. Boutelier, P. M. Chadwick, A. Charbonnier, R. C. G. Chaves, A. Cheesebrough, L.-M. Chounet, A. C. Clapson, G. Coignet, M. Dalton, M. K. Daniel, I. D. Davids, B. Degrange, C. Deil, H. J. Dickinson, A. Djannati-Ataï, W. Domainko, L. O'C. Drury, F. Dubois, G. Dubus, J. Dyks, M. Dyrda, K. Egberts, D. Emmanoulopoulos, P. Espigat, C. Farnier, F. Feinstein, A. Fiasson, A. Förster, G. Fontaine, M. Füßling, S. Gabici, Y. A. Gallant, L. Gérard, D. Gerbig, B. Giebels, J. F. Glicenstein, B. Glück, P. Goret, D. Göring, D. Hauser, M. Hauser, S. Heinz, G. Heinzelmann, G. Henri, G. Hermann, J. A. Hinton, A. Hoffmann, W. Hofmann, M. Holleran, S. Hoppe, D. Horns, A. Jacholkowska, O. C. de Jager, C. Jahn, I. Jung, K. Katarzyński, U. Katz, S. Kaufmann, E. Kendziorra, M. Kerschhaggl, D. Khangulyan, B. Khélifi, D. Keogh, W. Kluźniak, T. Kneiske, N. Komin, K. Kosack, R. Kossakowski, G. Lamanna, J.-P. Lenain, T. Lohse, V. Marandon, J. M. Martin, O. Martineau-Huynh, A. Marcowith, J. Masbou, D. Maurin, T. J. L. McComb, M. C. Medina, R. Moderski, E. Moulin, M. Naumann-Godo, M. de Naurois, D. Nedbal, D. Nekrassov, B. Nicholas, J. Niemiec, S. J. Nolan, S. Ohm, J.-F. Olive, E. de Oña Wilhelmi, K. J. Orford, M. Ostrowski, M. Panter, M. Paz Arribas, G. Pedaletti, G. Pelletier, P.-O. Petrucci, S. Pita, G. Pühlhofer, M. Punch, A. Quirrenbach, B. C. Raubenheimer, M. Raue, S. M. Rayner, O. Reimer, M. Renaud, F. Rieger, J. Ripken, L. Rob, S. Rosier-Lees, G. Rowell, B. Rudak, C. B. Rulten, J. Ruppel, V. Sahakian, A. Santangelo, R. Schlickeiser, F. M. Schöck, R. Schröder, U. Schwanke, S. Schwarzburg, S. Schwemmer, A. Shalchi, M. Sikora, J. L. Skilton, H. Sol, D. Spangler, L. Stawarz, R. Steenkamp, C. Stegmann, F. Stinzing, G. Superina, A. Szostek, P. H. Tam, J.-P. Tavernet, R. Terrier, O. Tibolla, M. Tluczykont, C. van Eldik, G. Vasileiadis, C. Venter, L. Venter, J. P. Vialle, P. Vincent, M. Vivier, H. J. Völk, F. Volpe, S. J. Wagner, M. Ward, A. A. Zdziarski, and A. Zech, "Probing the ATIC peak in the cosmic-ray electron spectrum with H.E.S.S.," *Astronomy and Astrophysics* **508** (Dec., 2009) 561–564, `arXiv:0905.0105 [astro-ph.HE]`.

[158] D. Borla Tridon, "Measurement of the cosmic electron spectrum with the MAGIC telescopes," in *International Cosmic Ray Conference*, vol. 6 of *International Cosmic Ray Conference*, p. 43. 2011. arXiv:1110.4008 [astro-ph.HE].

[159] M. C. Chantell, C. W. Akerlof, H. M. Badran, J. Buckley, D. A. Carter-Lewis, M. F. Cawley, V. Connaughton, D. J. Fegan, P. Fleury, J. Gaidos, A. M. Hillas, R. C. Lamb, E. Pare, H. J. Rose, A. C. Rovero, X. Sarazin, G. Sembroski, M. S. Schubnell, M. Urban, T. C. Weekes, and C. Wilson, "A hybrid version of the Whipple observatory's air Cherenkov imaging camera for use in moonlight," *Astroparticle Physics* **6** (Feb., 1997) 205–214.

[160] D. Pomarède, P. J. Boyle, M. Urban, H. M. Badran, L. Behr, M. T. Brunetti, D. J. Fegan, and T. C. Weekes, "Search for shadowing of primary cosmic radiation by the moon at TeV energies," *Astroparticle Physics* **14** (Jan., 2001) 287–317.

[161] P. Colin, "Probing the CR positron/electron ratio at few hundreds GeV through Moon shadow observation with the MAGIC telescopes," in *International Cosmic Ray Conference*, vol. 6 of *International Cosmic Ray Conference*, p. 189. 2011. arXiv:1110.0183 [astro-ph.HE].

[162] O. Adriani, G. C. Barbarino, G. A. Bazilevskaya, R. Bellotti, M. Boezio, E. A. Bogomolov, L. Bonechi, M. Bongi, V. Bonvicini, S. Borisov, S. Bottai, A. Bruno, F. Cafagna, D. Campana, R. Carbone, P. Carlson, M. Casolino, G. Castellini, L. Consiglio, M. P. De Pascale, C. De Santis, N. De Simone, V. Di Felice, A. M. Galper, W. Gillard, L. Grishantseva, P. Hofverberg, G. Jerse, A. V. Karelin, S. V. Koldashov, S. Y. Krutkov, A. N. Kvashnin, A. Leonov, V. Malvezzi, L. Marcelli, A. G. Mayorov, W. Menn, V. V. Mikhailov, E. Mocchiutti, A. Monaco, N. Mori, N. Nikonov, G. Osteria, P. Papini, M. Pearce, P. Picozza, C. Pizzolotto, M. Ricci, S. B. Ricciarini, L. Rossetto, M. Simon, R. Sparvoli, P. Spillantini, Y. I. Stozhkov, A. Vacchi, E. Vannuccini, G. Vasilyev, S. A. Voronov, J. Wu, Y. T. Yurkin, G. Zampa, N. Zampa, and V. G. Zverev, "PAMELA Results on the Cosmic-Ray Antiproton Flux from 60 MeV to 180 GeV in Kinetic Energy," *Phys. Rev. Lett.* **105** (Sep, 2010) 121101. http://link.aps.org/doi/10.1103/PhysRevLett.105.121101.

[163] M. Cirelli, M. Kadastik, M. Raidal, and A. Strumia, "Model-independent implications of the $e^{\pm}$, $\bar{p}$ cosmic ray spectra on properties of Dark Matter," *Nuclear Physics B* **813** (May, 2009) 1–21, arXiv:0809.2409 [hep-ph].

[164] F. W. Stecker and A. W. Wolfendale, "The case for antiparticles in the extragalactic cosmic radiation," *Nature* **309** (May, 1984) 37.

[165] A. Barrau, G. Boudoul, F. Donato, D. Maurin, P. Salati, and R. Taillet, "Antiprotons from primordial black holes," *A&A* **388** (June, 2002) 676–687, arXiv:astro-ph/0112486.

[166] A. A. Abdo, M. Ackermann, M. Ajello, W. B. Atwood, M. Axelsson, L. Baldini, J. Ballet, G. Barbiellini, D. Bastieri, M. Battelino, B. M. Baughman, K. Bechtol, R. Bellazzini, B. Berenji, R. D. Blandford, E. D. Bloom, G. Bogaert, E. Bonamente, A. W. Borgland, J. Bregeon, A. Brez, M. Brigida, P. Bruel, T. H. Burnett, G. A. Caliandro, R. A. Cameron, P. A. Caraveo, P. Carlson, J. M. Casandjian, C. Cecchi, E. Charles, A. Chekhtman, C. C. Cheung, J. Chiang, S. Ciprini, R. Claus, J. Cohen-Tanugi, L. R. Cominsky, J. Conrad, S. Cutini, C. D. Dermer, A. de Angelis, F. de Palma, S. W. Digel, G. di Bernardo, E. Do Couto E Silva, P. S. Drell, R. Dubois, D. Dumora, Y. Edmonds, C. Farnier, C. Favuzzi, W. B. Focke, M. Frailis, Y. Fukazawa, S. Funk, P. Fusco, D. Gaggero, F. Gargano, D. Gasparrini, N. Gehrels, S. Germani, B. Giebels, N. Giglietto, F. Giordano, T. Glanzman, G. Godfrey, D. Grasso, I. A. Grenier, M.-H. Grondin, J. E. Grove, L. Guillemot, S. Guiriec, Y. Hanabata, A. K. Harding, R. C. Hartman, M. Hayashida, E. Hays, R. E. Hughes, G. Jóhannesson, A. S. Johnson, R. P. Johnson, W. N. Johnson, T. Kamae, H. Katagiri, J. Kataoka, N. Kawai, M. Kerr, J. Knödlseder, D. Kocevski, F. Kuehn,

M. Kuss, J. Lande, L. Latronico, M. Lemoine-Goumard, F. Longo, F. Loparco, B. Lott, M. N. Lovellette, P. Lubrano, G. M. Madejski, A. Makeev, M. M. Massai, M. N. Mazziotta, W. McConville, J. E. McEnery, C. Meurer, P. F. Michelson, W. Mitthumsiri, T. Mizuno, A. A. Moiseev, C. Monte, M. E. Monzani, E. Moretti, A. Morselli, I. V. Moskalenko, S. Murgia, P. L. Nolan, J. P. Norris, E. Nuss, T. Ohsugi, N. Omodei, E. Orlando, J. F. Ormes, M. Ozaki, D. Paneque, J. H. Panetta, D. Parent, V. Pelassa, M. Pepe, M. Pesce-Rollins, F. Piron, M. Pohl, T. A. Porter, S. Profumo, S. Rainò, R. Rando, M. Razzano, A. Reimer, O. Reimer, T. Reposeur, S. Ritz, L. S. Rochester, A. Y. Rodriguez, R. W. Romani, M. Roth, F. Ryde, H. F.-W. Sadrozinski, D. Sanchez, A. Sander, P. M. Saz Parkinson, J. D. Scargle, T. L. Schalk, A. Sellerholm, C. Sgrò, D. A. Smith, P. D. Smith, G. Spandre, P. Spinelli, J.-L. Starck, T. E. Stephens, M. S. Strickman, A. W. Strong, D. J. Suson, H. Tajima, H. Takahashi, T. Takahashi, T. Tanaka, J. B. Thayer, J. G. Thayer, D. J. Thompson, L. Tibaldo, O. Tibolla, D. F. Torres, G. Tosti, A. Tramacere, Y. Uchiyama, T. L. Usher, A. van Etten, V. Vasileiou, N. Vilchez, V. Vitale, A. P. Waite, E. Wallace, P. Wang, B. L. Winer, K. S. Wood, T. Ylinen, and M. Ziegler, "Measurement of the Cosmic Ray e^++e^- Spectrum from 20GeV to 1TeV with the Fermi Large Area Telescope," *Physical Review Letters* **102** no. 18, (May, 2009) 181101, `arXiv:0905.0025 [astro-ph.HE]`.

[167] M. Schubnell, C. Bower, S. Coutu, and et al., "The Cosmic Ray Electron Synchrotron Telescope (CREST) Experiment," in *International Cosmic Ray Conference*, vol. 2 of *International Cosmic Ray Conference*, pp. 305–308. 2008.

[168] B. F. Rauch and CALET Collaboration, "Using the earth's geomagnetic field to measure ultra-heavy cosmic ray abundances and electron and positron fluxes with CALET," in *American Institute of Physics Conference Series*, J. F. Ormes, ed., vol. 1516 of *American Institute of Physics Conference Series*, pp. 293–293. Feb., 2013.

[169] T. Linden and S. Profumo, "Probing the Pulsar Origin of the Anomalous Positron Fraction with AMS-02 and Atmospheric Cherenkov Telescopes," *Ap. J.* **772** (July, 2013) 18, `arXiv:1304.1791 [astro-ph.HE]`.

[170] D. Pomarède, P. J. Boyle, M. Urban, H. M. Badran, L. Behr, M. T. Brunetti, D. J. Fegan, and T. C. Weekes, "Search for shadowing of primary cosmic radiation by the moon at TeV energies," *Astroparticle Physics* **14** (Jan., 2001) 287–317.

[171] P. Colin, D. Borla Tridon, D. Britzger, E. Lorenz, R. Mirzoyan, T. Schweizer, M. Teshima, and for the MAGIC Collaboration, "Observation of shadowing of the cosmic electrons and positrons by the Moon with IACT," *ArXiv e-prints* (July, 2009) , `arXiv:0907.1026 [astro-ph.IM]`.

[172] T. Jogler, M. D. Wood, J. Dumm, and CTA Consortium, "Monte Carlo comparison of mid-size telescope designs for the Cherenkov Telescope Array," in *American Institute of Physics Conference Series*, F. A. Aharonian, W. Hofmann, and F. M. Rieger, eds., vol. 1505 of *American Institute of Physics Conference Series*, pp. 765–768. Dec., 2012. `arXiv:1211.3181 [astro-ph.IM]`.

[173] F. Donato, N. Fornengo, and P. Salati, "Antideuterons as a signature of supersymmetric dark matter," *Physics Review D* **62** no. 4, (Aug., 2000) 043003, `arXiv:hep-ph/9904481`.

[174] H. Fuke, T. Maeno, K. Abe, S. Haino, Y. Makida, S. Matsuda, H. Matsumoto, J. W. Mitchell, A. A. Moiseev, J. Nishimura, M. Nozaki, S. Orito, J. F. Ormes, M. Sasaki, E. S. Seo, Y. Shikaze, R. E. Streitmatter, J. Suzuki, K. Tanaka, K. Tanizaki, T. Yamagami, A. Yamamoto, Y. Yamamoto, K. Yamato, T. Yoshida, and K. Yoshimura, "Search for Cosmic-Ray Antideuterons," *Physical Review Letters* **95** no. 8, (Aug., 2005) 081101, `arXiv:astro-ph/0504361`.

[175] V. Choutko and F. Giovacchini, "Cosmic Rays Antideuteron Sensitivity for AMS-02 Experiment," in *International Cosmic Ray Conference*, vol. 4 of *International Cosmic Ray Conference*, pp. 765–768. 2008.

[176] C. J. Hailey, "An indirect search for dark matter using antideuterons: the GAPS experiment," *New Journal of Physics* **11** no. 10, (Oct., 2009) 105022.

[177] S. A. I. Mognet, T. Aramaki, N. Bando, S. E. Boggs, P. von Doetinchem, H. Fuke, F. H. Gahbauer, C. J. Hailey, J. E. Koglin, N. Madden, K. Mori, S. Okazaki, R. A. Ong, K. M. Perez, G. Tajiri, T. Yoshida, and J. Zweerink, "The Prototype GAPS (pGAPS) Experiment," *ArXiv e-prints* (Mar., 2013) , arXiv:1303.1615 [astro-ph.IM].

[178] M. Kadastik, M. Raidal, and A. Strumia, "Enhanced anti-deuteron Dark Matter signal and the implications of PAMELA," *Physics Letters B* **683** (Jan., 2010) 248–254, arXiv:0908.1578 [hep-ph].

[179] A. Ibarra and S. Wild, "Prospects of antideuteron detection from dark matter annihilations or decays at AMS-02 and GAPS," *JCAP* **2** (Feb., 2013) 21, arXiv:1209.5539 [hep-ph].

[180] L. A. Dal and M. Kachelrieß, "Antideuterons from dark matter annihilations and hadronization model dependence," *Physics Review D* **86** no. 10, (Nov., 2012) 103536, arXiv:1207.4560 [hep-ph].

[181] J. Lavalle, J. Pochon, P. Salati, and R. Taillet, "Clumpiness of dark matter and the positron annihilation signal," *Astronomy and Astrophysics* **462** (Feb., 2007) 827–840, arXiv:astro-ph/0603796.

[182] F. Donato, N. Fornengo, and D. Maurin, "Antideuteron fluxes from dark matter annihilation in diffusion models," *Physics Review D* **78** no. 4, (Aug., 2008) 043506, arXiv:0803.2640 [hep-ph].

[183] C. J. Hailey, T. Aramaki, S. E. Boggs, P. v. Doetinchem, H. Fuke, F. Gahbauer, J. E. Koglin, N. Madden, S. A. I. Mognet, R. Ong, T. Yoshida, T. Zhang, and J. A. Zweerink, "Antideuteron based dark matter search with GAPS: Current progress and future prospects," *Advances in Space Research* **51** (Jan., 2013) 290–296.

[184] R. Bernabei, P. Belli, F. Cappella, R. Cerulli, C. J. Dai, A. D'Angelo, H. L. He, A. Incicchitti, H. H. Kuang, X. H. Ma, F. Montecchia, F. Nozzoli, D. Prosperi, X. D. Sheng, R. G. Wang, and Z. P. Ye, "New results from DAMA/LIBRA," *European Physical Journal C* **67** (May, 2010) 39–49, arXiv:1002.1028 [astro-ph.GA].

[185] CDMS Collaboration, R. Agnese, Z. Ahmed, A. J. Anderson, S. Arrenberg, D. Balakishiyeva, R. Basu Thakur, D. A. Bauer, J. Billard, A. Borgland, D. Brandt, P. L. Brink, T. Bruch, R. Bunker, B. Cabrera, D. O. Caldwell, D. G. Cerdeno, H. Chagani, J. Cooley, B. Cornell, C. H. Crewdson, P. Cushman, M. Daal, F. Dejongh, E. D. C. E. Silva, T. Doughty, L. Esteban, S. Fallows, E. Figueroa-Feliciano, J. Filippini, J. Fox, M. Fritts, G. L. Godfrey, S. R. Golwala, J. Hall, R. H. Harris, S. A. Hertel, T. Hofer, D. Holmgren, L. Hsu, M. E. Huber, A. Jastram, O. Kamaev, B. Kara, M. H. Kelsey, A. Kennedy, P. Kim, M. Kiveni, K. Koch, M. Kos, S. W. Leman, B. Loer, E. Lopez Asamar, R. Mahapatra, V. Mandic, C. Martinez, K. A. McCarthy, N. Mirabolfathi, R. A. Moffatt, D. C. Moore, P. Nadeau, R. H. Nelson, K. Page, R. Partridge, M. Pepin, A. Phipps, K. Prasad, M. Pyle, H. Qiu, W. Rau, P. Redl, A. Reisetter, Y. Ricci, T. Saab, B. Sadoulet, J. Sander, K. Schneck, R. W. Schnee, S. Scorza, B. Serfass, B. Shank, D. Speller, K. M. Sundqvist, A. N. Villano, B. Welliver, D. H. Wright, S. Yellin, J. J. Yen, J. Yoo, B. A. Young, and J. Zhang, "Dark Matter Search Results Using the Silicon Detectors of CDMS II," *ArXiv e-prints* (Apr., 2013) , arXiv:1304.4279 [hep-ex].

[186] C. E. Aalseth, P. S. Barbeau, J. Colaresi, J. I. Collar, J. Diaz Leon, J. E. Fast, N. E. Fields, T. W. Hossbach, A. Knecht, M. S. Kos, M. G. Marino, H. S. Miley, M. L. Miller, J. L. Orrell, and K. M. Yocum, "CoGeNT: A search for low-mass dark matter using p-type point contact germanium detectors," *Physics Review D* **88** no. 1, (July, 2013) 012002, arXiv:1208.5737 [astro-ph.CO].

[187] G. Gelmini and P. Gondolo, "Neutralino with the right cold dark matter abundance in (almost) any supersymmetric model," *Physics Review D* **74** no. 2, (July, 2006) 023510, arXiv:hep-ph/0602230.

[188] Pierre Auger Collaboration, J. Abraham, P. Abreu, M. Aglietta, C. Aguirre, D. Allard, I. Allekotte, J. Allen, P. Allison, J. Alvarez-Muñiz, and et al., "Upper limit on the cosmic-ray photon flux above 10^{19} eV using the surface detector of the Pierre Auger Observatory," *Astroparticle Physics* **29** (May, 2008) 243–256, arXiv:0712.1147.

[189] The Pierre Auger Collaboration, P. Abreu, M. Aglietta, E. J. Ahn, I. F. M. Albuquerque, D. Allard, I. Allekotte, J. Allen, P. Allison, J. Alvarez Castillo, and et al., "The Pierre Auger Observatory III: Other Astrophysical Observations," *ArXiv e-prints* (July, 2011) , arXiv:1107.4805 [astro-ph.HE].

[190] P. Gondolo and J. Silk, "Dark Matter Annihilation at the Galactic Center," *Physical Review Letters* **83** (Aug., 1999) 1719–1722, arXiv:astro-ph/9906391.

[191] P. Gondolo and J. Silk, "Dark Matter at the Galactic Center," *Nuclear Physics B Proceedings Supplements* **87** (June, 2000) 87–89, arXiv:hep-ph/0001070.

[192] L. Sadeghian, F. Ferrer, and C. M. Will, "Dark matter distributions around massive black holes: A general relativistic analysis," *ArXiv e-prints* (May, 2013) , arXiv:1305.2619 [astro-ph.GA].

[193] A. V. Belikov, M. R. Buckley, and D. Hooper, "Searching for dark matter subhalos in the Fermi-LAT second source catalog," *Physics Review D* **86** no. 4, (Aug., 2012) 043504, arXiv:1111.2613 [hep-ph].

[194] R. A. Ong, V. A. Acciari, T. Arlen, T. Aune, M. Beilicke, W. Benbow, D. Boltuch, S. M. Bradbury, J. H. Buckley, V. Bugaev, K. Byrum, A. Cannon, A. Cesarini, L. Ciupik, Y. C. Chow, P. Cogan, W. Cui, C. Duke, S. J. Fegan, J. P. Finley, G. Finnegan, P. Fortin, L. Fortson, A. Furniss, N. Galante, D. Gall, G. H. Gillanders, S. Godambe, J. Grube, R. Guenette, G. Gyuk, D. Hanna, J. Holder, D. Horan, C. M. Hui, T. B. Humensky, A. Imran, P. Kaaret, N. Karlsson, M. Kertzman, D. Kieda, A. Konopelko, H. Krawczynski, F. Krennrich, M. J. Lang, G. Maier, S. McArthur, A. McCann, M. McCutcheon, J. Millis, P. Moriarty, A. N. Otte, D. Pandel, J. S. Perkins, A. Pichel, M. Pohl, J. Quinn, K. Ragan, L. C. Reyes, P. T. Reynolds, E. Roache, H. J. Rose, M. Schroedter, G. H. Sembroski, A. W. Smith, D. Steele, S. P. Swordy, M. Theiling, S. Thibadeau, J. A. Toner, A. Varlotta, V. V. Vassiliev, S. Vincent, R. G. Wagner, S. P. Wakely, J. E. Ward, T. C. Weekes, A. Weinstein, D. A. Williams, S. Wissel, M. Wood, and B. Zitzer, "Highlight Talk: Recent Results from VERITAS," *ArXiv e-prints* (Dec., 2009) , arXiv:0912.5355 [astro-ph.HE].

[195] V. A. Acciari, T. Arlen, T. Aune, M. Beilicke, W. Benbow, D. Boltuch, S. M. Bradbury, J. H. Buckley, V. Bugaev, K. Byrum, A. Cannon, A. Cesarini, J. L. Christiansen, L. Ciupik, W. Cui, R. Dickherber, C. Duke, J. P. Finley, G. Finnegan, A. Furniss, N. Galante, S. Godambe, J. Grube, R. Guenette, G. Gyuk, D. Hanna, J. Holder, C. M. Hui, T. B. Humensky, A. Imran, P. Kaaret, N. Karlsson, M. Kertzman, D. Kieda, A. Konopelko, H. Krawczynski, F. Krennrich, G. Maier, S. McArthur, A. McCann, M. McCutcheon, P. Moriarty, R. A. Ong, A. N. Otte, D. Pandel, J. S. Perkins, M. Pohl, J. Quinn, K. Ragan, L. C. Reyes, P. T. Reynolds, E. Roache, H. J. Rose, M. Schroedter, G. H. Sembroski, G. D. Senturk, A. W. Smith, D. Steele, S. P. Swordy, G. Tešić, M. Theiling, S. Thibadeau, A. Varlotta, V. V. Vassiliev, S. Vincent, R. G. Wagner, S. P. Wakely, J. E. Ward, T. C. Weekes, A. Weinstein, T. Weisgarber, D. A. Williams, S. Wissel, B. Zitzer, and VERITAS Collaboration, "VERITAS Search for VHE Gamma-ray Emission from Dwarf Spheroidal Galaxies," *Astrophysical Journal* **720** (Sept., 2010) 1174–1180, arXiv:1006.5955 [astro-ph.CO].

[196] M. Beilicke and VERITAS Collaboration, "The Galactic Center region imaged by VERITAS," *Nuclear Instruments and Methods in Physics Research A* **692** (Nov., 2012) 208–211, arXiv:1109.6836 [astro-ph.HE].

[197] D. B. Kieda for the VERITAS Collaboration, "The Gamma Ray Detection sensitivity of the upgraded VERITAS Observatory," *ArXiv e-prints* (Aug., 2013) , arXiv:1308.4849 [astro-ph.IM].

[198] M. Doro, J. Conrad, D. Emmanoulopoulos, M. A. Sànchez-Conde, J. A. Barrio, E. Birsin, J. Bolmont, P. Brun, S. Colafrancesco, S. H. Connell, J. L. Contreras, M. K. Daniel, M. Fornasa, M. Gaug, J. F. Glicenstein, A. González-Muñoz, T. Hassan, D. Horns, A. Jacholkowska, C. Jahn, R. Mazini, N. Mirabal, A. Moralejo, E. Moulin, D. Nieto, J. Ripken, H. Sandaker, U. Schwanke, G. Spengler, A. Stamerra, A. Viana, H.-S. Zechlin, S. Zimmer, and CTA Consortium, "Dark matter and fundamental physics with the Cherenkov Telescope Array," *Astroparticle Physics* **43** (Mar., 2013) 189–214, arXiv:1208.5356 [astro-ph.IM].

[199] A. Abramowski, F. Acero, F. Aharonian, A. G. Akhperjanian, G. Anton, A. Barnacka, U. Barres de Almeida, A. R. Bazer-Bachi, Y. Becherini, J. Becker, B. Behera, K. Bernlöhr, A. Bochow, C. Boisson, J. Bolmont, P. Bordas, V. Borrel, J. Brucker, F. Brun, P. Brun, T. Bulik, I. Büsching, S. Carrigan, S. Casanova, M. Cerruti, P. M. Chadwick, A. Charbonnier, R. C. G. Chaves, A. Cheesebrough, L.-M. Chounet, A. C. Clapson, G. Coignet, J. Conrad, M. Dalton, M. K. Daniel, I. D. Davids, B. Degrange, C. Deil, H. J. Dickinson, A. Djannati-Ataï, W. Domainko, L. O. . Drury, F. Dubois, G. Dubus, J. Dyks, M. Dyrda, K. Egberts, P. Eger, P. Espigat, L. Fallon, C. Farnier, S. Fegan, F. Feinstein, M. V. Fernandes, A. Fiasson, G. Fontaine, A. Förster, M. Füßling, Y. A. Gallant, H. Gast, L. Gérard, D. Gerbig, B. Giebels, J. F. Glicenstein, B. Glück, P. Goret, D. Göring, J. D. Hague, D. Hampf, M. Hauser, S. Heinz, G. Heinzelmann, G. Henri, G. Hermann, J. A. Hinton, A. Hoffmann, W. Hofmann, P. Hofverberg, D. Horns, A. Jacholkowska, O. C. de Jager, C. Jahn, M. Jamrozy, I. Jung, M. A. Kastendieck, K. Katarzyński, U. Katz, S. Kaufmann, D. Keogh, M. Kerschhaggl, D. Khangulyan, B. Khélifi, D. Klochkov, W. Kluźniak, T. Kneiske, N. Komin, K. Kosack, R. Kossakowski, H. Laffon, G. Lamanna, D. Lennarz, T. Lohse, A. Lopatin, C.-C. Lu, V. Marandon, A. Marcowith, J. Masbou, D. Maurin, N. Maxted, T. J. L. McComb, M. C. Medina, J. Méhault, R. Moderski, E. Moulin, C. L. Naumann, M. Naumann-Godo, M. de Naurois, D. Nedbal, D. Nekrassov, N. Nguyen, B. Nicholas, J. Niemiec, S. J. Nolan, S. Ohm, J.-F. Olive, E. de Oña Wilhelmi, B. Opitz, M. Ostrowski, M. Panter, M. Paz Arribas, G. Pedaletti, G. Pelletier, P.-O. Petrucci, S. Pita, G. Pühlhofer, M. Punch, A. Quirrenbach, M. Raue, S. M. Rayner, A. Reimer, O. Reimer, M. Renaud, R. de Los Reyes, F. Rieger, J. Ripken, L. Rob, S. Rosier-Lees, G. Rowell, B. Rudak, C. B. Rulten, J. Ruppel, F. Ryde, V. Sahakian, A. Santangelo, R. Schlickeiser, F. M. Schöck, A. Schönwald, U. Schwanke, S. Schwarzburg, S. Schwemmer, A. Shalchi, M. Sikora, J. L. Skilton, H. Sol, G. Spengler, L. Stawarz, R. Steenkamp, C. Stegmann, F. Stinzing, I. Sushch, A. Szostek, J.-P. Tavernet, R. Terrier, O. Tibolla, M. Tluczykont, K. Valerius, C. van Eldik, G. Vasileiadis, C. Venter, J. P. Vialle, A. Viana, P. Vincent, M. Vivier, H. J. Völk, F. Volpe, S. Vorobiov, M. Vorster, S. J. Wagner, M. Ward, A. Wierzcholska, A. Zajczyk, A. A. Zdziarski, A. Zech, and H.-S. Zechlin, "Search for a Dark Matter Annihilation Signal from the Galactic Center Halo with H.E.S.S.," *Physical Review Letters* **106** no. 16, (Apr., 2011) 161301, arXiv:1103.3266 [astro-ph.HE].

[200] A. Charbonnier, C. Combet, M. Daniel, S. Funk, J. A. Hinton, D. Maurin, C. Power, J. I. Read, S. Sarkar, M. G. Walker, and M. I. Wilkinson, "Dark matter profiles and annihilation in dwarf spheroidal galaxies: prospectives for present and future γ-ray observatories - I. The classical dwarf spheroidal galaxies," *MNRAS* **418** (Dec., 2011) 1526–1556, arXiv:1104.0412 [astro-ph.HE].

[201] V. A. Acciari, T. Arlen, T. Aune, M. Beilicke, W. Benbow, D. Boltuch, S. M. Bradbury, J. H. Buckley, V. Bugaev, K. Byrum, A. Cannon, A. Cesarini, J. L. Christiansen, L. Ciupik, W. Cui, R. Dickherber,

C. Duke, J. P. Finley, G. Finnegan, A. Furniss, N. Galante, S. Godambe, J. Grube, R. Guenette, G. Gyuk, D. Hanna, J. Holder, C. M. Hui, T. B. Humensky, A. Imran, P. Kaaret, N. Karlsson, M. Kertzman, D. Kieda, A. Konopelko, H. Krawczynski, F. Krennrich, G. Maier, S. McArthur, A. McCann, M. McCutcheon, P. Moriarty, R. A. Ong, A. N. Otte, D. Pandel, J. S. Perkins, M. Pohl, J. Quinn, K. Ragan, L. C. Reyes, P. T. Reynolds, E. Roache, H. J. Rose, M. Schroedter, G. H. Sembroski, G. D. Senturk, A. W. Smith, D. Steele, S. P. Swordy, G. Tešić, M. Theiling, S. Thibadeau, A. Varlotta, V. V. Vassiliev, S. Vincent, R. G. Wagner, S. P. Wakely, J. E. Ward, T. C. Weekes, A. Weinstein, T. Weisgarber, D. A. Williams, S. Wissel, B. Zitzer, and VERITAS Collaboration, "VERITAS Search for VHE Gamma-ray Emission from Dwarf Spheroidal Galaxies," *Astrophysical Journal* **720** (Sept., 2010) 1174–1180, `arXiv:1006.5955 [astro-ph.CO]`.

[202] J. Aleksić, E. A. Alvarez, L. A. Antonelli, P. Antoranz, M. Asensio, M. Backes, J. A. Barrio, D. Bastieri, J. Becerra González, W. Bednarek, A. Berdyugin, K. Berger, E. Bernardini, A. Biland, O. Blanch, R. K. Bock, A. Boller, G. Bonnoli, D. Borla Tridon, I. Braun, T. Bretz, A. Cañellas, E. Carmona, A. Carosi, P. Colin, E. Colombo, J. L. Contreras, J. Cortina, L. Cossio, S. Covino, F. Dazzi, A. De Angelis, E. De Cea del Pozo, B. De Lotto, C. Delgado Mendez, A. Diago Ortega, M. Doert, A. Domínguez, D. Dominis Prester, D. Dorner, M. Doro, D. Elsaesser, D. Ferenc, M. V. Fonseca, L. Font, C. Fruck, R. J. García López, M. Garczarczyk, D. Garrido, G. Giavitto, N. Godinović, D. Hadasch, D. Häfner, A. Herrero, D. Hildebrand, D. Höhne-Mönch, J. Hose, D. Hrupec, B. Huber, T. Jogler, S. Klepser, T. Krähenbühl, J. Krause, A. La Barbera, D. Lelas, E. Leonardo, E. Lindfors, S. Lombardi, M. López, E. Lorenz, M. Makariev, G. Maneva, N. Mankuzhiyil, K. Mannheim, L. Maraschi, M. Mariotti, M. Martínez, D. Mazin, M. Meucci, J. M. Miranda, R. Mirzoyan, H. Miyamoto, J. Moldón, A. Moralejo, P. Munar-Androver, D. Nieto, K. Nilsson, R. Orito, I. Oya, S. Paiano, D. Paneque, R. Paoletti, S. Pardo, J. M. Paredes, S. Partini, M. Pasanen, F. Pauss, M. A. Perez-Torres, M. Persic, L. Peruzzo, M. Pilia, J. Pochon, F. Prada, P. G. Prada Moroni, E. Prandini, I. Puljak, I. Reichardt, R. Reinthal, W. Rhode, M. Ribó, J. Rico, S. Rügamer, A. Saggion, K. Saito, T. Y. Saito, M. Salvati, K. Satalecka, V. Scalzotto, V. Scapin, C. Schultz, T. Schweizer, M. Shayduk, S. N. Shore, A. Sillanpää, J. Sitarek, D. Sobczynska, F. Spanier, S. Spiro, A. Stamerra, B. Steinke, J. Storz, N. Strah, T. Surić, L. Takalo, H. Takami, F. Tavecchio, P. Temnikov, T. Terzić, D. Tescaro, M. Teshima, M. Thom, O. Tibolla, D. F. Torres, A. Treves, H. Vankov, P. Vogler, R. M. Wagner, Q. Weitzel, V. Zabalza, F. Zandanel, R. Zanin, M. Fornasa, R. Essig, N. Sehgal, and L. E. Strigari, "Searches for dark matter annihilation signatures in the Segue 1 satellite galaxy with the MAGIC-I telescope," *JCAP* **6** (June, 2011) 35, `arXiv:1103.0477 [astro-ph.HE]`.

[203] J. Albert, E. Aliu, H. Anderhub, P. Antoranz, M. Backes, C. Baixeras, J. A. Barrio, H. Bartko, D. Bastieri, J. K. Becker, W. Bednarek, K. Berger, C. Bigongiari, A. Biland, R. K. Bock, P. Bordas, V. Bosch-Ramon, T. Bretz, I. Britvitch, M. Camara, E. Carmona, A. Chilingarian, S. Commichau, J. L. Contreras, J. Cortina, M. T. Costado, V. Curtef, V. Danielyan, F. Dazzi, A. De Angelis, C. Delgado, R. de los Reyes, B. De Lotto, M. De Maria, F. De Sabata, D. Dorner, M. Doro, M. Errando, M. Fagiolini, D. Ferenc, E. Fernández, R. Firpo, M. V. Fonseca, L. Font, M. Fuchs, N. Galante, R. J. García-López, M. Garczarczyk, M. Gaug, F. Goebel, D. Hakobyan, M. Hayashida, T. Hengstebeck, A. Herrero, D. Höhne, J. Hose, S. Huber, C. C. Hsu, P. Jacon, T. Jogler, R. Kosyra, D. Kranich, A. Laille, E. Lindfors, S. Lombardi, F. Longo, M. López, E. Lorenz, P. Majumdar, G. Maneva, N. Mankuzhiyil, K. Mannheim, M. Mariotti, M. Martínez, D. Mazin, C. Merck, M. Meucci, M. Meyer, J. M. Miranda, R. Mirzoyan, S. Mizobuchi, M. Moles, A. Moralejo, D. Nieto, K. Nilsson, J. Ninkovic, E. Oña-Wilhelmi, N. Otte, I. Oya, M. Panniello, R. Paoletti, J. M. Paredes, M. Pasanen, D. Pascoli, F. Pauss, R. Pegna, M. A. Pérez-Torres, M. Persic, L. Peruzzo, A. Piccioli, F. Prada, E. Prandini, N. Puchades, A. Raymers, W. Rhode, M. Ribó, J. Rico, M. Rissi, A. Robert, S. Rügamer, A. Saggion, T. Y. Saito, A. Sánchez, M. Sánchez-Conde, P. Sartori, V. Scalzotto, V. Scapin, R. Schmitt, T. Schweizer, M. Shayduk, K. Shinozaki, S. N. Shore, N. Sidro, A. Sillanpää, D. Sobczynska,

F. Spanier, A. Stamerra, L. S. Stark, L. Takalo, P. Temnikov, D. Tescaro, M. Teshima, D. F. Torres, N. Turini, H. Vankov, A. Venturini, V. Vitale, R. M. Wagner, W. Wittek, F. Zandanel, R. Zanin, and J. Zapatero, "Upper Limit for γ-Ray Emission above 140 GeV from the Dwarf Spheroidal Galaxy Draco," *Astrophysical Journal* **679** (May, 2008) 428–431, arXiv:0711.2574.

[204] E. Aliu, H. Anderhub, L. A. Antonelli, P. Antoranz, M. Backes, C. Baixeras, S. Balestra, J. A. Barrio, H. Bartko, D. Bastieri, J. B. González, J. K. Becker, W. Bednarek, K. Berger, E. Bernardini, A. Biland, R. K. Bock, G. Bonnoli, P. Bordas, D. B. Tridon, V. Bosch-Ramon, D. Bose, T. Bretz, I. Britvitch, M. Camara, E. Carmona, S. Commichau, J. L. Contreras, J. Cortina, M. T. Costado, S. Covino, V. Curtef, F. Dazzi, A. DeAngelis, E. DeCea del Pozo, R. de los Reyes, B. DeLotto, M. DeMaria, F. DeSabata, C. D. Mendez, A. Dominguez, D. Dorner, M. Doro, D. Elsaesser, M. Errando, D. Ferenc, E. Fernández, R. Firpo, M. V. Fonseca, L. Font, N. Galante, R. J. García López, M. Garczarczyk, M. Gaug, F. Goebel, D. Hadasch, M. Hayashida, A. Herrero, D. Höhne-Mönch, J. Hose, C. C. Hsu, S. Huber, T. Jogler, D. Kranich, A. L. Barbera, A. Laille, E. Leonardo, E. Lindfors, S. Lombardi, F. Longo, M. López, E. Lorenz, P. Majumdar, G. Maneva, N. Mankuzhiyil, K. Mannheim, L. Maraschi, M. Mariotti, M. Martínez, D. Mazin, M. Meucci, M. Meyer, J. M. Miranda, R. Mirzoyan, J. Moldón, M. Moles, A. Moralejo, D. Nieto, K. Nilsson, J. Ninkovic, N. Otte, I. Oya, R. Paoletti, J. M. Paredes, M. Pasanen, D. Pascoli, F. Pauss, R. G. Pegna, M. A. Perez-Torres, M. Persic, L. Peruzzo, F. Prada, E. Prandini, N. Puchades, W. Rhode, M. Ribó, J. Rico, M. Rissi, A. Robert, S. Rügamer, A. Saggion, T. Y. Saito, M. Salvati, M. Sanchez-Conde, K. Satalecka, V. Scalzotto, V. Scapin, T. Schweizer, M. Shayduk, K. Shinozaki, S. N. Shore, N. Sidro, A. Sierpowska-Bartosik, A. Sillanpää, J. Sitarek, D. Sobczynska, F. Spanier, A. Stamerra, L. S. Stark, L. Takalo, F. Tavecchio, P. Temnikov, D. Tescaro, M. Teshima, M. Tluczykont, D. F. Torres, N. Turini, H. Vankov, R. M. Wagner, W. Wittek, V. Zabalza, F. Zandanel, R. Zanin, and J. Zapatero, "Upper Limits on the VHE Gamma-Ray Emission from the Willman 1 Satellite Galaxy with the Magic Telescope," *Astrophysical Journal* **697** (June, 2009) 1299–1304, arXiv:0810.3561.

[205] E. Aliu, S. Archambault, T. Arlen, T. Aune, M. Beilicke, W. Benbow, A. Bouvier, S. M. Bradbury, J. H. Buckley, V. Bugaev, K. Byrum, A. Cannon, A. Cesarini, J. L. Christiansen, L. Ciupik, E. Collins-Hughes, M. P. Connolly, W. Cui, G. Decerprit, R. Dickherber, J. Dumm, M. Errando, A. Falcone, Q. Feng, F. Ferrer, J. P. Finley, G. Finnegan, L. Fortson, A. Furniss, N. Galante, D. Gall, S. Godambe, S. Griffin, J. Grube, G. Gyuk, D. Hanna, J. Holder, H. Huan, G. Hughes, T. B. Humensky, P. Kaaret, N. Karlsson, M. Kertzman, Y. Khassen, D. Kieda, H. Krawczynski, F. Krennrich, K. Lee, A. S. Madhavan, G. Maier, P. Majumdar, S. McArthur, A. McCann, P. Moriarty, R. Mukherjee, R. A. Ong, M. Orr, A. N. Otte, N. Park, J. S. Perkins, M. Pohl, H. Prokoph, J. Quinn, K. Ragan, L. C. Reyes, P. T. Reynolds, E. Roache, H. J. Rose, J. Ruppel, D. B. Saxon, M. Schroedter, G. H. Sembroski, G. D. Şentürk, C. Skole, A. W. Smith, D. Staszak, I. Telezhinsky, G. Tešić, M. Theiling, S. Thibadeau, K. Tsurusaki, A. Varlotta, V. V. Vassiliev, S. Vincent, M. Vivier, R. G. Wagner, S. P. Wakely, J. E. Ward, T. C. Weekes, A. Weinstein, T. Weisgarber, D. A. Williams, and B. Zitzer, "VERITAS deep observations of the dwarf spheroidal galaxy Segue 1," *Physical Review D* **85** no. 6, (Mar., 2012) 062001, arXiv:1202.2144 [astro-ph.HE].

[206] J. Aleksic, "Segue 1: the best dark matter candidate dwarf galaxy surveyed by MAGIC," in *International Cosmic Ray Conference*, vol. 5 of *International Cosmic Ray Conference*, p. 149. 2011. arXiv:1109.6781 [astro-ph.CO].

[207] F. Aharonian, A. G. Akhperjanian, A. R. Bazer-Bachi, M. Beilicke, W. Benbow, D. Berge, K. Bernlöhr, C. Boisson, O. Bolz, V. Borrel, I. Braun, E. Brion, A. M. Brown, R. Bühler, I. Büsching, T. Boutelier, S. Carrigan, P. M. Chadwick, L.-M. Chounet, G. Coignet, R. Cornils, L. Costamante, B. Degrange, H. J. Dickinson, A. Djannati-Ataï, L. O. . Drury, G. Dubus, K. Egberts, D. Emmanoulopoulos, P. Espigat, C. Farnier, F. Feinstein, E. Ferrero, A. Fiasson, G. Fontaine, S. Funk, S. Funk, M. Füßling,

Y. A. Gallant, B. Giebels, J. F. Glicenstein, B. Glück, P. Goret, C. Hadjichristidis, D. Hauser, M. Hauser, G. Heinzelmann, G. Henri, G. Hermann, J. A. Hinton, A. Hoffmann, W. Hofmann, M. Holleran, S. Hoppe, D. Horns, A. Jacholkowska, O. C. de Jager, E. Kendziorra, M. Kerschhaggl, B. Khélifi, N. Komin, K. Kosack, G. Lamanna, I. J. Latham, R. Le Gallou, A. Lemière, M. Lemoine-Goumard, T. Lohse, J. M. Martin, O. Martineau-Huynh, A. Marcowith, C. Masterson, G. Maurin, T. J. L. McComb, E. Moulin, M. de Naurois, D. Nedbal, S. J. Nolan, A. Noutsos, E. Nuss, J.-P. Olive, K. J. Orford, J. L. Osborne, M. Panter, G. Pelletier, P.-O. Petrucci, S. Pita, G. Pühlhofer, M. Punch, S. Ranchon, B. C. Raubenheimer, M. Raue, S. M. Rayner, J. Ripken, L. Rob, L. Rolland, S. Rosier-Lees, G. Rowell, V. Sahakian, A. Santangelo, L. Saugé, S. Schlenker, R. Schlickeiser, R. Schröder, U. Schwanke, S. Schwarzburg, S. Schwemmer, A. Shalchi, H. Sol, D. Spangler, F. Spanier, R. Steenkamp, C. Stegmann, G. Superina, P. H. Tam, J.-P. Tavernet, R. Terrier, M. Tluczykont, C. van Eldik, G. Vasileiadis, C. Venter, J. P. Vialle, P. Vincent, M. Vivier, H. J. Völk, S. J. Wagner, and M. Ward, "Observations of the Sagittarius dwarf galaxy by the HESS experiment and search for a dark matter signal," *Astroparticle Physics* **29** (Feb., 2008) 55–62, arXiv:0711.2369.

[208] H.E.S.S. Collaboration, A. Abramowski, F. Acero, F. Aharonian, A. G. Akhperjanian, G. Anton, A. Barnacka, U. Barres de Almeida, A. R. Bazer-Bachi, Y. Becherini, J. Becker, B. Behera, K. Bernlöhr, A. Bochow, C. Boisson, J. Bolmont, P. Bordas, V. Borrel, J. Brucker, F. Brun, P. Brun, T. Bulik, I. Büsching, S. Carrigan, S. Casanova, M. Cerruti, P. M. Chadwick, A. Charbonnier, R. C. G. Chaves, A. Cheesebrough, L.-M. Chounet, A. C. Clapson, G. Coignet, J. Conrad, M. Dalton, M. K. Daniel, I. D. Davids, B. Degrange, C. Deil, H. J. Dickinson, A. Djannati-Ataï, W. Domainko, L. O. C. Drury, F. Dubois, G. Dubus, J. Dyks, M. Dyrda, K. Egberts, P. Eger, P. Espigat, L. Fallon, C. Farnier, S. Fegan, F. Feinstein, M. V. Fernandes, A. Fiasson, G. Fontaine, A. Förster, M. Füßling, Y. A. Gallant, H. Gast, L. Gérard, D. Gerbig, B. Giebels, J. F. Glicenstein, B. Glück, P. Goret, D. Göring, J. D. Hague, D. Hampf, M. Hauser, S. Heinz, G. Heinzelmann, G. Henri, G. Hermann, J. A. Hinton, A. Hoffmann, W. Hofmann, P. Hofverberg, D. Horns, A. Jacholkowska, O. C. de Jager, C. Jahn, M. Jamrozy, I. Jung, M. A. Kastendieck, K. Katarzyński, U. Katz, S. Kaufmann, D. Keogh, M. Kerschhaggl, D. Khangulyan, B. Khélifi, D. Klochkov, W. Kluźniak, T. Kneiske, N. Komin, K. Kosack, R. Kossakowski, H. Laffon, G. Lamanna, D. Lennarz, T. Lohse, A. Lopatin, C.-C. Lu, V. Marandon, A. Marcowith, J. Masbou, D. Maurin, N. Maxted, T. J. L. McComb, M. C. Medina, J. Méhault, R. Moderski, E. Moulin, C. L. Naumann, M. Naumann-Godo, M. de Naurois, D. Nedbal, D. Nekrassov, N. Nguyen, B. Nicholas, J. Niemiec, S. J. Nolan, S. Ohm, J.-F. Olive, E. de Oña Wilhelmi, B. Opitz, M. Ostrowski, M. Panter, M. Paz Arribas, G. Pedaletti, G. Pelletier, P.-O. Petrucci, S. Pita, G. Pühlhofer, M. Punch, A. Quirrenbach, M. Raue, S. M. Rayner, A. Reimer, O. Reimer, M. Renaud, R. de Los Reyes, F. Rieger, J. Ripken, L. Rob, S. Rosier-Lees, G. Rowell, B. Rudak, C. B. Rulten, J. Ruppel, F. Ryde, V. Sahakian, A. Santangelo, R. Schlickeiser, F. M. Schöck, A. Schönwald, U. Schwanke, S. Schwarzburg, S. Schwemmer, A. Shalchi, M. Sikora, J. L. Skilton, H. Sol, G. Spengler, L. Stawarz, R. Steenkamp, C. Stegmann, F. Stinzing, I. Sushch, A. Szostek, J.-P. Tavernet, R. Terrier, O. Tibolla, M. Tluczykont, K. Valerius, C. van Eldik, G. Vasileiadis, C. Venter, J. P. Vialle, A. Viana, P. Vincent, M. Vivier, H. J. Völk, F. Volpe, S. Vorobiov, M. Vorster, S. J. Wagner, M. Ward, A. Wierzcholska, A. Zajczyk, A. A. Zdziarski, A. Zech, H.-S. Zechlin, and H.E.S.S. Collaboration, "H.E.S.S. constraints on dark matter annihilations towards the sculptor and carina dwarf galaxies," *Astroparticle Physics* **34** (Mar., 2011) 608–616, arXiv:1012.5602 [astro-ph.HE].

[209] M. Battaglia, A. D. Roeck, J. Ellis, F. Gianotti, K. A. Olive, and L. Pape, "Updated post-WMAP benchmarks for supersymmetry," *European Physical Journal C* **33** (Mar., 2004) 273–296, arXiv:hep-ph/0306219.

[210] N. Kaiser, H. Aussel, B. E. Burke, H. Boesgaard, K. Chambers, M. R. Chun, J. N. Heasley, K.-W. Hodapp, B. Hunt, R. Jedicke, D. Jewitt, R. Kudritzki, G. A. Luppino, M. Maberry, E. Magnier, D. G.

Monet, P. M. Onaka, A. J. Pickles, P. H. H. Rhoads, T. Simon, A. Szalay, I. Szapudi, D. J. Tholen, J. L. Tonry, M. Waterson, and J. Wick, "Pan-STARRS: A Large Synoptic Survey Telescope Array," in *Society of Photo-Optical Instrumentation Engineers (SPIE) Conference Series*, J. A. Tyson and S. Wolff, eds., vol. 4836 of *Society of Photo-Optical Instrumentation Engineers (SPIE) Conference Series*, pp. 154–164. Dec., 2002.

[211] **Dark Energy Survey Collaboration** Collaboration, T. Abbott *et al.*, "The dark energy survey," arXiv:astro-ph/0510346 [astro-ph].

[212] Z. Ivezic, J. A. Tyson, T. Axelrod, D. Burke, C. F. Claver, K. H. Cook, S. M. Kahn, R. H. Lupton, D. G. Monet, P. A. Pinto, M. A. Strauss, C. W. Stubbs, L. Jones, A. Saha, R. Scranton, C. Smith, and LSST Collaboration, "LSST: From Science Drivers To Reference Design And Anticipated Data Products," in *American Astronomical Society Meeting Abstracts #213*, vol. 41 of *Bulletin of the American Astronomical Society*, p. 460.03. Jan., 2009.

[213] CTA Consortium, B. S. Acharya, M. Actis, T. Aghajani, G. Agnetta, J. Aguilar, F. Aharonian, M. Ajello, A. Akhperjanian, M. Alcubierre, and et al., "Introducing the CTA concept," *Astroparticle Physics* **43** (Mar., 2013) 3–18.

[214] K. Bernlöhr, A. Barnacka, Y. Becherini, O. Blanch Bigas, E. Carmona, P. Colin, G. Decerprit, F. Di Pierro, F. Dubois, C. Farnier, S. Funk, G. Hermann, J. A. Hinton, T. B. Humensky, B. Khélifi, T. Kihm, N. Komin, J.-P. Lenain, G. Maier, D. Mazin, M. C. Medina, A. Moralejo, S. J. Nolan, S. Ohm, E. de Oña Wilhelmi, R. D. Parsons, M. Paz Arribas, G. Pedaletti, S. Pita, H. Prokoph, C. B. Rulten, U. Schwanke, M. Shayduk, V. Stamatescu, P. Vallania, S. Vorobiov, R. Wischnewski, T. Yoshikoshi, A. Zech, and CTA Consortium, "Monte Carlo design studies for the Cherenkov Telescope Array," *Astroparticle Physics* **43** (Mar., 2013) 171–188, arXiv:1210.3503 [astro-ph.IM].

[215] T. Jogler, M. D. Wood, J. Dumm, and A. B. f. t. CTA Consortium, "Monte Carlo comparison of medium-size telescope designs for the Cherenkov Telescope Array," *ArXiv e-prints* (July, 2013) , arXiv:1307.5905 [astro-ph.IM].

[216] G. F. Giudice, R. Rattazzi, M. A. Luty, and H. Murayama, "Gaugino mass without singlets," *Journal of High Energy Physics* **12** (Dec., 1998) 27, arXiv:hep-ph/9810442.

[217] L. Randall and R. Sundrum, "Out of this world supersymmetry breaking," *Nuclear Physics B* **557** (Sept., 1999) 79–118, arXiv:hep-th/9810155.

[218] M. Ibe, S. Matsumoto, S. Shirai, and T. T. Yanagida, "AMS-02 Positrons from Decaying Wino in the Pure Gravity Mediation Model," *ArXiv e-prints* (May, 2013) , arXiv:1305.0084 [hep-ph].

[219] **LAT collaboration** Collaboration, M. Ackermann *et al.*, "Constraints on the Galactic Halo Dark Matter from Fermi-LAT Diffuse Measurements," *Astrophys.J.* **761** (2012) 91, arXiv:1205.6474 [astro-ph.CO].

[220] M. Cirelli and G. Giesen, "Antiprotons from Dark Matter: Current constraints and future sensitivities," *JCAP* **1304** (2013) 015, arXiv:1301.7079 [hep-ph].

[221] M. Cirelli, E. Moulin, P. Panci, P. D. Serpico, and A. Viana, "Gamma ray constraints on Decaying Dark Matter," *Phys.Rev.* **D86** (2012) 083506, arXiv:1205.5283 [astro-ph.CO].

[222] **Fermi-LAT collaboration** Collaboration, A. Abdo *et al.*, "The Spectrum of the Isotropic Diffuse Gamma-Ray Emission Derived From First-Year Fermi Large Area Telescope Data," *Phys.Rev.Lett.* **104** (2010) 101101, arXiv:1002.3603 [astro-ph.HE].

[223] H. Silverwood, P. Scott, M. Danninger, C. Savage, J. Edsj, *et al.*, "Sensitivity of IceCube-DeepCore to neutralino dark matter in the MSSM-25," *JCAP* **1303** (2013) 027, arXiv:1210.0844 [hep-ph].

[224] A. Gould, "Evaporation of WIMPs with arbitrary cross sections," *Astrophysical Journal* **356** (June, 1990) 302–309.

[225] W. H. Press and D. N. Spergel, "Capture by the sun of a galactic population of weakly interacting, massive particles," *Astrophysical Journal* **296** (Sept., 1985) 679–684.

[226] T. K. Gaisser, G. Steigman, and S. Tilav, "Limits on cold-dark-matter candidates from deep underground detectors," *Physics Review D* **34** (Oct., 1986) 2206–2222.

[227] K. Griest and D. Seckel, "Cosmic asymmetry, neutrinos and the Sun.," *Nucl. Phys. B* **283** (1987) 681–705.

[228] A. Gould, "Resonant enhancements in weakly interacting massive particle capture by the earth," *Astrophysical Journal* **321** (Oct., 1987) 571–585.

[229] A. Gould, "Weakly interacting massive particle distribution in and evaporation from the sun," *Astrophysical Journal* **321** (Oct., 1987) 560–570.

[230] J. Edsjö and P. Gondolo, "WIMP mass determination with neutrino telescopes.," *Phys. Lett. B* **357** (Sept., 1995) 595–601, arXiv:hep-ph/9504283.

[231] J. Edsjö, *Aspects of Neutrino Detection of Neutralino Dark Matter*. PhD thesis, Uppsala Univ., Oct., 1997. arXiv:hep-ph/9704384.

[232] A. H. G. Peter, "Dark matter in the Solar System. II. WIMP annihilation rates in the Sun," *Physics Review D* **79** no. 10, (May, 2009) 103532–+, arXiv:0902.1347.

[233] S. Sivertsson and J. Edsjö, "WIMP diffusion in the Solar System including solar WIMP-nucleon scattering," *Physics Review D* **85** no. 12, (June, 2012) 123514.

[234] T. Bruch, A. H. G. Peter, J. Read, L. Baudis, and G. Lake, "Dark matter disc enhanced neutrino fluxes from the Sun and Earth," *Phys. Lett. B* **674** (Apr., 2009) 250–256, arXiv:0902.4001.

[235] J. Diemand, B. Moore, and J. Stadel, "Earth-mass dark-matter haloes as the first structures in the early Universe," *Nature* **433** (Jan., 2005) 389–391, arXiv:astro-ph/0501589.

[236] M. Kamionkowski, S. M. Koushiappas, and M. Kuhlen, "Galactic substructure and dark-matter annihilation in the Milky Way halo," *Physics Review D* **81** no. 4, (Feb., 2010) 043532, arXiv:1001.3144 [astro-ph.GA].

[237] S. M. Koushiappas and M. Kamionkowski, "Galactic Substructure and Energetic Neutrinos from the Sun and Earth," *Physical Review Letters* **103** no. 12, (Sept., 2009) 121301–+, arXiv:0907.4778 [astro-ph.CO].

[238] M. Kuhlen, N. Weiner, J. Diemand, P. Madau, B. Moore, D. Potter, J. Stadel, and M. Zemp, "Dark matter direct detection with non-Maxwellian velocity structure," *JCAP* **2** (Feb., 2010) 30–+, arXiv:0912.2358 [astro-ph.GA].

[239] M. Lisanti, L. E. Strigari, J. G. Wacker, and R. H. Wechsler, "Dark matter at the end of the Galaxy," *Physics Review D* **83** no. 2, (Jan., 2011) 023519, arXiv:1010.4300 [astro-ph.CO].

[240] Y.-Y. Mao, L. E. Strigari, R. H. Wechsler, H.-Y. Wu, and O. Hahn, "Halo-to-halo Similarity and Scatter in the Velocity Distribution of Dark Matter," *Astrophysical Journal* **764** (Feb., 2013) 35, arXiv:1210.2721 [astro-ph.CO].

[241] A. Schneider, L. Krauss, and B. Moore, "Impact of dark matter microhalos on signatures for direct and indirect detection," *Physics Review D* **82** no. 6, (Sept., 2010) 063525, arXiv:1004.5432 [astro-ph.GA].

[242] **AMANDA Collaboration** Collaboration, A. Achterberg *et al.*, "Limits on the muon flux from neutralino annihilations at the center of the Earth with AMANDA," *Astropart.Phys.* **26** (2006) 129–139.

[243] **IceCube collaboration** Collaboration, M. Aartsen *et al.*, "Search for dark matter annihilations in the Sun with the 79-string IceCube detector," *Phys.Rev.Lett.* **110** (2013) 131302, arXiv:1212.4097 [astro-ph.HE].

[244] **IceCube Collaboration** Collaboration, R. Abbasi *et al.*, "Search for Dark Matter from the Galactic Halo with the IceCube Neutrino Observatory," *Phys.Rev.* **D84** (2011) 022004, arXiv:1101.3349 [astro-ph.HE].

[245] **IceCube collaboration** Collaboration, R. Abbasi *et al.*, "Search for Neutrinos from Annihilating Dark Matter in the Direction of the Galactic Center with the 40-String IceCube Neutrino Observatory," arXiv:1210.3557 [hep-ex].

[246] **IceCube Collaboration** Collaboration, R. Abbasi *et al.*, "The IceCube Neutrino Observatory IV: Searches for Dark Matter and Exotic Particles," arXiv:1111.2738 [astro-ph.HE].

[247] P. Gondolo, J. Edsjö, P. Ullio, L. Bergström, M. Schelke, and E. A. Baltz, "DarkSUSY: computing supersymmetric dark matter properties numerically," *JCAP* **7** (July, 2004) 8, arXiv:astro-ph/0406204.

[248] **Super-Kamiokande Collaboration** Collaboration, T. Tanaka *et al.*, "An Indirect Search for WIMPs in the Sun using 3109.6 days of upward-going muons in Super-Kamiokande," *Astrophys.J.* **742** (2011) 78, arXiv:1108.3384 [astro-ph.HE].

[249] C. Rott, J. Siegal-Gaskins, and J. F. Beacom, "New Sensitivity to Solar WIMP Annihilation using Low-Energy Neutrinos," *Phys.Rev.* **D88** (2013) 055005, arXiv:1208.0827 [astro-ph.HE].

[250] N. Bernal, J. Martn-Albo, and S. Palomares-Ruiz, "A novel way of constraining WIMPs annihilations in the Sun: MeV neutrinos," *JCAP* **1308** (2013) 011, arXiv:1208.0834 [hep-ph].

[251] K. Abe, T. Abe, H. Aihara, Y. Fukuda, Y. Hayato, *et al.*, "Letter of Intent: The Hyper-Kamiokande Experiment — Detector Design and Physics Potential —," arXiv:1109.3262 [hep-ex].

[252] C. Savage, G. Gelmini, P. Gondolo, and K. Freese, "Compatibility of DAMA/LIBRA dark matter detection with other searches," *JCAP* **0904** (2009) 010, arXiv:0808.3607 [astro-ph].

[253] J. L. Feng, J. Kumar, D. Marfatia, and D. Sanford, "Isospin-Violating Dark Matter," *Phys.Lett.* **B703** (2011) 124–127, arXiv:1102.4331 [hep-ph].

[254] G. B. Rybicki and A. P. Lightman, *Radiative processes in astrophysics*. 1979.

[255] P. Gondolo, "Either neutralino dark matter or cuspy dark halos," *Phys.Lett.* **B494** (2000) 181–186, arXiv:hep-ph/0002226 [hep-ph].

[256] G. Bertone, G. Sigl, and J. Silk, "Astrophysical limits on massive dark matter," *Monthly Notices of the Royal Astronomical Society* **326** (Sept., 2001) 799–804, arXiv:astro-ph/0101134.

[257] R. Aloisio, P. Blasi, and A. V. Olinto, "Neutralino annihilation at the galactic centre revisited," *JCAP* **5** (May, 2004) 7, arXiv:astro-ph/0402588.

[258] E. A. Baltz and L. Wai, "Diffuse inverse Compton and synchrotron emission from dark matter annihilations in galactic satellites," *Physics Review D* **70** no. 2, (July, 2004) 023512, arXiv:astro-ph/0403528.

[259] S. Colafrancesco, S. Profumo, and P. Ullio, "Detecting dark matter WIMPs in the Draco dwarf: A multiwavelength perspective," *Physics Review D* **75** no. 2, (Jan., 2007) 023513, arXiv:astro-ph/0607073.

[260] S. Profumo, "Nonthermal x rays from the Ophiuchus galaxy cluster and dark matter annihilation," *Physics Review D* **77** no. 10, (May, 2008) 103510, arXiv:0801.0740.

[261] S. Colafrancesco, P. de Bernardis, S. Masi, G. Polenta, and P. Ullio, "Direct probes of dark matter in the cluster 1ES0657-556 through microwave observations," *Astronomy and Astrophysics* **467** (May, 2007) L1–L5, arXiv:astro-ph/0702568.

[262] M. Regis and P. Ullio, "Multiwavelength signals of dark matter annihilations at the Galactic center," *Physics Review D* **78** no. 4, (Aug., 2008) 043505, arXiv:0802.0234 [hep-ph].

[263] D. P. Finkbeiner, "WMAP Microwave Emission Interpreted as Dark Matter Annihilation in the Inner Galaxy," *ArXiv Astrophysics e-prints* (Sept., 2004) , arXiv:astro-ph/0409027.

[264] D. Hooper, D. P. Finkbeiner, and G. Dobler, "Possible evidence for dark matter annihilations from the excess microwave emission around the center of the Galaxy seen by the Wilkinson Microwave Anisotropy Probe," *Physics Review D* **76** no. 8, (Oct., 2007) 083012, arXiv:0705.3655.

[265] D. Hooper, G. Zaharijas, D. P. Finkbeiner, and G. Dobler, "Prospects for detecting dark matter with GLAST in light of the WMAP haze," *Physics Review D* **77** no. 4, (Feb., 2008) 043511, arXiv:0709.3114.

[266] D. Hooper, "Constraining supersymmetric dark matter with synchrotron measurements," *Physics Review D* **77** no. 12, (June, 2008) 123523, arXiv:0801.4378 [hep-ph].

[267] M. L. Mateo, "Dwarf Galaxies of the Local Group," *Annual Review of Astron and Astrophys* **36** (1998) 435–506, arXiv:astro-ph/9810070.

[268] T. E. Jeltema and S. Profumo, "Searching for Dark Matter with X-Ray Observations of Local Dwarf Galaxies," *Astrophysical Journal* **686** (Oct., 2008) 1045–1055, arXiv:0805.1054.

[269] T. E. Jeltema and S. Profumo, "Dark matter detection with hard X-ray telescopes," *Monthly Notices of the Royal Astronomical Society* **421** (Apr., 2012) 1215–1221, arXiv:1108.1407 [astro-ph.HE].

[270] A. Hillas, "The Origin of Ultrahigh-Energy Cosmic Rays," *Ann.Rev.Astron.Astrophys.* **22** (1984) 425–444.

[271] A. K. Konopelko and A. V. Plyasheshnikov, "Ability of Cosmic Ray Rejection Based on Simultaneous Registration of the Integral Cherenkov Light Intensities from Air Showers by Multitelescope System Used in VHE γ-Ray," in *International Cosmic Ray Conference*, vol. 2 of *International Cosmic Ray Conference*, p. 556. 1995.

[272] A. Daum, G. Hermann, M. Heß, W. Hofmann, H. Lampeitl, G. Pühlhofer, F. Aharonian, A. G. Akhperjanian, J. A. Barrio, A. S. Beglarian, K. Bernlöhr, J. J. G. Beteta, S. M. Bradbury, J. L. Contreras, J. Cortina, T. Deckers, E. Feigl, J. Fernandez, V. Fonseca, A. Fraß, B. Funk, J. C. Gonzalez, G. Heinzelmann, M. Hemberger, A. Heusler, I. Holl, D. Horns, R. Kankanyan, O. Kirstein, C. Köhler, A. Konopelko, D. Kranich, H. Krawczynski, H. Kornmayer, A. Lindner, E. Lorenz, N. Magnussen, H. Meyer, R. Mirzoyan, H. Möller, A. Moralejo, L. Padilla, M. Panter, D. Petry, R. Plaga, J. Prahl, C. Prosch, G. Rauterberg, W. Rhode, A. Röhring, V. Sahakian, M. Samorski, J. A. Sanchez, D. Schmele, W. Stamm, M. Ulrich, H. J. Völk, S. Westerhoff, B. Wiebel-Sooth, C. A. Wiedner, M. Willmer, and H. Wirth, "First results on the performance of the HEGRA IACT array," *Astroparticle Physics* **8** (Dec., 1997) 1–11.

[273] M. G. Aartsen, R. Abbasi, Y. Abdou, M. Ackermann, J. Adams, J. A. Aguilar, M. Ahlers, D. Altmann, J. Auffenberg, X. Bai, and et al., "Search for Dark Matter Annihilations in the Sun with the 79-String IceCube Detector," *Physical Review Letters* **110** no. 13, (Mar., 2013) 131302.

[274] T. Tanaka, K. Abe, Y. Hayato, T. Iida, J. Kameda, Y. Koshio, Y. Kouzuma, M. Miura, S. Moriyama, M. Nakahata, S. Nakayama, Y. Obayashi, H. Sekiya, M. Shiozawa, Y. Suzuki, A. Takeda, Y. Takenaga, K. Ueno, K. Ueshima, S. Yamada, T. Yokozawa, C. Ishihara, S. Hazama, H. Kaji, T. Kajita, K. Kaneyuki, T. McLachlan, K. Okumura, Y. Shimizu, N. Tanimoto, F. Dufour, E. Kearns, M. Litos, J. L. Raaf, J. L. Stone, L. R. Sulak, J. P. Cravens, K. Bays, W. R. Kropp, S. Mine, C. Regis, M. B. Smy, H. W. Sobel, K. S. Ganezer, J. Hill, W. E. Keig, J. S. Jang, J. Y. Kim, I. T. Lim, J. B. Albert, K. Scholberg, C. W. Walter, R. Wendell, T. Wongjirad, T. Ishizuka, S. Tasaka, J. G. Learned, S. Matsuno, S. Smith, K. Martens, M. Vagins, Y. Watanabe, T. Hasegawa, T. Ishida, T. Ishii, T. Kobayashi, T. Nakadaira, K. Nakamura, K. Nishikawa, H. Nishino, Y. Oyama, K. Sakashita, T. Sekiguchi, T. Tsukamoto, A. T. Suzuki, Y. Takeuchi, M. Ikeda, A. Minamino, T. Nakaya, L. Labarga, Y. Fukuda, Y. Itow, G. Mitsuka, C. K. Jung, C. McGrew, G. Lopez, C. Yanagisawa, N. Tamura, H. Ishino, A. Kibayashi, M. Sakuda, Y. Kuno, M. Yoshida, S. B. Kim, B. S. Yang, H. Okazawa, Y. Choi, K. Nishijima, Y. Yokosawa, M. Koshiba, Y. Totsuka, M. Yokoyama, S. Chen, Y. Heng, Z. Yang, H. Zhang, D. Kielczewska, P. Mijakowski, K. Connolly, M. Dziomba, E. Thrane, R. J. Wilkes, and Super-Kamiokande Collaboration, "An Indirect Search for Weakly Interacting Massive Particles in the Sun Using 3109.6 Days of Upward-going Muons in Super-Kamiokande," *Astrophysical Journal* **742** (Dec., 2011) 78, `arXiv:1108.3384 [astro-ph.HE]`.

[275] C. Rott, J. Siegal-Gaskins, and J. F. Beacom, "New Sensitivity to Solar WIMP Annihilation using Low-Energy Neutrinos," *ArXiv e-prints* (Aug., 2012) , `arXiv:1208.0827 [astro-ph.HE]`.

[276] N. Bernal, J. Martin-Albo, and S. Palomares-Ruiz, "A novel way of constraining WIMPs annihilations in the Sun: MeV neutrinos," *ArXiv e-prints* (Aug., 2012) , `arXiv:1208.0834 [hep-ph]`.